



The Rigid Limit in Special Kahler Geometry: From K3-Fibrations to Special Riemann Surfaces: A Detailed Case Study

The Harvard community has made this
article openly available. [Please share](#) how
this access benefits you. Your story matters

Citation	Billo, Marco, Frederik Denef, Pietro Fre, Igor Pesando, Walter Troost, Antoine Van Proeyen, and Daniela Zanon. 1998. The rigid limit in Special Kahler geometry: From K3-fibrations to Special Riemann surfaces: A detailed case study. <i>Classical and Quantum Gravity</i> 15(8): 2083-2152.
Published Version	http://dx.doi.org/10.1088/0264-9381/15/8/003
Citable link	http://nrs.harvard.edu/urn-3:HUL.InstRepos:2770489
Terms of Use	This article was downloaded from Harvard University's DASH repository, and is made available under the terms and conditions applicable to Other Posted Material, as set forth at http://nrs.harvard.edu/urn-3:HUL.InstRepos:dash.current.terms-of-use#LAA

The rigid limit in Special Kähler geometry

From K3-fibrations to Special Riemann surfaces: a detailed case study.

Marco Billó¹, Frederik Denef^{1,+},
Pietro Frè², Igor Pesando², Walter Troost^{1,*},
Antoine Van Proeyen^{1,†} and Daniela Zanon³

¹ Instituut voor theoretische fysica,
Katholieke Universiteit Leuven, B-3001 Leuven, Belgium

² Dipartimento di Fisica Teorica dell' Università,
via P. Giuria 1, I-10125 Torino, Italy

³ Dipartimento di Fisica dell'Università di Milano and
INFN, Sezione di Milano, via Celoria 16, I-20133 Milano, Italy.

ABSTRACT

The limiting procedure of special Kähler manifolds to their rigid limit is studied for moduli spaces of Calabi–Yau manifolds in the neighbourhood of certain singularities. In two examples we consider all the periods in and around the rigid limit, identifying the non-trivial ones in the limit as periods of a meromorphic form on the relevant Riemann surfaces. We show how the Kähler potential of the special Kähler manifold reduces to that of a rigid special Kähler manifold. We make extensive use of the structure of these Calabi–Yau manifolds as $K3$ fibrations, which is useful to obtain the periods even before the $K3$ degenerates to an ALE manifold in the limit. We study various methods to calculate the periods and their properties. The development of these methods is an important step to obtaining exact results from supergravity on Calabi–Yau manifolds.

Work supported by the European Commission TMR programme ERBFMRX-CT96-0045, in which D.Z. is associated to U. Torino.

+ Aspirant FWO, Belgium

* Onderzoeksleider FWO, Belgium

† Onderzoeksdirecteur FWO, Belgium

1 Introduction

String theory has proven to be a quite valuable tool in obtaining exact results for non-trivial supersymmetric quantum field theories. In particular, the relation of type II theories on Calabi–Yau manifolds to $N = 2$ supersymmetric $D = 4$ theories has been studied extensively [1, 2], see also [3, 4] and references therein. In many instances, special Kähler geometry [5] and its rigid version [6], and, in particular, the extraction of the rigid limit, play a key role. Special geometry is the geometric structure defined by the two derivative actions of the scalars in vector multiplets of $N = 2$, $D = 4$ theories. The highly constrained structure of the special geometry makes it possible to find exact analytical expressions for many low-energy effective actions [7].

There are two types of special Kähler geometry: ‘rigid’ and ‘local’. Local special geometry applies to local supersymmetry, i.e. supergravity and strings, while rigid special geometry applies to rigid supersymmetry, i.e. $N = 2$ supersymmetric gauge theory in flat spacetime. In spite of the obvious similarities, their precise relation is not completely straightforward. In fact, even in the context of supergravity it is not completely obvious how to decouple gravitons, gravitinos and their graviphoton supersymmetrically. One particular limiting procedure was discussed in [8]. In the present paper we want to identify the essential steps which are involved in this limiting procedure. We want to embed the rigid theory in the supergravity theory. This also implies the calculation of parts of the action which decouple from the field theory degrees of freedom. The detailed explanation of the methods involved can contribute towards the calculation of the next-to-leading terms in the expansion of a phenomenologically important class of supergravity actions, namely those which are obtained from compactifications on $K3$ fibred Calabi–Yau manifolds.

Type IIB string theory compactified on a Calabi–Yau (CY) manifold leads to an $N = 2$ theory in four dimensions. In this case the (local) special geometry of the vector multiplet moduli space is given by the classical geometry of the CY complex structure moduli [9] (see [10] for a review), and it is known to receive no quantum corrections. Therefore, by going to a rigid limit of this classical moduli space and identifying the corresponding rigid low-energy quantum theory (usually a field theory) one should obtain an exact solution for the two-derivative low-energy effective action [1, 2]. The identification of the rigid theory is conceptually the most non-trivial part of this programme, and indeed it was solved only after the discovery of heterotic/type II duality [11] (suggesting non-Abelian gauge theories) and D -branes as solitonic states [12] (providing the ‘missing’ massive gauge vector multiplets). The relevant rigid special geometry often turns out to be naturally associated to the rigid special geometry of a certain class of Riemann surfaces, reproducing and extending the Seiberg–Witten (SW) solution of $N = 2$ quantum Yang–Mills theory. Furthermore, within this framework many features of quantum field theory have a beautiful geometrical interpretation and this provides quite elegant solutions to problems which would be hard to tackle with ordinary field theory techniques, like for example the existence and stability of BPS states [2, 3, 4].

By now, a very large class of $N = 2$, $d = 4$ quantum field theories (and even more exotic theories) can be ‘engineered’ and solved geometrically in this way. The usual procedure

[13, 14] is to find a local IIA model which in the rigid limit produces the field theory to be solved; to map this IIA theory into an equivalent IIB theory using local mirror symmetry and finally to solve this IIB theory exactly (in the low-energy field theory limit) using classical geometry. One argues that the restriction to local models and local mirror symmetry—where ‘local’ means that one only considers a certain small region of the Calabi–Yau manifold—is allowed roughly because the relevant (light brane) degrees of freedom are all localized well inside that region.

An alternative, but not unrelated, approach consists in making use of M -theory brane configurations in flat space [15].

In this paper we study in detail the rigid limit on the type IIB side, without assuming *a priori* that we can restrict ourselves to the local considerations mentioned above. In [2] it was explained how one finds the periods of a Riemann surface and the associated rigid special Kähler structure of its moduli space by expanding the Calabi–Yau 3-fold around singular points and reducing it to an ALE-fibration. This idea is also instrumental for the present work, and many of the results obtained here were already contained in those papers. However, the limiting theory does not teach us how the rigid limit is approached in supergravity. For this we study in detail the behaviour of the full Kähler potential and its rigid limit. Hence we will keep *all* Calabi–Yau periods (which are the building blocks of local special Kähler geometry), not just those that stay finite in the ALE limit. This may also be useful for a possible continuation of the present work, namely a computation of the next-to-leading terms in the expansion of supergravity.

We will study the rigid limit very explicitly in two examples. The corresponding Calabi–Yau surfaces are $K3$ -fibrations, which is a generic feature of type II Calabi–Yau compactifications dual to heterotic strings [16, 17]. We obtain exact expressions for all the periods using the $K3$ -fibration structure. Only afterwards will the expansion be made, and the reduction of special Kähler geometry from local to rigid will be demonstrated explicitly. We will see how certain periods decouple from the Kähler potential to lowest order, and how the latter reduces from its general $Sp(2n + 2)$ structure (where n is the complex dimension of the special Kähler moduli space) to the $Sp(2r)$ structure (where r is the complex dimension of the rigid special Kähler moduli space, with, in our examples, $r = n - 1$). For one of the examples we consider, we obtain the Seiberg–Witten Riemann surfaces corresponding to the different rigid limits as degenerating branches of a genus-5 Riemann surface, defined for *all* values of the Calabi–Yau moduli. The same genus-5 surface gives rise to a genus-2 surface in the $SU(3)$ rigid limit and to the genus-1 surfaces for the $SU(2)$ and $SU(2) \times SU(2)$ limits.

In section 2 we present some of the essential ingredients. First we give a definition of special geometry, the one which is most useful for our purpose [18, 19]. Then we review how moduli spaces of Calabi–Yau and Riemann surfaces realize special Kähler geometry, and we point out the difference between rigid and local special geometry. Then we explain how we expect to make the transition between the two, i.e. how to perform the rigid limit.

Section 3 is devoted to a description of CY surfaces realized as $K3$ fibrations in weighted projective spaces. We illustrate some aspects of $K3$ manifolds, in particular, the distinction between cycles in the Picard and in the transcendental lattice [20, 21]. As the former have trivial periods, the latter are the relevant ones. Then we describe a class of $K3$ fibrations

in which our two examples will fit and we explain how the CY periods can be computed by taking advantage of this $K3$ approach.

In section 4 we introduce the two examples which we will study in detail. In particular, we analyse the structure of the moduli spaces, using a parametrization which allows us to keep the gauge invariances related to redefinitions of the coordinates on the manifolds unfixed. Then we discuss the singularity structures and recall how one can expand the manifolds around these singularities in such a way that they reduce locally to fibrations of ALE spaces.

In section 5 we present a detailed study of the first example. We construct cycles and periods on the CY manifold in terms of the corresponding ones on the $K3$ fibre. The aim is to obtain the periods in a basis with known intersection matrix, which is necessary to calculate the Kähler potential. Although not strictly necessary for our discussion, we derive exact expressions of the periods since these quantities would be useful if we were to consider an expansion of the full supergravity action in the vicinity of its rigid limit. In order to obtain closed expressions of the periods in an integral basis we have found it convenient to combine two approaches: the use of the Picard–Fuchs differential equations [22] and the explicit integration over one particular cycle in a certain region of moduli space. Analytic continuation then leads to the construction of all the other periods.

In section 6 the analysis is extended to the second example. Since in this case the CY manifold can be viewed as a double fibration, first a $K3$ and then a torus fibration, the CY periods are constructed taking advantage of this feature. We obtain exact expressions for the periods and determine monodromy matrices and the intersection matrix.

Finally, in section 7 the limiting procedure is applied and the rigid limit is described. We show that the Kähler potential of (local) special geometry indeed reduces to that of rigid special geometry. We show how the scheme, set out in section 2, emerges from the limiting behaviour of the CY periods. We finally compare the result in the limit with the periods of the Seiberg–Witten Riemann surfaces.

Section 8 contains a summary of the results obtained in our work and some conclusive remarks. We also make some connections to the M theory 2/5-brane picture, albeit only at the formal level.

In the appendices we have collected some additional material. Appendix A presents the structure of the duality and monodromy groups from the point of view of general group-theoretical considerations. Appendix B contains instead the relevant calculations for obtaining the Picard–Fuchs equations and their solutions in the two examples considered in the main text. These are derived using a method inspired by toric geometry, which amounts in practice to simple manipulations of Griffith’s representation of the periods. Finally, appendix C gives an alternative way to define cycles in the first example, which makes contact with [23], and allows us to obtain a compact expression of the intersection matrix.

2 Ingredients

2.1 Special geometry

The first construction of general couplings of vector multiplets to $N = 2$ supergravity [5] used conformal tensor calculus. The geometry of the scalars, ‘special Kähler geometry’, was described in terms of ‘special coordinates’. The construction started from a ‘prepotential’ which corresponds to the function of the vector superfields which is the superspace density. It was realized in [24] that coordinate-independent formulations would be more useful. Meanwhile it was recognized that a special Kähler geometry occurs in the moduli space of Calabi–Yau (CY) manifolds, and in [25] an attempt was made to give definitions of the special geometry which are more useful from that point of view. Crucial in these formulations is the symplectic group, $Sp(2(n+1))$ for the coupling of n physical vector multiplets, which is the group of dualities of the vectors. This structure was already apparent in the conformal tensor calculus in which vector multiplets realize this $Sp(2(n+1))$ group. For defining the special geometry, the symplectic structure is a more natural starting point than the prepotential. This point of view is supported by the observation that some actions cannot be obtained directly from a prepotential [26] (in that case they are dual to an action obtained from a prepotential [19]). In the conformal tensor calculus these theories can be obtained from defining the symplectic vector of superconformal multiplets [27], rather than from a superconformal invariant action. Finally, the symplectic definition which we will describe below is also most useful for the application in moduli spaces.

First we summarize the relevant geometric concepts, both for the rigid¹ and for the local case. We consider symplectic vectors $V(u)$ (rigid), respectively $v(z)$ (local) which are holomorphic functions of r , (respectively n) complex scalars $\{u^i\}$ (respectively $\{z^\alpha\}$). These are $2r$ -vectors for the rigid case (in correspondence with the electric and magnetic field strengths), and $2(n+1)$ -vectors in the local case (because in that case there is also the graviphoton). A symplectic inner product is defined as

$$\langle V, W \rangle = V^T Q^{-1} W ; \quad \langle v, w \rangle = v^T q^{-1} w , \quad (2.1)$$

where Q (and q) is a real, invertible, antisymmetric matrix (we wrote Q^{-1} in (2.1) in view of the meaning which Q will get in the moduli space realizations). Canonically, Q (or q) is

$$Q = \begin{pmatrix} 0 & \mathbf{1} \\ -\mathbf{1} & 0 \end{pmatrix} , \quad (2.2)$$

but we will use also other symplectic metrics.

The Kähler potential is, for the rigid and local manifold, respectively,

$$K(u, \bar{u}) = i \langle V(u), \bar{V}(\bar{u}) \rangle ; \quad \mathcal{K}(z, \bar{z}) = -\log(-i \langle v(z), \bar{v}(\bar{z}) \rangle) . \quad (2.3)$$

In the rigid case there is a rigid invariance $V \rightarrow e^{i\theta} V$, but in the local case there is a symmetry with a holomorphic dependence: $v(z) \rightarrow e^{f(z)} v(z)$. This gives a Kähler transformation $\mathcal{K}(z, \bar{z}) \rightarrow \mathcal{K}(z, \bar{z}) - f(z) - \bar{f}(\bar{z})$. Because of this local symmetry we have to introduce covariant derivatives

$$\mathcal{D}_{\bar{\alpha}} v = \partial_{\bar{\alpha}} v = 0 ; \quad \mathcal{D}_{\alpha} v = \partial_{\alpha} v + (\partial_{\alpha} \mathcal{K}) v . \quad (2.4)$$

¹Rigid special geometry was first found in [6].

There also exists a more symmetrical formulation, using as symplectic sections $e^{\mathcal{K}/2}v$, but we will restrict here to one formulation. In both cases we still need one more constraint (leading to the ‘almost always’ existence of a prepotential), which is for rigid (respectively local) supersymmetry:

$$\langle \partial_i V, \partial_j V \rangle = 0 ; \quad \langle \mathcal{D}_\alpha v, \mathcal{D}_\beta v \rangle = 0 . \quad (2.5)$$

There are further global requirements, such as that in overlaps of regions the symplectic vectors should be related by $ISp(2r, \mathbb{R})$, respectively $Sp(2(n+1), \mathbb{R}) \times \mathbb{C}$ transformations, and the Hodge–Kähler nature of the local manifold, but for an exact formulation we refer to [18, 19].

2.2 Special Kähler geometry in moduli spaces

Although the concept of special Kähler geometry includes cases that are not necessarily related to moduli spaces of surfaces, and although the rigid limit can also be addressed for these cases, in the present paper we focus on such moduli spaces.

Hence, we recall how special geometry (of both kinds) is realized in the moduli spaces of certain complex manifolds. We consider first a CY manifold. It has $n = h^{2,1}$ complex structure moduli to be identified with the complex scalars z^α . The $h^{1,1}$ Kähler moduli do not play any role in this paper: in $N = 2$ supergravity they are associated with the scalars in hypermultiplets, which we do not consider here.

There are $2(n+1)$ cohomologically different 3-cycles c_Λ , and their intersection matrix will be identified with the symplectic metric $q_{\Lambda\Sigma} = c_\Lambda \cap c_\Sigma$. Canonically these are the A and B cycles with intersection matrix (2.2). One identifies v with the ‘period’ vector formed by integration of the $(3,0)$ form over the $2(n+1)$ three-cycles:

$$v_\Lambda = \int_{c_\Lambda} \Omega^{(3,0)} ; \quad \mathcal{D}_\alpha v_\Lambda = \int_{c_\Lambda} \Omega_{(\alpha)}^{(2,1)} . \quad (2.6)$$

With a $(3,0)$ form which is holomorphic in the moduli space, we satisfy all requirements for *local* special geometry automatically [28], e.g.

$$\langle \mathcal{D}_\alpha v, \mathcal{D}_\beta v \rangle = \int_{c_\Lambda} \Omega_{(\alpha)}^{(2,1)} \cdot q^{\Lambda\Sigma} \cdot \int_{c_\Sigma} \Omega_{(\beta)}^{(2,1)} = - \int_{CY} \Omega_{(\alpha)}^{(2,1)} \wedge \Omega_{(\beta)}^{(2,1)} = 0 . \quad (2.7)$$

Rigid special Kähler geometry is realized in moduli spaces of Riemann surfaces (RS). A RS of genus g has g holomorphic $(1,0)$ forms. Now, in general, we need a family of Riemann surfaces with r complex moduli u^i , such that one can isolate r $(1,0)$ -forms which are the derivatives of a meromorphic 1-form λ up to a total derivative:

$$\gamma_i = \partial_i \lambda + d\eta_i ; \quad \alpha = 1, \dots, r \leq g . \quad (2.8)$$

Then one should also identify $2r$ 1-cycles c_A forming a complete basis for the cycles over which the integrals of λ are non-zero. We identify the symplectic vector of rigid special geometry as

$$V_A = \int_{c_A} \lambda . \quad (2.9)$$

As follows from the above explanation, this construction of rigid special geometry is much less straightforward than the construction of local special geometry in the CY moduli space, since except for genus 1 it is not clear *a priori* how to find the subspace of moduli space that has the required special property.

2.3 The rigid limit

Let us start from a manifold with local special geometry. We expect, in some limit, to find the structure of *rigid* special geometry; we will call this the *rigid limit*. We will investigate the rigid limit at the level of the Kähler potential. One may think of the construction as in section 2.2, but the treatment here is more general. The scalar fields $\{z^\alpha\}$, with $\alpha = 1, \dots, n$, are moduli of this manifold, and we consider a region in moduli space where they are expanded in terms of a small expansion parameter ϵ . This expansion is made keeping some (functions of the) moduli $\{u^i\}$ with $i = 1, \dots, r$ fixed:

$$z^\alpha = z^\alpha(\epsilon, u^i) . \tag{2.10}$$

An example of such a procedure was given in section 10 of [8] in which case $r = n$, while in the examples which we will consider below $r = n - 1$, and (2.10) can be considered as a local coordinate change from z^α to $\{\epsilon, u^i\}$. We now imagine that the period vector (or more generally the symplectic vector) is the sum of pieces with different ϵ dependence, of the form

$$v = v_0(\epsilon) + \epsilon^a v_1(u) + v_2(\epsilon, u) . \tag{2.11}$$

The dominant piece in the $\epsilon \rightarrow 0$ limit is imagined to be v_0 , a piece independent of the surviving moduli. v_1 is a vector such that the derivatives with respect to the moduli form a matrix of rank r . The pieces v_1 and v_2 are assumed to contribute to the local Kähler potential \mathcal{K} of (2.3) in a progressively less dominant manner as follows:

$$\langle v, \bar{v} \rangle = iM^2(\epsilon) + |\epsilon|^{2a} \langle v_1(u), \bar{v}_1(\bar{u}) \rangle + R(\epsilon, u, \bar{u}) , \tag{2.12}$$

where

$$iM^2(\epsilon) = \langle v_0(\epsilon), \bar{v}_0(\epsilon) \rangle , \tag{2.13}$$

$$\frac{|\epsilon|^{2a}}{M^2} \xrightarrow{\epsilon \rightarrow 0} 0 ; \quad \frac{R}{|\epsilon|^{2a}} \xrightarrow{\epsilon \rightarrow 0} 0 . \tag{2.14}$$

and a is some real number (which could be normalized to 1 by choosing ϵ appropriately). For this one needs that $\text{Im} \langle v_0(\epsilon), \bar{v}_1(\epsilon) \rangle = o(|\epsilon|^{2a})$, and similar conditions for v_2 . If this structure is realized, the local Kähler potential \mathcal{K} of (2.3) can be written as

$$\mathcal{K} = -\log(M^2) + i \frac{|\epsilon|^{2a}}{M^2} \langle v_1(u), \bar{v}_1(\bar{u}) \rangle + \dots = -\log(M^2) + \frac{|\epsilon|^{2a}}{M^2} K(v_1(u), \bar{v}_1(\bar{u})) + \dots . \tag{2.15}$$

This indicates that the local Kähler potential thus reduces to the Kähler potential for a rigid special geometry up to an additive constant and an overall multiplicative renormalization, see also (2.3) with the identification of $V(z)$ with $v_1(u)$.

To confirm this interpretation, we also have to consider the covariant derivative in (2.4). The expansion (2.11) implies for the derivatives with respect to the surviving moduli

$$D_u v = \epsilon^a \partial_u v_1 + \dots, \quad (2.16)$$

where the dots indicate subleading terms that can be neglected in the limit. This implies that the first expression of (2.5) is implied by the second, in this limit. The constraints of local special Kähler thus reduce to those of rigid special Kähler geometry.

Relating ϵ to the inverse Planck mass, in this way one should obtain the limit of the theory when gravitational interactions are switched off. One of our tasks is therefore to show how to obtain the structure anticipated in (2.11) and (2.12). In [8] it was proposed that v_0 is a constant vector, orthogonal to $v_1(z^\alpha)$ (of rank $2n$), and v_2 is of order $\epsilon^{3\alpha}$. The various objects appearing in rigid and local special geometry were then related. ϵ is in our case one of the fields of the supergravity model which is fixed in the rigid theory. We will have to demonstrate that the structure required for (2.12), like the approximate orthogonality of v_0 and v_1 , really holds.

In previous work [2], the $\epsilon \rightarrow 0$ limit was taken by considering not the full CY space, but only its structure around the specific singularity in moduli space. The CY surfaces treated there are $K3$ fibrations, and in the rigid limit they degenerate into fibrations of an asymptotically locally Euclidean (ALE) space, with a corresponding set of forms and cycles. One expects that in the rigid limit only the periods corresponding to these forms and cycles are relevant. The particular ALE space then determines the Seiberg–Witten auxiliary surface for the corresponding Yang–Mills theory. We will not make use of this degeneration, but rather work on the full CY space. Nevertheless, inspired by [2], we will also consider CY manifolds that are $K3$ fibrations. Therefore in section 3.1 we discuss some common properties of the particular CY and $K3$ surfaces we need in the following.

2.4 Monodromies and the Picard–Lefschetz formula

In the course of the programme sketched above, we will often use monodromy matrices. Let us state explicitly our convention about monodromy and intersection matrices.

Consider a set of functions $U_i(\mu)$ (e.g. a basis of solutions to a differential equation, to fix the ideas), with a cut running from $\mu = 0$. Consider the analytic continuation of $U_i(\mu)$, following $\mu \rightarrow e^{i\phi}\mu$ from $\phi = 0$ to $\phi = 2\pi$, with $|\mu|$ small (which we will indicate by $\mu \rightarrow e^{2\pi i}\mu$). After crossing the cut, these continuations, U'_i , will be re-expressed in the U_i are still solutions of the same differential equations, and can be expressed in the U_i basis by $U'_i = M_i^j U_j$; M_i^j is the monodromy matrix around $\mu = 0$. We remark that the monodromy is thus connected to the crossing of the cut. If more than one cut runs from $\mu = 0$, the monodromy matrix can depend on the base point, i.e. the value of μ where we start. This dependence is in practice only on the order in which different cuts to the singular points are crossed during the loop.

If we cross two cuts, the first one related to the monodromy matrix M , and the second one to N , then the combined monodromy is ordered as $M N$, because the monodromies are

always defined with respect to the original basis U_i . With these conventions we have for I an intersection matrix, M a monodromy matrix, and $U' = SU$ a change of basis:

$$MIM^T = I; \quad I' = SISO^T; \quad M' = SMS^{-1} \quad (2.17)$$

for the new intersection and monodromy matrices I' and M' .

A useful ingredient is the Picard–Lefschetz formula. This says that for a cycle C going around a singularity where ν is the vanishing cycle

$$C \rightarrow C - s^N (-1)^{N(N+1)/2} (\nu \cdot C) \nu, \quad (2.18)$$

where N is the complex dimension of the manifold, $s = \pm 1$, the conventional intersection number $X \cdot Y$ of the real axis X and the imaginary axis Y in the complex plane. We used $s = +1$. Further, the dot product means the intersection number. Note that for $K3$, as for any manifold with $N = 2 \bmod 4$, this implies $\nu \cdot \nu = -2$. For CY and $K3$ we can thus use

$$C \rightarrow C + (C \cdot \nu) \nu. \quad (2.19)$$

3 $K3$ fibrations, singularities and periods

3.1 Description of the CY and $K3$ in weighted projective spaces

The complex manifolds we shall be concerned with in this paper are all described as hypersurfaces in a *weighted projective ambient space*; they correspond to loci of a complex *polynomial equation* $W(x) = 0$ with $(x_1, \dots, x_{N+2}) \sim (\lambda^{w_1} x_1, \dots, \lambda^{w_{N+2}} x_{N+2})$, i.e. with $x \in \mathbb{P}^{w_1, \dots, w_{N+2}}$, and with $W(\lambda x) = \lambda^d W(x)$, if they are N dimensional. The first Chern class of such a manifold vanishes provided the sum of the weights equals the homogeneity degree of W , i.e. if $\sum w_i = d$; if this is the case, the hypersurface is named a CY manifold if three dimensional, it is $K3$ if two dimensional and the torus if one dimensional.

We adopt the standard notation to denote such manifolds: for example, $X_{24}[1, 1, 2, 8, 12]$ is a CY space defined by $W(x) = 0$ with $x \in \mathbb{P}^{1,1,2,8,12}$ and $W(\lambda x) = \lambda^{24} W(x)$.

A general quasi-homogeneous polynomial W in weighted projected space is specified by many coefficients, 335 in the example above. Coordinate transformations in the ambient weighted projective space, however, induce ‘gauge transformations’ of these coefficients, numbering 92 in the present case. Fixing the gauge reduces the number of true parameters, to 243 in the example.

We will consider surfaces for which a discrete group of additional *global identifications* is imposed on the ambient space. This group we will call G for CY and G' for $K3$. For instance, for $X_{24}^*[1, 1, 2, 8, 12]$, which is one of those we will treat extensively, we impose, with respect to its unasterisked version², additional identifications

$$\begin{aligned} x_j &\simeq \exp\left(n_j \frac{2\pi i}{24}\right) x_j, \\ (n_1, n_2, n_3, n_4, n_5) &= m_1(1, -1, 0, 0, 0) + m_2(-1, -1, 2, 0, 0), \end{aligned} \quad (3.1)$$

²The * in the notation in facts indicates the mirror manifold, for which a particular set of global identifications is necessary, as we will do in our examples.

where $m_i \in \mathbb{Z} \bmod 24$. Using a shorthand notation, the group G in (3.1) is generated by the rescalings $(1, -1, 0, 0, 0)_{24}$ and $(-1, -1, 2, 0, 0)_{24}$. Notice that these rescalings are defined mod $(1, 1, 2, 8, 12)_{24}$ because of the projective identifications. The defining polynomial W is then restricted to a sum of those monomials that are invariant under these identifications. In this way the number of parameters is reduced to 11 and the number of gauge invariances to 8. We thus remain with three true complex structure moduli. The manifold turns out to be the dual of the one without the identifications, and we have $h^{2,1} = 3$ and $h^{1,1} = 243$.

For some purposes it is useful to keep (at least some of) the gauge invariances, rather than fixing them, as we will see.

The relevant forms both for local as for rigid special geometry can be represented using the Griffiths residue theorem [29, 30]. We will use this representation for the holomorphic forms $\Omega^{(N,0)}$, with $N = 3$ for the CY (3, 0) form and $N = 2$ for the (2, 0) form in $K3$. In that case the theorem states that

$$\Omega^{(N,0)} = \frac{|G|}{(2\pi i)^{N+1}} \int \frac{\omega}{W}, \quad (3.2)$$

where $|G|$ is the number of elements in the group G (or G' for the $K3$). the normalization is chosen for later convenience and the integral is over a 1-cycle that encircles the surface $W = 0$ in the ambient space $\mathbb{P}^{w_1, \dots, w_{N+2}}$, of which ω is the volume form [31]:

$$\omega = w_1 x^1 dx^2 \dots dx^{N+2} - w_2 x^2 dx^1 \dots dx^{N+2} + \dots + (-)^{N+1} w_{N+2} x^{N+2} dx^1 \dots dx^{N+1}. \quad (3.3)$$

The relevant periods are obtained by performing integrals of these forms over integral 3-cycles on the CY surface.

The expression (3.2) makes it clear that periods of $\Omega^{(N,0)}$ over N -cycles depend holomorphically on the moduli (not on their complex conjugates) appearing in the polynomial W . This remains true if the normalization of $\Omega^{(N,0)}$ is redefined by any holomorphic function of the moduli. This freedom leads in the local Kähler potential to a Kähler transformation. To obtain the expansion of the periods into the form of (2.12) it may be necessary to perform such a Kähler transformation.

3.2 $K3$ and its Picard and transcendental lattices

We will encounter $K3$ manifolds as fibres in a suitable description of the Calabi–Yau manifolds. It is thus perhaps useful to recall some properties of $K3$, also in comparison with those of the CY 3-folds themselves. The number of homology 2-cycles (and of cohomology 2-forms) of $K3$ is $b^2 = 22$: beside $\Omega^{(2,0)}$ and $\bar{\Omega}^{(0,2)}$ there are $h^{1,1} = 20$ elements in $H^{1,1}$.

Just as for the CYs we are interested in the periods of the holomorphic form $\Omega^{(3,0)}$, for $K3$ we will need the periods of $\Omega^{(2,0)}$. Yet, for their moduli spaces it is important to stress the following three important differences with respect to those of the Calabi–Yau 3-folds:

1. In contrast to what happens for a CY, where the number of 3-cycles along which we calculate the periods just equals the third Betti number: $b^3 = 2 + 2h^{2,1}$, for $K3$ the periods of $\Omega^{(2,0)}$ along a subset of 2-cycles, named ‘algebraic’ (see below), vanish.

Therefore in later sections, when discussing the 2-cycles for certain realizations of $K3$, we will consider exclusively the remaining ones, called ‘transcendental’.

2. In the Calabi–Yau case the calculation of the periods is instrumental for the very determination of the special Kähler metric $g_{\alpha\bar{\beta}}(z, \bar{z})$ on moduli space. In the $K3$ case the determination of the periods, for a fixed algebraic representation of $K3$, corresponds only to the solution of a uniformization problem, i.e. establishing the relation between a canonical and a non-canonical coordinate system. The metric on the complex structure moduli space is actually known *a priori* as this space is the homogeneous non-compact coset manifold $O(2, n)/O(2) \times O(n)$, where n is the number of transcendental cycles.
3. The moduli-space of a CY manifold is the direct product of its Kähler and complex structure moduli spaces. In contrast, the $K3$ moduli space, a homogeneous coset manifold modded by a discrete subgroup, has no such direct product structure.

Let us now be more precise, and consider a specific algebraic realization Σ_{K3} of the $K3$ manifold. The proper language for distinguishing between ‘*complex structure 2-cycles*’ and ‘*Kähler class 2-cycles*’ relative to such a realization, is by making use of the concept of the Picard lattice and its orthogonal complement, the transcendental lattice (see e.g. [21]). The *algebraic 2-cycles* are those that can be *holomorphically* embedded in Σ_{K3} , and the integral of $\Omega^{(2,0)}$ on them clearly vanish. The Picard lattice $\text{Pic}(\Sigma_{K3})$ is the sublattice of $H^2(K3, \mathbf{Z})$ spanned by their Poincaré duals. They have a purely $H^{1,1}(\Sigma_{K3})$ representative, and we can equivalently define

$$\text{Pic}(\Sigma_{K3}) \equiv H^{1,1}(\Sigma_{K3}) \cap H^2(K3, \mathbf{Z}) . \quad (3.4)$$

Also with this formulation it is clear that the periods of $\Omega^{(2,0)}$ along cycles dual to the 2-forms in the Picard lattice are always zero. Fixing a certain lattice to be the Picard lattice puts a constraint on the allowed complex structure deformations, whose number is reduced to $n \equiv 20 - \rho(\Sigma_{K3})$, where $\rho(\Sigma_{K3})$, the ‘Picard number’, is the rank of the Picard lattice. A completely generic $K3$ has Picard number zero. For an algebraic $K3$ however, $\rho(\Sigma_{K3}) \geq 1$ and the lattice has signature $(1, \rho(\Sigma_{K3}) - 1)$. Indeed, the Kodaira–Spencer theorem ensures that in a projective algebraic manifold the Kähler class is proportional to an integer class. The generic quartic has $\rho(\Sigma_3) = 1$. Here the curve $x_i = 0$, with x_i any homogeneous coordinate on \mathbb{P}^3 , is algebraic. Hence there are 19 complex structure deformations. The purely Fermat quartic has $\rho(\Sigma_{K3}) = 20$. The two examples which we will consider have Picard number 19 and 18, respectively. The orthogonal complement of $\text{Pic}(\Sigma_{K3})$ in $H^2(K3, \mathbf{Z})$ is called the *transcendental lattice*

$$\Lambda^{\text{tr}} = \left\{ \hat{C} \in H^2(K3, \mathbf{Z}) \mid \hat{C} \cdot \text{Pic} = 0 \right\} , \quad (3.5)$$

the dot product being determined by the intersection of the dual cycles. This lattice has rank $22 - \rho(\Sigma_{K3})$ and signature $(2, 20 - \rho(\Sigma_{K3}))$. Denote by $\{\hat{c}_A\}$ for $A = 1, \dots, 22$ a basis of $H^2(K3, \mathbf{Z})$, by $\{\hat{c}_a\}$ for $a = 1, \dots, \rho(\Sigma_{K3})$ a basis of Pic , and $\{\hat{c}_I\}$ for $I = \rho(\Sigma_{K3}) + 1, \dots, 22$ a basis of the transcendental lattice. We thus have

$$\hat{c}_a = \mathcal{G}_a^A \hat{c}_A \quad \text{with } \mathcal{G}_a^A \in \mathbf{Z}$$

$$\hat{c}_I = \mathcal{G}_I^A \hat{c}_A \quad \text{with} \quad \begin{cases} \mathcal{G}_I^A \in \mathbf{Z} \\ \mathcal{I}_{Ia} \equiv \mathcal{G}_I^A \mathcal{I}_{AB} \mathcal{G}_a^B = 0 \end{cases} , \quad (3.6)$$

with $\text{rank}(\mathcal{G}_a^A) = \rho(\Sigma_{K3})$. The total transformation of basis for the 22 two-cycles is thus determined by the matrix

$$\begin{pmatrix} \mathcal{G}_a^A \\ \mathcal{G}_I^A \end{pmatrix} . \quad (3.7)$$

If this matrix is of determinant 1, then $H^2(K3, \mathbf{Z}) = \text{Pic} \oplus \Lambda^{\text{tr}}$, but in general the b^2 vectors $\{c_a, c_I\}$, do *not* form a lattice basis of $H^2(K3, \mathbf{Z})$.

Since the periods of the (2,0)-form over the algebraic cycles (the Poincaré duals of the forms in Pic) vanish, the complex structure moduli space at fixed Picard lattice is (over)parametrized by the periods along the transcendental cycles (dual to elements of Λ^{tr}).

Consider the general relation

$$\int_{c_A} \lambda \mathcal{I}^{AB} \int_{c_B} \omega = \int_{K3} \lambda \wedge \omega , \quad (3.8)$$

for any 2-forms λ and ω and with c_A a complete basis of cycles with \mathcal{I}^{AB} the inverse of the complete intersection matrix. This relation remains true for any change of basis, even if not integral. Therefore, using the transformation (3.7), this equation reduces for $\lambda = \omega = \Omega^{(2,0)}$ to a sum over the cycles \hat{c}_I forming a basis of the Λ^{tr} . Defining the periods

$$\theta_I = \int_{\hat{c}_I} \Omega^{(2,0)} , \quad (3.9)$$

we obtain

$$\theta_I \mathcal{I}^{IJ} \theta_J = \int_{K3} \Omega^{(2,0)} \wedge \Omega^{(2,0)} = 0 , \quad (3.10)$$

where the symmetric matrix \mathcal{I}^{IJ} , of signature $(2, 20 - \rho(\Sigma_{K3}))$, is the inverse of the intersection matrix of the transcendental 2-cycles:

$$\mathcal{I}_{IJ} \equiv \hat{c}_I \cap \hat{c}_J . \quad (3.11)$$

In the next section we shall introduce a class of CY manifolds that admits a $K3$ fibration. This class includes the two examples that will subsequently be treated in detail. We will indicate how the fibration can be used to reduce the calculation of the CY periods to that of the $K3$ periods, and discuss some strategies to carry out this computation.

3.3 A class of $K3$ fibrations

We consider Calabi–Yau manifolds of the form³

$$X_{2K}[1, 1, 2k_3, 2k_4, 2k_5] \quad \text{with} \quad K = 1 + k_3 + k_4 + k_5 , \quad (3.12)$$

³Here we write X_{2K} for a manifold which has at least some global identifications as we will explain. In practice we will use the one with all identifications such that it is $X_{2K}^*[1, 1, 2k_3, 2k_4, 2k_5]$.

that is, zero-loci of a quasi-homogeneous polynomial $W(x) = \lambda^{2K}W(\lambda x)$ in the weighted projective space $\mathbb{P}^{1,1,2k_3,2k_4,2k_5}$, where a point of coordinates $(x_1, x_2, x_3, x_4, x_5)$ is identified with $(\lambda x_1, \lambda x_2, \lambda^{2k_3}x_3, \lambda^{2k_4}x_4, \lambda^{2k_5}x_5)$. The ambient space is subject to a group of discrete identifications G of the form

$$G = \mathbf{Z}_K \times G' , \quad (3.13)$$

where the first factor corresponds to the identifications

$$x_1 \sim e^{\frac{2\pi i}{2K}} x_1 ; \quad x_2 \sim e^{\frac{-2\pi i}{2K}} x_2 \quad (3.14)$$

(note that the K th power of (3.14) is a projective transformation) and G' leaves invariant the ratio x_1/x_2 . The most general polynomial of degree $2K$ in the x 's invariant under (3.14) can be written (up to a rescaling of x_1/x_2) as

$$W = \frac{B}{2K} (x_1^{2K} + x_2^{2K}) + \hat{W}(x_1x_2, x_3, x_4, x_5; \psi_i) - \frac{1}{K}\psi_s(x_1x_2)^K , \quad (3.15)$$

where B , ψ_i , ψ_s are moduli and \hat{W} is a polynomial of weight K in the projective space $\mathbb{P}^{1,k_3,k_4,k_5}$. The $K3$ -fibration of the CY manifold we are considering is exhibited introducing new coordinates x_0 and ζ , invariant under (3.14), by

$$x_1 = \zeta^{1/(2K)} \sqrt{x_0} ; \quad x_2 = \zeta^{-1/(2K)} \sqrt{x_0} . \quad (3.16)$$

In these coordinates the potential W becomes

$$W = B' \frac{1}{K} x_0^K + \hat{W}(x_0, x_3, x_4, x_5; \psi_i) , \quad (3.17)$$

where we have introduced

$$B' = \frac{1}{2} \left(B\zeta + \frac{B}{\zeta} - 2\psi_s \right) . \quad (3.18)$$

The polynomial W in (3.17) then describes a $K3$ manifold of type $X_K[1, k_3, k_4, k_5]$ (subject to a discrete identification group G'), with one of the moduli, namely B' , varying from point to point in the base as in (3.18).

Note that the 'gauge invariances' in the moduli space of both the CY and the $K3$ always include the projective transformation

$$B' \rightarrow \lambda^K B' ; \quad \psi_i \rightarrow \psi_i \lambda^{a_i} ; \quad \lambda \in \mathbb{C}_0 , \quad (3.19)$$

where the weights a_i are determined so as to reabsorb the coordinate rescaling $x_0 \rightarrow \lambda^{-1}x_0$:

$$W(x_0, x_3, x_4, x_5; B', \psi_i) = W\left(\frac{1}{\lambda}x_0, x_3, x_4, x_5; B'\lambda^K, \psi_i\lambda^{a_i}\right) . \quad (3.20)$$

3.4 Using the $K3$ fibration for the periods

In the calculation of periods and monodromy matrices for Calabi–Yau 3-folds one may take full advantage of the fibration structure of the manifold. In the expression for the $(3, 0)$ -form, (3.2), we can make use of the relation between the volume forms

$$\begin{aligned}\omega_{CY} &= \frac{1}{K} \omega_{K3} \frac{d\zeta}{\zeta}; & \Omega^{(3,0)} &= \Omega^{(2,0)} \frac{d\zeta}{2\pi i \zeta} \\ \omega_{K3} &= x_0 dx_3 dx_4 dx_5 - dx_0 (k_3 x_3 dx_4 dx_5 + k_4 x_4 dx_5 dx_3 + k_5 x_5 dx_3 dx_4) .\end{aligned}\quad (3.21)$$

The factor K is cancelled in the relation between the forms due to (3.2) and (3.13). To make full use of this factorized form, it is convenient to also describe the relevant CY 3-cycles in a factorized form: this allows us to integrate first over 2-cycles in the $K3$ manifold, thus giving periods of the $K3$, leaving the ζ integral to the end. The structure of this last integration will eventually lead to the auxiliary Riemann surfaces of [7], and the associated special Kähler geometry. Let us therefore first consider the structure of the 3-cycles. The homology cycles C of the Calabi–Yau manifold can be constructed as fibrations⁴ of homology cycles c of the $K3$ -fibre over (possibly *open*) paths γ in the base manifold \mathbb{P}^1 ; that is, there is a fibration $f : C \rightarrow \gamma$ such that for every point $p \in \gamma$, the fibre $f^{-1}(p)$ is a $K3$ 2-cycle c . The intersection of two 3-cycles C_1, C_2 is then

$$C_1 \cdot C_2 = \sum_{p \in \gamma_1 \cap \gamma_2} s(p) f_1^{-1}(p) \cdot f_2^{-1}(p), \quad (3.22)$$

where $s(p)$ is the sign of the intersection in p of the paths γ_1 and γ_2 . This simply means that we have to add (with the appropriate sign) the $K3$ intersections of the fibres (which are 2-cycles) above the intersection points in the base⁵.

Consider a particular non-trivial 2-cycle in the $K3$ manifold. This cycle may nevertheless vanish for a value of the moduli that makes the $K3$ singular. For a fixed Calabi–Yau manifold this singularity corresponds to a certain value of ζ . Now one can make two constructions

- One can consider a path between two (singular) points in the ζ -base space where the same $K3$ cycle vanishes. The $K3$ 2-cycle along this path gives a closed 3-cycle in the CY manifold.
- One can consider a non-trivial loop in the base space transporting a cycle that has trivial monodromy around that loop.

3.5 Strategies for obtaining $K3$ periods

In view of this fibration structure we will first address the calculation of periods, monodromies and intersection matrix for the $K3$ manifold, leaving the dependence of the moduli on the \mathbb{P}^1 base coordinate ζ for later.

⁴In the following, for simplicity, we write just $C = \gamma \times c$, but we understand a fibration.

⁵Note that, in general, $f_1^{-1}(p) \cdot f_2^{-1}(p)$ will be p -dependent (due to monodromies). The sum factorizes only if the CY cycles have a true global direct product structure.

The most straightforward approach to the computation of the $K3$ periods would be to explicitly integrate the $(2,0)$ form over an integral basis of 2-cycles⁶. This is, however, not always practical. In the first example, in fact, we will use a variation on this method [23]. We explicitly integrate over one specific cycle, which is easy to parametrize, in the neighbourhood of the ‘large complex structure’ point in moduli space; this gives the so-called ‘fundamental period’. Analytic continuation of this period, as a function of the modulus, outside the original neighbourhood reveals cuts. Associated monodromy transformations change it into (integer) linear combinations of a basis of integral periods. An approach which is complementary in this respect is the use of the *Picard–Fuchs equations* satisfied by the periods of the $(2,0)$ form. Using (3.10) the intersection matrix is obtained modulo a multiplicative constant. In turn, while a generic basis of solutions of the PF equation is a basis for the $K3$ periods, it does not necessarily correspond to integrals over *integer* cycles: it is not an *integral basis*, and the explicit expression of the period over the fundamental cycle is needed in order to be able to define such a basis.

Finally one can try to apply the strategy used for the Calabi–Yau periods to the $K3$ periods themselves. In the second example this works because the $K3$ is itself a *torus fibration*. The forms and cycles can be decomposed in forms and cycles on the torus, fibred over a second \mathbb{P}^1 base space. For that example this procedure has the advantage that the starting point is the torus, where much more is known explicitly for cycles, periods and the intersection matrix.

4 Introducing the examples: fibrations and singularities

In this section, we turn to the explicit description of the two examples of CY manifolds that we study in detail, the $K3$ fibrations that we use in this study, and their singularity structures. We use the notation introduced in subsection 3.3.

4.1 Description and fibration of $X_8^*[1, 1, 2, 2, 2]$

The first example is the Calabi–Yau manifold in the class (3.12) with $k_3 = k_4 = k_5 = 1$. The group G contains the identifications

$$x_j \simeq \exp\left(n_j \frac{2\pi i}{8}\right) x_j \tag{4.1}$$

with

$$\begin{aligned} (n_1, n_2, n_3, n_4, n_5) = & m_0(1, 1, 2, 2, 2) + m_1(1, -1, 0, 0, 0) \\ & + m_2(0, 0, 2, -2, 0) + m_3(0, 0, 2, 0, -2) , \end{aligned} \tag{4.2}$$

⁶We will further consider only the transcendental cycles, and will therefore just talk about these as ‘the cycles’.

where $m_1, m_2, m_3 \in \mathbb{Z}$. The transformation parametrized with m_0 is the identifying relation for the weighted projective space in which our CY is embedded. If m_0 is an integer, (4.1) leaves the polynomial invariant. The identification m_1 is the transformation (3.14). The group G is thus \mathbb{Z}_4^3 as in (3.13) with $G' = \mathbb{Z}_4^2$.

The most general polynomial of degree 8 in the variables x_1, \dots, x_5 , invariant under (4.2), is (up to rescalings of the x_i)

$$W^{(1)} = \frac{b_1}{8}x_1^8 + \frac{b_2}{8}x_2^8 + \frac{b_3}{4}x_3^4 + \frac{b_4}{4}x_4^4 + \frac{b_5}{4}x_5^4 - \psi_0 x_1 x_2 x_3 x_4 x_5 - \frac{1}{4}\psi_s (x_1 x_2)^4. \quad (4.3)$$

There are still 5 gauge invariances, induced by rescaling the x_i , such that there remain 2 independent moduli. We could take as invariants, for example, $\psi_s^2/(b_1 b_2)$ and $\psi_0^4/(\psi_s b_3 b_4 b_5)$. This would be valid in a patch where $\psi_s b_1 b_2 b_3 b_4 b_5 \neq 0$. We will regularly make such choices without further comments. For example, in the form of (3.15), the gauge invariance has already been used⁷ also to put $b_1 = b_2 = B$. It is sometimes useful to postpone such choices, notably for the discussion of singularities (section 4.3), and also for the derivation of Picard–Fuchs equations (section B).

We continue with the $K3$ fibration, following the general pattern of section 3.3: introducing $x_1 x_2 = x_0$ leads to (3.17), which in this case becomes

$$W^{(1)} = \frac{B'}{4}x_0^4 + \frac{b_3}{4}x_3^4 + \frac{b_4}{4}x_4^4 + \frac{b_5}{4}x_5^4 - \psi_0 x_0 x_3 x_4 x_5. \quad (4.4)$$

The remaining gauge invariances are the rescalings of the x_i . Therefore the moduli space of this fibre is in fact 1-complex dimensional. The truly invariant variable is

$$z = -\frac{B' b_3 b_4 b_5}{\psi_0^4}. \quad (4.5)$$

(with minus signs for later convenience). Mostly we will partially gauge fix the rescalings by putting $b_3 = b_4 = b_5 = 1$, such that the polynomial is

$$W^{(1)}(x; B', \psi_0) = \frac{1}{4} \left(B' x_0^4 + x_3^4 + x_4^4 + x_5^4 \right) - \psi_0 x_0 x_3 x_4 x_5 \quad (4.6)$$

with B' given in (3.18). The moduli space has the projective transformations given in general in (3.19) (with $K = 4$, $a_0 = 1$). The identifications in (4.2) give rise to corresponding identifications on the $K3$ manifold

$$x_j \simeq \exp\left(n_j \frac{2\pi i}{4}\right) x_j \quad (4.7)$$

with

$$(n_0, n_3, n_4, n_5) = m_0(1, 1, 1, 1) + m_2(0, 1, -1, 0) + m_3(0, 1, 0, -1). \quad (4.8)$$

We stress that ζ , defined in (3.16), is invariant under the identifications (4.1) so that the change of variables (3.14) is one to one.

⁷Although $b_1 = 0$ will be of interest for our work, this is not a limitation: see footnote 10 on page 21.

4.2 Description and fibrations of $X_{24}^*[1, 1, 2, 8, 12]$

As a second example, we start from the polynomials of degree 24 in the variables x_1, \dots, x_5 with weights 1, 1, 2, 8, 12, respectively, which is in the class (3.12) with $K = 12$ and $k_3 = 1$, $k_4 = 4$, $k_5 = 6$. As mentioned before, in section 3.1, we impose the global identifications (3.1). This leads to a Calabi–Yau manifold with three complex structure moduli. The generic polynomial compatible with the identification group G contains 11 arbitrary coefficients:

$$\begin{aligned}
W^{(2)} &= \frac{1}{24}(b_1x_1^{24} + b_2x_2^{24}) + \frac{b_3}{12}x_3^{12} + \frac{b_4}{3}x_4^3 + \frac{b_5}{2}x_5^2 \\
&\quad - \psi_0 x_1x_2x_3x_4x_5 - \frac{1}{6}\psi_1 (x_1x_2x_3)^6 - \frac{1}{12}\psi_s (x_1x_2)^{12} \\
&\quad - \frac{1}{4}\psi_3 (x_1x_2x_3x_4)^2 - \frac{1}{4}\psi_4 (x_1x_2x_3)^4 x_4 - \frac{1}{3}\psi_5 (x_1x_2x_3)^3 x_5 . \tag{4.9}
\end{aligned}$$

Again we will take $b_1 = b_2 = B$ and use the form (3.15).

4.2.1 The Calabi–Yau as a $K3$ fibration

The general fibration scheme of section 3.3 then gives

$$\begin{aligned}
W^{(2)} &= \frac{B'}{12}x_0^{12} + \frac{b_3}{12}x_3^{12} + \frac{b_4}{3}x_4^3 + \frac{b_5}{2}x_5^2 - \psi_0 x_0x_3x_4x_5 - \frac{1}{6}\psi_1 (x_0x_3)^6 \\
&\quad - \frac{1}{4}\psi_3 (x_0x_3x_4)^2 - \frac{1}{4}\psi_4 (x_0x_3)^4 x_4 - \frac{1}{3}\psi_5 (x_0x_3)^3 x_5 . \tag{4.10}
\end{aligned}$$

In this case the identification group that restricts the available deformations to those listed above acts on the homogeneous coordinates as follows:

$$x_j \simeq \exp(n_j \frac{2\pi i}{12}) x_j \tag{4.11}$$

with

$$(n_0, n_3, n_4, n_5) = m_0(1, 1, 4, 6) + m_2(-1, 1, 0, 0) . \tag{4.12}$$

The group G is as in (3.13) with $K = 12$ and $G' = \mathbf{Z}_6$ (as $m_0 = m_2 = 6$ gives the identity). The gauge transformations on the moduli space are induced by redefinitions

$$\begin{aligned}
\tilde{x}_0 &= \lambda_0 x_0 , & \tilde{x}_4 &= \lambda_4 x_4 + \lambda'_4 (x_0 x_3)^2 , \\
\tilde{x}_3 &= \lambda_3 x_3 , & \tilde{x}_5 &= \lambda_5 x_5 + \lambda'_5 x_0 x_3 x_4 + \lambda''_5 (x_0 x_3)^3 ,
\end{aligned} \tag{4.13}$$

so that the moduli space of the fibre is 2-complex dimensional. The polynomial is invariant in the sense that

$$W^{(2)}(\tilde{x}; B', b, \psi) = W^{(2)}(x; \tilde{B}', \tilde{b}, \tilde{\psi}) , \tag{4.14}$$

where

$$\tilde{B}' = B' \lambda_0^{12} ; \quad \tilde{b}_3 = b_3 \lambda_3^{12} ; \quad \tilde{b}_4 = b_4 \lambda_4^3 ; \quad \tilde{b}_5 = b_5 \lambda_5^2$$

$$\begin{aligned}
\tilde{\psi}_0 &= \psi_0 \lambda_{03} \lambda_4 \lambda_5 - b_5 \lambda'_5 \lambda_5 \\
\tilde{\psi}_1 &= \psi_1 \lambda_{03}^6 - 3b_5 \lambda_5'^2 - 2b_4 \lambda_4'^3 + 6\lambda_5'' \lambda'_4 \lambda_{03} \psi_0 + \frac{3}{2} \lambda_4'^2 \lambda_0^2 \lambda_3^2 \psi_3 + \frac{3}{2} \lambda'_4 \lambda_{03}^4 \psi_4 + 2\lambda_5'' \lambda_{03}^3 \psi_5 \\
\tilde{\psi}_3 &= \psi_3 (\lambda_{03} \lambda_4)^2 - 2b_5 \lambda_5'^2 - 4b_4 \lambda_4' \lambda_4^2 + 4\lambda_5' \lambda_{03} \lambda_4 \psi_0 \\
\tilde{\psi}_4 &= \psi_4 \lambda_{03}^4 \lambda_4 - 4b_4 \lambda_4'^2 \lambda_4 \psi_0 + 4\lambda_5'' \lambda_{03} \lambda_4 \psi_0 + 2\lambda_4' \lambda_{03}^2 \lambda_4 \psi_3 + 4\lambda_5' (\lambda_4' \lambda_{03} - b_5 \lambda_5'' + \frac{1}{3} \lambda_{03}^3 \psi_5) \\
\tilde{\psi}_5 &= (\psi_5 \lambda_{03}^3 - 3b_5 \lambda_5'' + 3\lambda_4' \lambda_{03} \psi_0) \lambda_5 ,
\end{aligned} \tag{4.15}$$

where $\lambda_{03} = \lambda_0 \lambda_3$. Introducing the auxiliary combinations

$$\begin{aligned}
I_0 &= \psi_3 + 2 \frac{\psi_0^2}{b_5} ; & I_1 &= \psi_4 + \frac{I_0^2}{4b_4} + \frac{4}{3} \frac{\psi_0 \psi_5}{b_5} , \\
I_2 &= \psi_1 + \frac{3}{8} \frac{I_0 I_1}{b_4} - \frac{1}{32} \frac{I_0^3}{b_4^2} + \frac{1}{3} \frac{\psi_5^2}{b_5} ,
\end{aligned} \tag{4.16}$$

we parametrize the moduli space with the invariants

$$\nu_1 = I_1^3 (B' b_3 b_4)^{-1} ; \quad \nu_2 = I_2^2 (B' b_3)^{-1} . \tag{4.17}$$

For most of the paper we will use the gauge

$$b_3 = b_4 = b_5 = 1 ; \quad \psi_3 = \psi_4 = \psi_5 = 0 , \tag{4.18}$$

which is also the one used in earlier work. For later reference we give the polynomial in this gauge,

$$W^{(2)}(x; B', \psi_0, \psi_1) = \frac{1}{12} (B' x_0^{12} + x_3^{12}) + \frac{1}{3} x_4^3 + \frac{1}{2} x_5^2 - \psi_0 x_0 x_3 x_4 x_5 - \frac{1}{6} \psi_1 x_0^6 x_3^6 , \tag{4.19}$$

and the expressions for the invariants,

$$\begin{aligned}
I_0 &= 2\psi_0^2 ; & I_1 &= \psi_0^4 , & I_2 &= \psi_1 + \frac{1}{2} \psi_0^6 ; \\
\nu_1 &= \psi_0^{12} / B' , & \nu_2 &= \left(\psi_1 + \frac{1}{2} \psi_0^6 \right)^2 / B' .
\end{aligned} \tag{4.20}$$

The remaining projective transformations on the moduli space coordinates are as in (3.19) with $K = 12$, $a_0 = 1$ and $a_1 = 6$.

With this gauge choice there is, however, a remaining discrete transformation identifying

$$(\psi_0^6, \psi_1) \sim (-\psi_0^6, \psi_1 + \psi_0^6) . \tag{4.21}$$

For some purposes, the alternative gauge choice

$$b_3 = b_4 = b_5 = 1 ; \quad \psi_0 = \psi_3 = \psi_5 = 0 , \tag{4.22}$$

is more convenient: that choice fixes the gauge completely. Note that in this gauge ψ_4 and ψ_1 are I_1 and I_2 and thus according to (4.20) correspond to ψ_0^4 and $(\frac{1}{2} \psi_0^6 + \psi_1)$ in the gauge (4.18).

The CY has a \mathbb{Z}_2 symmetry, which is most clearly exhibited in the alternative gauge as $x_5 \rightarrow -x_5$. When one of the invariants ν_i vanishes, this symmetry is enhanced. If ν_1 vanishes, which in the alternative gauge corresponds to $\psi_4 = 0$, then the symmetry becomes \mathbb{Z}_6 , represented as $x_3 \rightarrow e^{2\pi i/6} x_3$. This includes the above-mentioned \mathbb{Z}_2 as $x_3 \rightarrow -x_3$ is by (4.12) with $m_0 = m_2 = 3$ the same as $x_5 \rightarrow -x_5$. If $\nu_2 = 0$ (or $\psi_1 = 0$ in this gauge), the symmetry is enhanced to \mathbb{Z}_4 , represented by $x_3 \rightarrow e^{2\pi i/4} x_3$.

This fibration has been used in [2] to develop the reduction of the CY manifold, in the neighbourhood of a singular point in its moduli space. In that neighbourhood the $K3$ fibre is seen to degenerate into an ALE space. We will continue to work without taking this singular limit at this stage, and therefore will not approximate the $K3$ fibre as an ALE space. Instead, we develop additional techniques to work with the $K3$ exactly. One of these techniques is a further fibration of the $K3$ itself.

4.2.2 The $K3$ as a torus fibration

In this example the $K3$ manifold itself is an elliptic fibration. Actually, it can be fibred further in two different ways. The possibility of these fibrations can be seen from toric geometry considerations (see, for instance, [32]). To this end, we construct the (reflexive) polyhedron that describes this manifold. The following variables are invariant under projective and global identifications:

$$\xi = \left(\frac{x_3}{x_0}\right)^6 ; \quad x = \frac{x_4}{y_0^2} ; \quad y = \frac{x_5}{y_0^3} , \quad (4.23)$$

where the introduction of

$$y_0 = x_0 x_3 \quad (4.24)$$

and ξ again follows the general pattern of section 3.3, and the other variables are introduced to write the Laurent polynomial defining the manifold in a standard form:

$$\begin{aligned} \frac{W^{(2)}}{x_0 x_3 x_4 x_5} &= -\psi_0 - \frac{1}{3}\psi_5 x^{-1} + \frac{1}{3}b_4 x^2 y^{-1} - \frac{1}{4}\psi_4 y^{-1} - \frac{1}{4}\psi_3 x y^{-1} + \frac{1}{2}b_5 x^{-1} y \\ &\quad - \frac{1}{6}\psi_1 x^{-1} y^{-1} + \frac{1}{12}b_3 \xi x^{-1} y^{-1} + \frac{1}{12}B' \xi^{-1} x^{-1} y^{-1} . \end{aligned} \quad (4.25)$$

From this expression, we read off the polyhedron in figure 1. Fibrations of the $K3$ correspond to any 2-plane in this 3-dimensional picture on which the restriction of the polyhedron is itself reflexive, which implies that it should include a central point. This is clearly the case for the plane of the drawing (orthogonal to the ξ -axis), which corresponds to a first elliptic fibration, with ξ parametrizing the base. The second possibility is the plane perpendicular to the picture through the line of b_5 and ψ_1 . The base manifold in this case can be parametrized by x .

The first fibration takes ξ as the coordinate on the base, and the fibre is a torus presented as $X_6[1, 2, 3]$, in the projective space of $\{y_0, x_4, x_5\}$. Using the gauge (4.18) the polynomial takes the form

$$W^{(2)} = \frac{1}{6}B'' y_0^6 + \frac{1}{3}x_4^3 + \frac{1}{2}x_5^2 - \psi_0 y_0 x_4 x_5 , \quad (4.26)$$

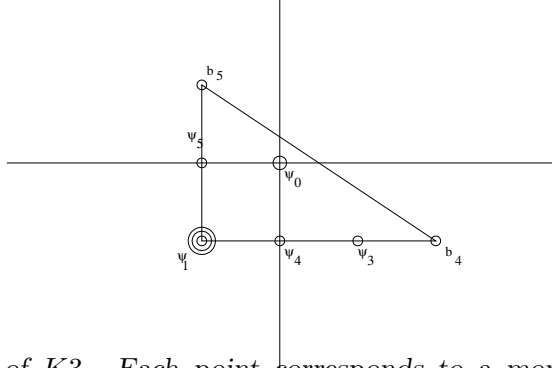


Fig. 1: The polyhedron of $K3$. Each point corresponds to a monomial in (4.25). The axes correspond to the powers of x and y in the monomials, while the ξ -axis is orthogonal to the plane of the drawing. The vertices corresponding to the B' and b_3 term are above and below the ψ_1 point.

where

$$B'' = \frac{1}{2} \left(\frac{B'}{\xi} + \xi - 2\psi_1 \right) . \quad (4.27)$$

The second fibration takes x as the coordinate of the base. In the alternative gauge (4.22) the $K3$ -polynomial turns into

$$W^{(2)} y_0^{-6} = \frac{1}{2} y^2 + \frac{1}{12} \left(\xi + \frac{B'}{\xi} \right) + \frac{1}{6} P(x) , \quad (4.28)$$

where

$$P(x) = 2x^3 - \frac{3}{2} \psi_4 x - \psi_1 . \quad (4.29)$$

4.3 Singularities

The rigid limit of the supergravity theory based on a Calabi–Yau manifold will correspond to the description of the behaviour of the theory in the vicinity of a certain singularity in the moduli space. At singular loci in the moduli space the CY manifold develops a singularity⁸. Hence we will first describe the singularity structure of the two CY 3-folds introduced above, relying on their $K3$ -fibred structure. Therefore we will first study the singularity structure on the $K3$ -fibre and then examine the total CY space. In the second example, we will make use of the fact that the $K3$ fibre itself is an elliptic fibration.

The rigid-limit singularity corresponds [16, 1] to the point at infinity on a line in moduli space where the CY develops a conifold singularity. At this point, the CY manifold becomes singular on the whole \mathbb{P}^1 base space of the fibration. This is the situation we are interested in.

In addition to the singularity structure itself, for both examples we will include a first look at the neighbourhood of such a singularity. This will be given by not only making an

⁸Recall that singularities occur when at the same time $W = 0$ and $dW = 0$. Since we are using homogeneous coordinates the above conditions are satisfied if $\frac{\partial W}{\partial x_i} = 0$.

expansion around the rigid-limit singular point in moduli space, but also by approximating the $K3$ fibre by an ALE space. Although we stress that this approximation will not be used in the remainder of this paper, we include it to make contact with [2], and also because it provides a useful picture to direct the ideas.

4.3.1 Singularities of $X_8^*[1, 1, 2, 2, 2]$

Singularities in the $K3$. We start from the defining polynomial of (4.6), with (4.5) giving the relevant modulus. Imposing the conditions for the simultaneous vanishing of derivatives of $W^{(1)}$, (4.4), we find, the following special points in $K3$ moduli space:

- a) $\psi_0^4 = B'$, i.e. $z = -1$. This is the conifold singularity. The point on the $K3$ where the singularity develops is $(x_0, x_3, x_4, x_5) \sim (1, \psi_0, \psi_0, \psi_0)$ up to identifications (4.1). The monodromy of the periods around $z = -1$ is diagonalizable (see after (5.15)).
- b) $B' = 0$, i.e.⁹ $z = 0$. Around this point the monodromy matrix is not diagonalizable and the singularity is referred to as ‘the large complex structure limit’. The point on the $K3$ at which the singularity develops is $\sim (x_0, 0, 0, 0)$ where x_0 can be scaled to 1.

Singularities in the Calabi–Yau. Using the results on singularities of the $K3$ fibre, we now examine the Calabi–Yau 3-fold. From (3.18) we find that each of the above $K3$ fibre singularities occurs at two points in the ζ -plane: $B' = 0$ (l.c.s.) and $B' = \psi_0^4$ (conifold) occur, respectively, at

$$e_0^\pm = \tilde{\psi}_s \pm \sqrt{\tilde{\psi}_s^2 - 1}; \quad e_1^\pm = \tilde{u} \pm \sqrt{\tilde{u}^2 - 1}, \quad (4.30)$$

where we have introduced the gauge-invariant combinations

$$\tilde{\psi}_s = \frac{\psi_s}{B}; \quad \tilde{u} \equiv \frac{\psi_s + \psi_0^4}{B}. \quad (4.31)$$

Note that, in terms of these, the $K3$ modulus is given by

$$z = \frac{\tilde{\psi}_s - \frac{1}{2}(\zeta + \frac{1}{\zeta})}{\tilde{u} - \tilde{\psi}_s}. \quad (4.32)$$

In the CY, ζ is an additional coordinate, and singularities occur if, beside the $K3$ fibre being singular, $\partial_\zeta W^{(1)} = 0$. This gives $\partial_\zeta B' = 0$, which imposes that $\zeta^2 = 1$ or $B = 0$. Thus the discriminant becomes

$$\Delta_{CY} \propto B^2 (B^2 - \psi_s^2) (B^2 - (\psi_s + \psi_0^4)^2) = B^6 (e_0^+ - e_0^-)^2 (e_1^+ - e_1^-)^2. \quad (4.33)$$

⁹There is some danger in this identification, since the proper treatment requires desingularization of the CY ambient space. This has been taken into account in the analysis of the CY singularity structure of the next paragraph.

We now take into account the desingularization mentioned in the previous paragraph, and also (temporarily) reinstate the b_i parameters, see (4.3), to retain the homogeneous description of the moduli space. The singular loci, the three components solving $\Delta_{CY} = 0$, are then given by

$$\begin{aligned} S_0 : \quad & b_1 b_2 b_3 b_4 b_5 = 0 \ , \\ S_1 : \quad & (b_3 b_4 b_5 \psi_s + \psi_0^4)^2 = b_1 b_2 (b_3 b_4 b_5)^2 \ , \\ S_b : \quad & \psi_s^2 = b_1 b_2 \ . \end{aligned} \tag{4.34}$$

The first locus has many components, but naturally splits into $b_1 b_2 = 0$ and $b_3 b_4 b_5 = 0$. We will only be interested in the former, and therefore limit the analysis to $b_3 b_4 b_5 \neq 0$: we will then choose the gauge $b_3 = b_4 = b_5 = 1$, as before. Also, we will largely ignore S_b in the following since the rigid limit in which we are interested in is the intersection of S_0 and S_1 .

We now indicate the location of the singularity on the CY for S_1 and S_0 . Taking into account the identifications (4.1), we find that $x_3 = x_4 = x_5$, and up to rescalings according to the weights in (3.12) we have:

$$\begin{aligned} S_1 - S_1 \cap S_0 : \quad & (x_1^8, x_2^8, x_3) \sim (1, 1, \psi_0) \\ S_0 - S_1 \cap S_0 : \quad & (x_1^8, x_2^8, x_3) \sim (1, 0, 0) \text{ if } b_1 = 0 \\ & (x_1^8, x_2^8, x_3) \sim (0, 1, 0) \text{ if } b_2 = 0 \\ S_1 \cap S_0 : \quad & \text{as } S_0 - S_1 \cap S_0, \text{ with in addition} \\ & (x_1^8, x_2^8, x_3) \sim (\zeta, \zeta^{-1}, \psi_0) \text{ if } b_1 = 0 = b_2 \ . \end{aligned} \tag{4.35}$$

Rigid limit. For $b_1 = 0 = b_2$ the CY becomes singular along a whole \mathbb{P}_1 , (with inhomogeneous coordinate ζ), that is the base space used for the fibration of the CY. All singular points in (4.35) can be parametrized as $(\zeta, \zeta^{-1}, \psi_0)$, where $\zeta = \pm 1$ correspond to the generic point on S_1 , and $\zeta = 0$ and $\zeta = \infty$ similarly correspond to S_0 . The rigid-limit point of interest is most easily described by using $b_1 = 0 = b_2$. The vicinity of this point can be explored by putting $b_1 = b_2 = B$, and we will use this simplification in all of what follows¹⁰.

ALE expansion. To see how the ALE approximation of the $K3$ fibre arises in the vicinity of the rigid-limit point in moduli space, we first fix coordinates on the CY manifold. At $B = 0$, the position of the singularity in the $K3$ fibre is at $(x_0, x_3, x_4, x_5) \sim (1, \psi_0, \psi_0, \psi_0)$. We choose the gauge $x_0 = 1$, and will approach the limit by keeping ψ_0 fixed while letting B become small. The following expansion parametrizes the neighbourhood of the singular point in moduli space:

$$B = 2\epsilon \ , \quad \psi_s + \psi_0^4 = 2\epsilon\tilde{u} \ , \tag{4.36}$$

¹⁰The rigid limit can also be explored by starting from the values $b_1 = 1, b_2 = 0$, in which case the singularity expressed in the x -coordinates is given by $(x_1, x_2, x_3, x_4, x_5) = (0, 1, 0, 0, 0)$. In this case one may fix $x_2 = 1$ as a gauge choice. The region around the singular point on the CY is parametrized to first order by a (common) value of $x_i, i = 3, 4, 5$ proportional to x_1 , which reinstates the coordinate ζ . To capture all the structure of the rigid limit, this is not sufficient however: the expansion has to be continued to higher order. This makes it less transparent, though equivalent to the one we give explicitly in the next paragraph, as can be seen by making a transformation of coordinates to map $b_1 = \epsilon, b_2 = \epsilon$ to $b_1 = 1, b_2 = \epsilon^2$.

where \tilde{u} , defined in (4.31), is kept fixed¹¹. Then the powers of ϵ in the expansion of the other variables around their critical values can be determined by examining explicitly the limiting form of the defining polynomial (4.6), and adjust¹² the powers of ϵ so that as many terms as possible are contributing in leading order in ϵ . The expansion that turns out to preserve the relevant structure of the fibre in the neighbourhood of its singular point is

$$\begin{aligned} x_3 &= \psi_0 + \sqrt{\epsilon} \left(\sqrt{\frac{1}{3}}y_1 - \sqrt{\frac{1}{6}}y_2 \right) \\ x_4 &= \psi_0 + \sqrt{\epsilon} \left(\sqrt{\frac{1}{3}}y_1 + \frac{1}{2\sqrt{6}}y_2 - \frac{1}{2\sqrt{2}}y_3 \right) \\ x_5 &= \psi_0 + \sqrt{\epsilon} \left(\sqrt{\frac{1}{3}}y_1 + \frac{1}{2\sqrt{6}}y_2 + \frac{1}{2\sqrt{2}}y_3 \right), \end{aligned} \tag{4.37}$$

in the gauge $x_0 = 1$, and the ALE limit of the fibre is given by

$$W_{ALE}^{(1)} = \frac{1}{2}\epsilon \left[\frac{1}{2}(\zeta + \frac{1}{\zeta}) + y_1^2 + y_2^2 + y_3^2 - \tilde{u} \right], \tag{4.38}$$

which shows the A_1 singularity structure.

4.3.2 Singularities of $X_{24}^*[1, 1, 2, 8, 12]$

The double fibration can be used to derive the singularity structure of the 2-modulus Calabi–Yau manifold $X_{24}^*[1, 1, 2, 8, 12]$ in a simple way.

Torus singularities. Working out the conditions for the simultaneous vanishing of derivatives of (4.26) we find:

- a) $B'' = \psi_0^6$
- b) $B'' = 0$

¹¹The coordinate \tilde{u} may be introduced on the grounds that the ratio $(\psi_s + \psi_0^4)/B$ is a gauge-invariant parameter of the moduli space (in the sense discussed in section 4.1) and left unspecified for the intersection $S_0 \cap S_1$. Alternatively, one may study the resolution of the singular point in moduli space by blowup as in [1, 4].

¹²Some care is needed in this procedure. In principle, one should show that the omitted terms disappear by changes of coordinates which are locally well defined. For example, for $W = x^2 + x^3 + y^2$: the x^3 term can be omitted because of the coordinate change $x' = x(1+x)^{1/2}$, which is well defined around $x = 0$. Consider, however, $W = x^3 + x^2 + 2xy + y^2$. Deleting the x^3 on the grounds that the ‘more relevant’ x^2 is present would also be too naive: after the change of coordinates $y' = y + x$, the polynomial is $W = x^3 + y'^2$, which shows that the x^3 term *is* relevant.

$K3$ singularities. Now we look at the $K3$ as an elliptic fibration with the above torus as fibre. The fibre is singular on the ξ base space at the following points in the $K3$ base:

- a) $\xi_{\alpha\pm} = (\psi_1 + \psi_0^6) \pm \sqrt{(\psi_1 + \psi_0^6)^2 - B'}$. The subscript $+$ is for the solution outside $|\xi| = \sqrt{|B'|}$, $-$ for the one inside this circle.
- b) $\xi_{\beta\pm} = \psi_1 \pm \sqrt{\psi_1^2 - B'}$.

Now the total $K3$ space is singular if in addition one has $\frac{\partial B'}{\partial \xi} = 0$. This implies $\xi^2 = B'$ and colliding singularities, i.e.

- a1) $B' = (\psi_1 + \psi_0^6)^2$ and thus $\xi_{\alpha+} = \xi_{\alpha-} = \psi_1 + \psi_0^6$.
- a2) $B' = \psi_1^2$ and thus $\xi_{\beta+} = \xi_{\beta-} = \psi_1$.
- b) $B' = 0$ and thus $\xi_{\alpha-} = \xi_{\beta-}$.

The cases a1) and a2) are identified by the gauge transformation (4.21). It will turn out that the monodromy matrices around this singularity are diagonalizable, and therefore we will refer to these as ‘conifold points’. Those around b) are not diagonalizable; they are referred to as the ‘large complex structure limit’.

Case a) generically exhibits an A_1 singularity. At the points where the manifold (both the $K3$ and the CY, in fact) has an enhanced symmetry however (see section 4.2.1), the character of the singularity changes. In the gauge we use, these points correspond to the intersections of a1) and a2). The change in the two cases is as follows:

- a,i) : $\nu_1 = 0$: $\psi_0 = 0$ and $B' = \psi_1^2$ or $\xi_{\alpha+} = \xi_{\alpha-} = \xi_{\beta+} = \xi_{\beta-}$. This is an A_2 singularity. The singularity on the $K3$ is a single point.
- a,ii) : $\nu_2 = 0$: $\psi_0^6 = -2\psi_1$ and $B' = \psi_1^2$ or $\xi_{\alpha+} = \xi_{\alpha-} = -\xi_{\beta+} = -\xi_{\beta-}$. This is an $A_1 \times A_1$ singularity. There are two singular points on the $K3$ manifold.

CY singularities. Let us now consider the Calabi–Yau 3-fold as a $K3$ -fibration with the above $K3$ as typical fibre. The above analysis says that the fibre has a singularity on ζ -base space when $B' = \frac{1}{2}(\zeta + 1/\zeta) - \psi_s$ satisfies a1) or a2) or b). The total space (i.e. the CY 3-fold) is singular when moreover $\frac{\partial B'}{\partial \zeta} = 0$, which implies $\zeta = \pm 1$ or $B = 0$. In the latter case, it is not difficult to see that the CY is singular without any further conditions. Summarizing, we obtain¹³

$$\begin{aligned}
 S_{a1}^{\pm} : (\psi_0^6 + \psi_1)^2 + \psi_s &= \pm B \\
 S_{a2}^{\pm} : \psi_1^2 + \psi_s &= \pm B \\
 S_b^{\pm} : \psi_s &= \pm B \\
 S_0 : B &= 0 .
 \end{aligned} \tag{4.39}$$

¹³If one does not fix $b_1 = b_2 = B$ from the start, the right-hand side in these is, in fact, $\sqrt{b_1 b_2}$, hence the signs. See also, *mutatis mutandis*, footnote 10.

Rigid limit(s). Generically, the singularities on the CY are isolated, i.e. they occur for a discrete set of values (usually a single one) of ζ and x_i . If $B = 0$, however, $W^{(2)}$ becomes independent of ζ and the singularity on the CY becomes a \mathbb{P}^1 , parametrized by ζ (the point at infinity corresponding to $x_2 = 0$): if the fibre is singular, it is singular over the *whole* base space of the fibration. The intersection points of S_0 with S_{a_1} and S_{a_2} correspond to rigid limits. We will treat in detail the point with the A_2 singularity, but will also comment on the $A_1 \times A_1$ point.

ALE expansion. In the neighbourhood of the singular point one may [2] approximate the $K3$ fibre by an ALE space. We first fix coordinates on the CY manifold. At the A_2 point in moduli space

$$A_2 \text{ point: } B = 0, \quad \psi_0 = 0, \quad \psi_s = -\psi_1^2, \quad (4.40)$$

the position of the singularity in the $K3$ fibre is at $(x_0, x_3, x_4, x_5) \sim (1, (-\psi_s)^{1/12}, 0, 0)$. We choose the gauge $x_0 = 1$, and approach the limit by keeping ψ_s fixed. The deviations from the singular point in the moduli space can be parametrized as

$$B = 2\epsilon; \quad \psi_0^6 \psi_1 = \epsilon \tilde{u}_0^6; \quad \psi_1^2 + \psi_s = \epsilon \tilde{u}_1. \quad (4.41)$$

where \tilde{u}_i are kept fixed. Then the powers of ϵ in the expansion of the other variables around their critical values can be determined by examining explicitly the limiting form of the defining polynomial $W^{(2)}$, and adjusting the powers of ϵ so that as many terms as possible contribute in leading order in ϵ . The relevant structure in the fibre is preserved by setting

$$\begin{aligned} x_3 &= (\psi_1)^{1/6} \left(1 + \left(\frac{\epsilon}{6} \right)^{1/2} \frac{y_3}{\psi_1} \right) \\ x_4 &= (\epsilon)^{1/3} (y_4 + \frac{1}{2} \tilde{u}_0^2) \\ x_5 &= \sqrt{\epsilon} \left(y_5 + \tilde{u}_0 (y_4 + \frac{1}{2} \tilde{u}_0^2) \right). \end{aligned} \quad (4.42)$$

The relevant terms in the expansion of $W^{(2)}$ are

$$W_{ALE}^{(2)} = \epsilon \left[\frac{1}{12} \left(\zeta + \frac{1}{\zeta} \right) + \frac{y_3^2}{2} + \frac{y_5^2}{2} + \frac{y_4^3}{3} - \frac{\tilde{u}_0^4}{4} y_4 - \frac{\tilde{u}_1 + \tilde{u}_0^6}{12} \right], \quad (4.43)$$

which shows the A_2 singularity structure.

5 Periods, monodromies and intersection matrix in the first example

In this section we consider $X_8^*[1, 1, 2, 2, 2]$. We compute periods and intersection matrices in an integral basis, constructing the results on the CY manifold in terms of the corresponding ones on the $K3$ fibre. We will thus have first to determine an integral basis of (transcendental) $K3$ periods. We will, as done in [23] for the CY (see appendix C), compute the *fundamental* period by explicit integration over an integer homology cycle and obtain the other periods by

analytic continuation. We also use explicit solutions of the Picard–Fuchs equations, which by itself, while providing exact expressions, does not lead to an integer basis. The information about the fundamental cycle and on the PF solutions together allow us to determine a basis of periods for which the monodromies and the intersection matrix are integer-valued.

We will then construct a basis of CY 3-cycles by fibring the $K3$ 2-cycles (associated to the above periods) as indicated in section 3.4. We want to determine the structure of the monodromies, which are the essential ingredients for the rigid limit, and in addition to obtain exact expressions of the periods that could be used in the future to analyse the expansion of the full supergravity action.

The $K3$ fibration of this CY manifold was described in detail in section 3 and we refer the reader to that section for the relevant definitions and formulae. Here we just recall that the potential of this manifold can be written as the potential for a $K3$ manifold $X_4^*[1, 1, 1, 1]$:

$$W^{(1)} = \frac{1}{4} \left(B' x_0^4 + x_3^4 + x_4^4 + x_5^4 \right) - \psi_0 x_0 x_3 x_4 x_5 . \quad (5.1)$$

where the complex structure modulus $z = -B'/\psi_0^4$, see (4.5), depends on the coordinate ζ of the \mathbb{P}^1 base, see (3.18).

Let us now study cycles and periods of the $K3$ fibre itself.

5.1 Cycles and periods of the $K3$ fibre

As discussed in [21] (and see (A.4)), the one-dimensional moduli space of complex structures is $\Gamma_D \backslash O(2, 1) / O(2)$. The $O(2, 1)$ vectors (generalized ‘Calabi–Visentini coordinates’) are the periods $\vartheta_I(z)$ ($I = 0, 1, 2$) of the $(2, 0)$ form computed on an integer basis of transcendental cycles. They are subject to the quadratic constraint (3.10), involving the inverse of the intersection matrix \mathcal{I}_{IJ} of the transcendental cycles c_I , which has signature $(2, 1)$. The discrete group Γ_D , the invariance group of the lattice of transcendental cycles, is generated by the monodromies of the periods around the singular points in the z -plane.

Now we explicitly construct a basis of periods $\hat{\vartheta}_I(z)$ with integer-valued monodromies and intersection matrix which therefore admit the above interpretation as periods over an integer basis of the transcendental lattice.

The fundamental period. We present the construction of the fundamental period of the $K3$ fibre following closely the steps in [23] where the corresponding period of the quintic CY manifold was defined and determined. One starts considering an integer homology cycle for large complex structure ψ_0

$$b_0 = \left\{ (x_0, x_3, x_4, x_5) \mid x_5 = \text{const.}, |x_0| = |x_3| = \delta, \right. \\ \left. x_4 \text{ the solution to } W^{(1)}(x) = 0 \text{ that tends to 0 as } \psi_0 \rightarrow \infty \right\} / |G'| . \quad (5.2)$$

We do not restrict the range of x_i , and therefore factor out $|G'| = 16$, the number of elements in the discrete identification group G' , as they act non-trivially on b_0 . We thus obtain an elementary cycle.

The holomorphic 2-form $\Omega^{(2,0)}$ of $X_4^*[1, 1, 1, 1]$ can be expressed via the Griffith map (3.2). We use here a rescaled 2-form

$$\hat{\Omega}^{(2,0)} = \psi_0 \Omega^{(2,0)} = \frac{|G'| \psi_0}{(2\pi i)^3} \int \frac{\omega_{K3}}{W^{(1)}}, \quad (5.3)$$

where ω_{K3} is given in (3.21). This choice ensures that $\lim_{z \rightarrow 0} \hat{\vartheta}_0(z) = 1$. Then the fundamental period $\hat{\vartheta}_0$ is (see [23], section 6)

$$\begin{aligned} \hat{\vartheta}_0(z) &\equiv \int_{b_0} \hat{\Omega}^{(2,0)} \\ &= -\frac{\psi_0}{(2\pi i)^3} \int_{\gamma_0 \times \gamma_3 \times \gamma_4} \frac{x_5 dx_0 dx_3 dx_4}{W^{(1)}} = -\frac{\psi_0}{(2\pi i)^4} \int_{\gamma_0 \times \gamma_3 \times \gamma_4 \times \gamma_5} \frac{dx_0 dx_3 dx_4 dx_5}{W^{(1)}}, \end{aligned} \quad (5.4)$$

where γ_i is the loop $|x_i| = \delta$. The second equality has been obtained by inserting unity in the form $(1/2\pi i) \int_{\gamma_5} (dx_5/x_5)$ [23]. Finally, writing $W^{(1)} = \hat{W}^{(1)} - \psi_0 x_0 x_3 x_4 x_5$, expanding in powers of $\hat{W}^{(1)}/(\psi_0 x_0 x_3 x_4 x_5)$ and performing the Cauchy integrations, one obtains for large ψ_0 , i.e. for small¹⁴ z ,

$$\hat{\vartheta}_0 = \sum_{n=0}^{\infty} \frac{(4n)!}{n!^4} \left(\frac{1}{4}\right)^{4n} (-z)^n, \quad (|z| < 1). \quad (5.5)$$

Our aim is now to find the desired integral basis of periods $\hat{\vartheta}_I(z)$ via analytic continuation to $|z| > 1$ of the fundamental one $\hat{\vartheta}_0(z)$. In order to achieve this we have found it convenient to rewrite first the fundamental period in terms of the solutions of the Picard–Fuchs equation, discussed in detail in Appendix B. At that stage the analytic properties of $\hat{\vartheta}_0(z)$ can be easily determined since the PF solutions are given by quadratic combinations of hypergeometric functions whose asymptotic forms are well known.

An integral basis via the Picard–Fuchs equation and analytic continuation. Making reference to the results presented in Appendix B, we start with the generic expression of the periods $\hat{\vartheta}$, thought of as solutions of the appropriate PF equation,

$$\hat{\vartheta}(z) = C_{\alpha\beta} U_{\alpha}(z) U_{\beta}(z), \quad (\alpha, \beta = 1, 2). \quad (5.6)$$

where $U_{1,2}$ are two linearly independent solutions of the hypergeometric equation of parameters $\{\frac{1}{8}, \frac{3}{8}, 1\}$, and $C_{\alpha\beta}$ are arbitrary constants.

We now want to express the integer period $\hat{\vartheta}_0(z)$, defined for $|z| < 1$ in (5.5), in terms of U_1 and U_2 . These solutions in the neighbourhood of $z = \infty$ are given by

$$\begin{aligned} U_1(z) &= \frac{\Gamma(\frac{1}{8})\Gamma(\frac{5}{8})}{\Gamma(\frac{3}{4})} \left(\frac{1}{z}\right)^{\frac{1}{8}} F\left(\frac{1}{8}, \frac{1}{8}, \frac{3}{4}; -\frac{1}{z}\right), \\ U_2(z) &= \frac{\Gamma(\frac{3}{8})\Gamma(\frac{7}{8})}{\Gamma(\frac{5}{4})} \left(\frac{1}{z}\right)^{\frac{3}{8}} F\left(\frac{3}{8}, \frac{3}{8}, \frac{5}{4}; -\frac{1}{z}\right). \end{aligned} \quad (5.7)$$

¹⁴That the convergence radius of the series (5.5) is 1 can be seen using Stirling's formula for $n \rightarrow \infty$.

We consider them for $|z| > 1$ and $-\pi - \epsilon < \arg z < \pi - \epsilon$. Having defined $z^\alpha = e^{\alpha \log z}$ we have chosen the cuts of $\log z$ in $\arg(z) = \pm\pi - \epsilon$. Thus in the fundamental domain $z \rightarrow e^{i\pi}$ corresponds to $z \rightarrow -1^+$ ‘above the cut’, and $z \rightarrow e^{-i\pi}$ to $z \rightarrow -1^-$ ‘below the cut’.

In order to make contact with $\hat{\vartheta}_0(z)$ we analytically continue these solutions near $z = 0$, i.e. in the large complex structure limit of the $K3$. Using standard formulae for $|z| < 1$ and $-\pi - \epsilon < \arg z < \pi - \epsilon$ one has

$$\begin{aligned} U_1(z) &= \log\left(\frac{1}{z}\right) F\left(\frac{1}{8}, \frac{3}{8}, 1; -z\right) + \sum_{n=0}^{\infty} \frac{\left(\frac{1}{8}\right)_n \left(\frac{3}{8}\right)_n}{(n!)^2} h_{1,n} (-z)^n, \\ U_2(z) &= \log\left(\frac{1}{z}\right) F\left(\frac{1}{8}, \frac{3}{8}, 1; -z\right) + \sum_{n=0}^{\infty} \frac{\left(\frac{1}{8}\right)_n \left(\frac{3}{8}\right)_n}{(n!)^2} h_{2,n} (-z)^n, \end{aligned} \quad (5.8)$$

where

$$\begin{aligned} h_{1n} &= 2\psi(n+1) - \psi\left(n + \frac{1}{8}\right) - \psi\left(n + \frac{3}{8}\right) - \pi \cot\left(\frac{3}{8}\pi\right), \\ h_{2n} &= 2\psi(n+1) - \psi\left(n + \frac{1}{8}\right) - \psi\left(n + \frac{3}{8}\right) - \pi \cot\left(\frac{1}{8}\pi\right). \end{aligned} \quad (5.9)$$

Since the fundamental period has to be quadratic in $U_{1,2}$ and, as shown in (5.5), it has a regular behaviour for $z \rightarrow 0$, from the expressions in (5.8) we easily conclude that it must be proportional to $(U_1 - U_2)^2$. More precisely, by comparing explicitly the coefficients of the series expansions, we find

$$\hat{\vartheta}_0 = \frac{1}{4\pi^2} (U_1 - U_2)^2 = F^2\left(\frac{1}{8}, \frac{3}{8}, 1; -z\right). \quad (5.10)$$

At this point the knowledge of the asymptotic forms of the functions U_i for large values of z given in (5.7) allows us to obtain the desired continuation of $\hat{\vartheta}_0(z)$ in the region $|z| > 1$.

Once the expressions in (5.7) are introduced in (5.10) we find the analytic continuation of the fundamental period in the form $\sum_{k \in \mathbb{Z}_4} z^{\frac{k}{4}} R_k(z)$ with $R_k(z)$ regular functions. Due to the presence of the fourth roots $\hat{\vartheta}_0(z)$ is no longer single valued. We choose to have the cut running from $z = -1$ to $z = \infty$ and define for $k = 1, 2, 3$,

$$\hat{\vartheta}_k(z) \equiv \hat{\vartheta}_0(e^{-2\pi i k} z), \quad |z| > 1, \quad \pi(2k-1) < \arg z < \pi(2k+1). \quad (5.11)$$

We immediately obtain

$$\hat{\vartheta}_1 = \frac{i}{4\pi^2} (U_1 - iU_2)^2, \quad \hat{\vartheta}_2 = -\frac{1}{4\pi^2} (U_1 + U_2)^2, \quad \hat{\vartheta}_3 = -\frac{i}{4\pi^2} (U_1 + iU_2)^2. \quad (5.12)$$

Being connected by a \mathbb{Z}_4 transformation, the $\hat{\vartheta}_k$ satisfy $\sum_{k=0}^3 \hat{\vartheta}_k = 0$, and only three of them are independent, for instance the first three $\hat{\vartheta}_I$, $I = 0, 1, 2$. In the $\hat{\vartheta}_I$ basis, the \mathbb{Z}_4 monodromy, $z \rightarrow e^{2\pi i} z$ for z large, acts thus by definition as $\hat{\vartheta} \rightarrow \mathcal{M}_\infty \hat{\vartheta}$, with

$$\mathcal{M}_\infty = \begin{pmatrix} 0 & 1 & 0 \\ 0 & 0 & 1 \\ -1 & -1 & -1 \end{pmatrix}. \quad (5.13)$$

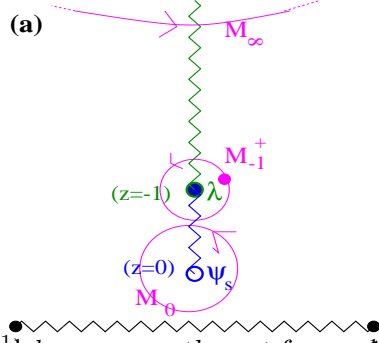


Fig. 2: Cuts in the $w = \frac{1}{2}(\zeta + \zeta^{-1})$ base space; the cut from -1 to 1 is associated to the ‘measure’ factor $\sqrt{1-w^2}$; the periods of the K3 fibre, of modulus $z(w)$ have a fourth-root cut from $z(\tilde{\psi}_s) \equiv 0$ to $z(\tilde{u}) \equiv -1$ and a logarithmic one to $z(\infty) \equiv \infty$; they have non-trivial monodromies along the indicated paths.

The analytic continuation of $\hat{\vartheta}_I(z)$ back to the region $|z| < 1$, $-\pi < \arg z < \pi$, obtained via (5.8), exhibits log and \log^2 cuts in the $\hat{\vartheta}_k$ periods with $k \neq 0$ ($\hat{\vartheta}_0$, is given by the regular expansion in (5.5)). Under $z \rightarrow e^{2\pi i} z$ with $|z| < 1$ we see from (5.8) that $U_\alpha \rightarrow U_\alpha - i(U_1 - U_2)$. Via (5.10, 5.12) this induces on the basis $\{\hat{\vartheta}_I\}$ the monodromy $\hat{\vartheta} \rightarrow \mathcal{M}_0 \hat{\vartheta}$ with

$$\mathcal{M}_0 = \begin{pmatrix} 1 & 0 & 0 \\ -1 & -1 & -1 \\ 6 & 4 & 3 \end{pmatrix}. \quad (5.14)$$

Since two different cuts depart from the conifold point $z = -1$ (see figure 2), in defining the monodromy at the conifold we have to specify the position of the basepoint of the small loop around $z = -1$. In both cases, i.e. if the starting point is ‘above’ or ‘below’ the cut, such a monodromy is obtained by combining the monodromies about $z = 0$ and $z = \infty$, but the order is different. If it is above (lower sign below) the cut, we have $\hat{\vartheta} \rightarrow \mathcal{M}_{-1}^\pm \hat{\vartheta}$, with

$$\mathcal{M}_{-1}^+ = \mathcal{M}_\infty^{-1} \mathcal{M}_0^{-1} = \begin{pmatrix} 0 & 1 & 0 \\ 1 & 0 & 0 \\ -3 & 3 & 1 \end{pmatrix}; \quad \mathcal{M}_{-1}^- = \mathcal{M}_0^{-1} \mathcal{M}_\infty^{-1} = \begin{pmatrix} -1 & -1 & -1 \\ 6 & 4 & 3 \\ -6 & -3 & -2 \end{pmatrix}. \quad (5.15)$$

The matrices \mathcal{M}_{-1}^\pm are diagonalisable with eigenvalues $(-1, 1, 1)$.

The condition (3.10) with (5.10), (5.12) determines the inverse intersection matrix \mathcal{I}^{IJ} up to a constant. In this basis of integer cycles, the intersection matrix \mathcal{I}_{IJ} has to be an integer, which implies that it is a multiple of

$$\mathcal{I} = \begin{pmatrix} 0 & 1 & -2 \\ 1 & 0 & 1 \\ -2 & 1 & 0 \end{pmatrix}. \quad (5.16)$$

Around $z = -1$ there is the vanishing cycle (above the cut) $\nu = \hat{\vartheta}_0 - \hat{\vartheta}_1$, which should have self-intersection -2 , which is the case with (5.16). One can then check that the Picard–Lefschetz formula (2.19) leads also to (5.15).

Expansion near the conifold. Now we want to obtain the expansion of the $K3$ periods $\hat{\vartheta}_I$ near the conifold singularity $z \rightarrow -1$. In order to do this we need consider the asymptotic expressions of the functions $U_{1,2}$ in the vicinity of¹⁵ $z = -1^+$ (or $z = -1^-$). This can be obtained in two steps, by first re-expressing U_1 and U_2 in terms of the basis

$$u_1(z) = 2\pi F\left(\frac{1}{8}, \frac{3}{8}, 1; -z\right), \quad u_2(z) = \frac{\Gamma(\frac{1}{8})\Gamma(\frac{3}{8})}{\Gamma(\frac{1}{2})} F\left(\frac{1}{8}, \frac{3}{8}, \frac{1}{2}; 1+z\right) \quad (5.17)$$

by comparing the U 's and the u 's in the neighbourhood¹⁶ of $z = 0$. The result is

$$U_1(z) = \sqrt{\frac{2-\sqrt{2}}{2}} e^{\frac{11\pi i}{8}} u_1 + u_2, \quad U_2(z) = -\sqrt{\frac{2+\sqrt{2}}{2}} e^{\frac{\pi i}{8}} u_1 + u_2. \quad (5.18)$$

The desired continuation to the neighbourhood of $z = -1^+$ is now obtained by the analytic continuation of u_1 , valid for $|\arg(1+z)| < \pi$, to this region:

$$u_{1(-1)}(z) = \frac{1}{\sqrt{2}} u_{2(-1)}(z) + 2\pi \frac{\Gamma(-\frac{1}{2})}{\Gamma(\frac{1}{8})\Gamma(\frac{3}{8})} (1+z)^{\frac{1}{2}} F\left(\frac{7}{8}, \frac{5}{8}, \frac{3}{2}; 1+z\right). \quad (5.19)$$

Substituting (5.19) into (5.18) one may rewrite the resulting expression as

$$\begin{aligned} U_1(z) &= K_1 \left[F\left(\frac{1}{8}, \frac{3}{8}, \frac{1}{2}; 1+z\right) - i(\sqrt{2}-1)(1+z)^{\frac{1}{2}} F\left(\frac{7}{8}, \frac{5}{8}, \frac{3}{2}; 1+z\right) \right], \\ U_2(z) &= K_1 \left[e^{-i\frac{\pi}{4}}(\sqrt{2}-1) F\left(\frac{1}{8}, \frac{3}{8}, \frac{1}{2}; 1+z\right) - e^{i\frac{\pi}{4}}(1+z)^{\frac{1}{2}} F\left(\frac{7}{8}, \frac{5}{8}, \frac{3}{2}; 1+z\right) \right], \end{aligned} \quad (5.20)$$

with $K_1 = e^{-i\frac{\pi}{8}} \sqrt{\frac{2+\sqrt{2}}{4}} \frac{\Gamma(\frac{1}{8})\Gamma(\frac{3}{8})}{\Gamma(\frac{1}{2})}$.

We have the ingredients to expand the periods $\hat{\vartheta}_I$ near $z = -1$, but before doing so we find it useful to define another integral basis, different from the one in (5.10) and (5.12), a basis that will enable us to compute the rigid limit efficiently. In particular, one of the periods in the new basis will be the ‘vanishing period’ at the conifold point, which will be fibred on the base space to give a CY cycle with S^3 topology and one with $S^2 \times S^1$, as described in general in section 3.5. Ultimately, the periods along these two CY cycles are the ones that reduce in the rigid limit to the periods of the meromorphic 1-form of the $SU(2)$ Seiberg–Witten theory, as we will show.

Thus we introduce the periods $\hat{\vartheta}'_I$ ($I = 0, 1, 2$) related to the previous ones by the integer change of basis

$$\hat{\vartheta}' = F \hat{\vartheta}, \quad F = \begin{pmatrix} -1 & 1 & 0 \\ 1 & -2 & -1 \\ 1 & 0 & 0 \end{pmatrix}. \quad (5.21)$$

¹⁵Some care is required in using the analytic continuation formulae because the range of $\arg z$ has to be appropriate to $z \rightarrow -1^+$ (or to $z \rightarrow -1^-$).

¹⁶The analytic continuation of u_2 reads $u_{2(0)}(z) = -\log(-z) F\left(\frac{1}{8}, \frac{3}{8}, 1; -z\right) + \sum_{n=0}^{\infty} \frac{(\frac{1}{8})_n (\frac{3}{8})_n}{(n!)^2} h_n (-z)^n$, for $|z| < 1$ and $-\pi + \epsilon < \arg(-z) < \pi + \epsilon$, i.e. $\epsilon < \arg(z) < 2\pi + \epsilon$, with $h_n = 2\psi(n+1) - \psi(n + \frac{1}{8}) - \psi(n + \frac{3}{8})$.

These periods are distinguished by their behaviour near the singularities. Indeed, $\hat{\vartheta}'_0 = \hat{\vartheta}'_1 - \hat{\vartheta}'_0$ is the vanishing period ‘above the cut’ at the conifold point $z \rightarrow -1^+$; $\hat{\vartheta}'_2 = \hat{\vartheta}'_0$ is the fundamental cycle; $\hat{\vartheta}'_1 = \hat{\vartheta}'_0 - 2\hat{\vartheta}'_1 - \hat{\vartheta}'_2$ is regular at the conifold and has no \log^2 term in its small- z expansion. This can be seen both by the form of the monodromies and by explicit expansions.

In the $\hat{\vartheta}'$ basis the monodromy matrix at the conifold, \mathcal{M}_{-1}^+ and the monodromy at large complex structure, \mathcal{M}_0 become

$$\mathcal{M}_{-1}^+ = \begin{pmatrix} -1 & 0 & 0 \\ 0 & 1 & 0 \\ 1 & 0 & 1 \end{pmatrix}, \quad \mathcal{M}'_0 = \begin{pmatrix} 1 & 1 & -2 \\ 0 & 1 & -4 \\ 0 & 0 & 1 \end{pmatrix}. \quad (5.22)$$

This is in agreement with the behaviours described above. The \mathbf{Z}_4 transformation and the intersection matrix \mathcal{I}' , (such that $\vartheta'_I \mathcal{I}'^{-1IJ} \vartheta'_J = 0$) become

$$\mathcal{M}_{\infty}' = \begin{pmatrix} -3 & -1 & -2 \\ 4 & 1 & 4 \\ 1 & 0 & 1 \end{pmatrix}, \quad \mathcal{I}' = \begin{pmatrix} -2 & 0 & 1 \\ 0 & 4 & 0 \\ 1 & 0 & 0 \end{pmatrix}. \quad (5.23)$$

5.2 Cycles and periods of the CY

Now we describe the 3-cycles of the CY manifold $X_8^*[1, 1, 2, 2, 2]$ by fibring $K3$ 2-cycles over paths in ζ in the two ways explained at the end of section 3.4. Correspondingly, the periods are integrals over such paths of the $K3$ periods. We will consider periods of the rescaled $(3, 0)$ -form

$$\hat{\Omega}^{(3,0)} \equiv \psi_0 \Omega^{(3,0)} = \int_{\gamma_4} \frac{\psi_0 |G| \omega_{CY}}{(2\pi i)^4 W^{(1)}} = \hat{\Omega}^{(2,0)} \frac{d\zeta}{2\pi i \zeta}. \quad (5.24)$$

and will sometimes make use of the variable

$$w = \frac{1}{2} \left(\zeta + \frac{1}{\zeta} \right), \quad (5.25)$$

First we can transport the three $K3$ cycles over the circle $|\zeta| = 1$. We will use the basis $\hat{\vartheta}'_I$ and will thus define

$$\begin{aligned} \mathcal{T}_v &\equiv \frac{1}{2\pi i} \int_C \frac{d\zeta}{\zeta} \hat{\vartheta}'_0 = \frac{1}{\pi} \int_{-1}^1 \frac{dw}{\sqrt{1-w^2}} \hat{\vartheta}'_0 \\ \mathcal{T}_1 &\equiv \frac{1}{2\pi i} \int_C \frac{d\zeta}{\zeta} \hat{\vartheta}'_1 = \frac{1}{\pi} \int_{-1}^1 \frac{dw}{\sqrt{1-w^2}} \hat{\vartheta}'_1 \\ \mathcal{T}_2 &\equiv \frac{1}{2\pi i} \int_C \frac{d\zeta}{\zeta} \hat{\vartheta}'_2 = \frac{1}{\pi} \int_{-1}^1 \frac{dw}{\sqrt{1-w^2}} \hat{\vartheta}'_2. \end{aligned} \quad (5.26)$$

Then we may transport $K3$ cycles between points where they vanish (see figure 3). First we consider the $K3$ period $\hat{\vartheta}'_0 = \hat{\vartheta}'_1 - \hat{\vartheta}'_0$, introduced in (5.21) and let c'_0 be its corresponding 2-cycle (a 2-sphere). It vanishes at the conifold point $z(w) = -1$, i.e. $\zeta = e_1^\pm$ (see (4.30)

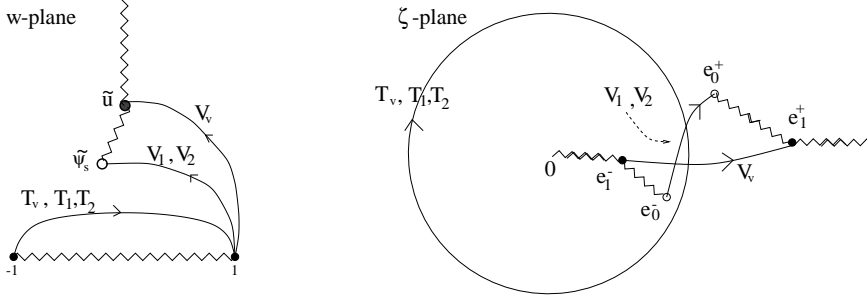


Fig. 3: An integer basis of cycles, suitable for taking the rigid limit, is depicted in the base space, parametrized by ζ or $w = \frac{1}{2}(\zeta + \frac{1}{\zeta})$. The cycles T_v, V_v are obtained by fibering over the indicated paths the K3 ‘vanishing cycle’ c'_0 ; the associated periods $\mathcal{T}_v, \mathcal{V}_v$ will reduce, in the rigid limit, to the section of the rigid $SU(2)$ special geometry, i.e. the periods of the meromorphic form λ . The cycles T_1, T_2 and V_{t_a}, V_{t_b} arise by fibering as indicated, respectively, the cycles c'_1, c'_2 and $2c'_2 - c'_1, 4c'_2$.

and figure 2), and we can thus consider its transport between these two points in ζ or, equivalently, on a path starting at $w = \tilde{u}$ and ending again at the same point (on the other sheet) after having crossed the square-root cut that runs from -1 to 1 . Clearly this 3-sphere collapses when $\tilde{u} = 1$. It is easy to see that the corresponding period is given by

$$\mathcal{V}_v \equiv \frac{1}{2\pi i} \int_{e_1^-}^{e_1^+} \frac{d\zeta}{\zeta} \hat{\vartheta}'_0 = \frac{1}{\pi} \int_1^{\tilde{u}} \frac{dw}{\sqrt{1-w^2}} \hat{\vartheta}'_0. \quad (5.27)$$

Similarly, we can consider which cycles vanish at the points e_0^\pm . This can be read from the monodromy matrix \mathcal{M}'_0 in (5.22). Indeed, comparing with the Picard–Lefschetz formula (2.19) shows that vanishing cycles are proportional to $\hat{\vartheta}'_1$ and $\hat{\vartheta}'_2$. So we define

$$\begin{aligned} \mathcal{V}_1 &\equiv \frac{1}{2\pi i} \int_{e_0^-}^{e_0^+} \frac{d\zeta}{\zeta} \hat{\vartheta}'_1 = \frac{1}{\pi} \int_1^{\tilde{\psi}_s} \frac{dw}{\sqrt{1-w^2}} \hat{\vartheta}'_1 \\ \mathcal{V}_2 &\equiv \frac{1}{2\pi i} \int_{e_0^-}^{e_0^+} \frac{d\zeta}{\zeta} \hat{\vartheta}'_2 = \frac{1}{\pi} \int_1^{\tilde{\psi}_s} \frac{dw}{\sqrt{1-w^2}} \hat{\vartheta}'_2. \end{aligned} \quad (5.28)$$

We have thus introduced the basis

$$v = \{\mathcal{V}_v, \mathcal{V}_1, \mathcal{V}_2, \mathcal{T}_v, \mathcal{T}_1, \mathcal{T}_v\}. \quad (5.29)$$

Intersection matrix. The intersection matrix can easily be obtained from considering the figure 3. We obtain in the basis (5.29):

$$q = \begin{pmatrix} q_{vv} & -\mathcal{I}' \\ \mathcal{I}' & 0 \end{pmatrix} = \begin{pmatrix} 0 & 0 & 1 & 2 & 0 & -1 \\ 0 & 0 & -2 & 0 & -4 & 0 \\ -1 & 2 & 0 & -1 & 0 & 0 \\ -2 & 0 & 1 & 0 & 0 & 0 \\ 0 & 4 & 0 & 0 & 0 & 0 \\ 1 & 0 & 0 & 0 & 0 & 0 \end{pmatrix}. \quad (5.30)$$

Only the derivation of the intersection between \mathcal{V}_1 and \mathcal{V}_2 is not trivial. We will explain in more detail the similar computation in the second example in section 6.4. In appendix C we derive cycles in another way, and obtain also an expression for the part q_{vv} in terms of a monodromy matrix and the intersection matrix of the $K3$ fibre.

6 Periods, monodromies and intersection matrix in the second example

We will work for the second example starting from its formulation as a double fibration: after the $K3$ fibration, we take the second torus fibration explained in section 4.2.2, and thus use the polynomial in the form (4.28). The holomorphic 3-form on the Calabi–Yau manifold is then (3.2) (we take y_0 constant)

$$\begin{aligned} \Omega^{(3,0)} &= \frac{|G|}{(2\pi i)^4} \int \frac{\omega_{CY}}{W^{(2)}} = \frac{|G'|}{(2\pi i)^4} \int \frac{\omega_{K3}}{W^{(2)}} \frac{d\zeta}{\zeta} = \frac{12}{(2\pi i)^4} \frac{d\zeta}{\zeta} \int \frac{1}{12} \frac{d\xi}{\xi} dx^4 dx^5 \frac{1}{W^{(2)} y_0^{-6}} \\ &= \frac{1}{(2\pi i)^4} \frac{d\zeta}{\zeta} \wedge \frac{d\xi}{\xi} \wedge dx \int dy \frac{1}{W^{(2)} y_0^{-6}} = \frac{1}{(2\pi i)^3} \frac{d\zeta}{\zeta} \wedge dx \wedge \frac{1}{y(\zeta, \xi, x)} \frac{d\xi}{\xi}, \end{aligned} \quad (6.1)$$

where we used the form (4.28) for $W^{(2)}$, and as path around the surface for Griffiths' residue theorem we used a loop in y , such that at the end $y(\zeta, \xi, x)$ is the solution to $W^{(2)} = 0$. Note that $\Omega^{(1,0)} \equiv \frac{1}{2\pi i} \frac{1}{y} \frac{d\xi}{\xi}$ is the (up to a constant factor unique) holomorphic 1-form on the torus fibre, and $\Omega^{(2,0)} \equiv \frac{1}{2\pi i} dx \wedge \Omega^{(1,0)}$ the holomorphic 2-form on the $K3$.

We will explicitly construct a basis of 3-cycles and their corresponding periods. To achieve this, we exploit the fibration structure of the model; first we study the cycles and periods of the torus fibre, then those of the $K3$, and finally those of the Calabi–Yau manifold itself. The explicit construction of the cycles allows us to compute monodromies and intersection forms in a straightforward way. For the torus and $K3$ fibres, we furthermore obtain closed expressions of the periods in terms of hypergeometric functions.

6.1 Torus cycles and periods

Branch points: If we consider the defining equation (4.28) to be an equation for y as a function of ξ , we get the torus as a 2-sheeted cover of the ξ plane. The sheets coincide at the branch points, which come in pairs symmetric under $\xi \leftrightarrow \frac{B'}{\xi}$, and are located at

$$\xi = -P \pm \sqrt{P^2 - B'} \quad (6.2)$$

and at

$$\xi = 0, \infty. \quad (6.3)$$

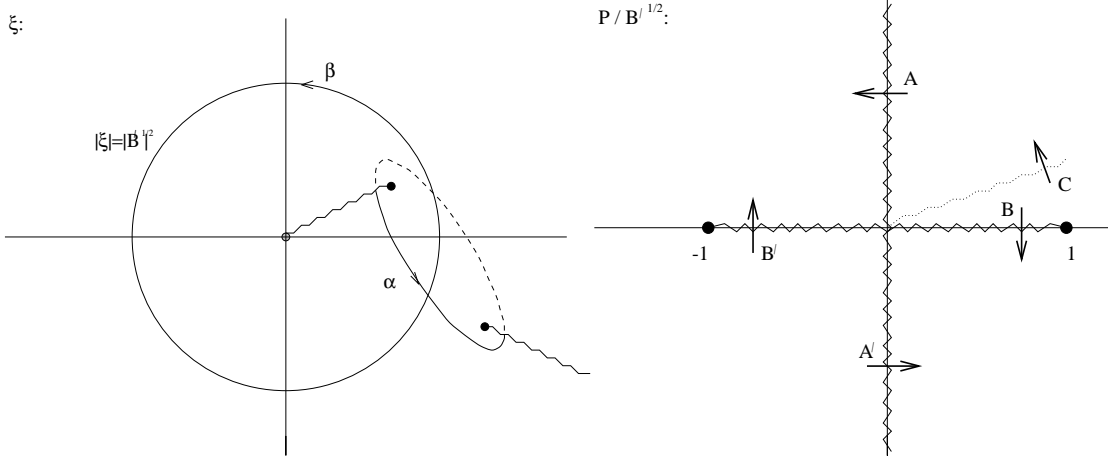


Fig. 4: (a) Branch points, cuts and cycles of the torus fibre in the ξ -plane. (b) Singularities and cuts in the $P/(B')^{1/2}$ -plane.

Cycles. Define β to be the 1-cycle $|\xi| = |B'|^{1/2}$ passing counterclockwise through the point¹⁷ ($\xi = i\sqrt{B'}, y = \frac{1}{\sqrt{3}}\sqrt{-P}$), and α the shortest cycle encircling the pair of branch points (6.2), with orientation such that $\alpha \cdot \beta = +1$. This is shown in figure 4(a).

Singularities and vanishing cycles. The torus degenerates when two branch points coincide. There are two possibilities:

- **$P^2 - B' = 0$:** the branch points (6.2) coincide and α vanishes. The locus in the (ζ, x) -plane where this occurs is a *genus-5* Riemann surface, as can be seen by substituting the expressions for $P(x)$ and $B'(\zeta)$. We denote this surface by Σ . Since α collapses to a point on Σ , this surface can be lifted trivially to the full Calabi–Yau. By slight abuse of notation, we denote the lifted surface by Σ as well. Thus Σ is the locus of elliptic fibre singularities of the Calabi–Yau. We could also view the full 10D spacetime $M_4 \times CY$ as an elliptic fibration. Then the locus of elliptic fibre singularities gets promoted to a $(5 + 1)$ -dimensional manifold $M_4 \times \Sigma$.
- **$B' = 0$:** one of the branch points (6.2) coincides with the branch point $\xi = 0$, and β vanishes. The surface where this occurs consists of two copies of the x -plane at fixed ζ positions, and is denoted by Σ' . Again, this surface can be lifted to the full Calabi–Yau or promoted to a $(5 + 1)$ -dimensional submanifold of spacetime.

Cuts. There are jumps (or cuts) in the definition of α at values of $P/\sqrt{B'}$ where there are two homologically different cycles encircling the two branch points with equal minimal length. This occurs when the branch points (6.2) are collinear, i.e. when $\frac{P}{\sqrt{B'}}$ is imaginary

¹⁷In the following, \sqrt{z} denotes the square root of z with positive real part.

(type A cut). Jumps in the definition of β occur when the branch points lie on the circle $|\xi| = |B'|^{1/2}$, i.e. when $\frac{P}{\sqrt{B'}} = 0$ lies on the real interval $[-1, 1]$ (type B cut). There is yet another type of cut, for both α and β , namely where our prescription for the location of β (and hence α) is ambiguous. For fixed B' , this is the case when P is real and positive (type C cut).

The cut structure in the $P/\sqrt{B'}$ -plane is shown in figure 4(b). For $B' \approx 1$ (which will be of special interest later), the C cut runs approximately over the positive real axis. The transformation rules for continuous transport of torus cycles across the cuts (yielding the monodromies) are

$$A, A' : \quad \alpha \rightarrow \alpha + 2\beta \quad (6.4)$$

$$B, B' : \quad \beta \rightarrow \beta + \alpha \quad (6.5)$$

$$C : \quad \alpha, \beta \rightarrow -\alpha, -\beta \quad (6.6)$$

Notice that the origin of the $P/\sqrt{B'}$ -plane is not really singular, as the monodromy about this point is, in fact, trivial.

Periods. The following expressions for the periods can be obtained by direct integration. Denoting $k_{\mp}^2 = \frac{1}{2}(1 \mp \frac{P}{\sqrt{B'}})$, we find

$$\int_{\alpha} \Omega^{(1,0)} = \frac{2\sqrt{6}i}{\pi} (\sqrt{B'})^{-1/2} \mathbf{K}(k_+^2) \text{ for } |k_+^2| < 1 \quad (6.7)$$

$$= \pm \frac{2\sqrt{6}}{\pi} (\sqrt{B'})^{-1/2} \mathbf{K}(k_{\pm}^2) \text{ for } |k_{\pm}^2| < 1 \text{ and } \pm \text{Im } P > 0 \quad (6.8)$$

where the imaginary part of P denotes a position above or below the C-cut, respectively,

$$\int_{\beta} \Omega^{(1,0)} = \frac{\sqrt{6}}{\pi} (\pm\sqrt{B'})^{-1/2} (\pm k_{\mp}^2)^{-1/2} \mathbf{K}(k_{\mp}^{-2}) \quad (6.9)$$

where the expressions are valid when the argument of the K -function is in the unit circle, and for P near the C-cut the square root in the prefactor is equal to $\pm i(\mp k_{\mp}^2)^{-1/2}$. Here $\mathbf{K}(u) = \frac{\pi}{2} F(\frac{1}{2}, \frac{1}{2}, 1; u)$ is the complete elliptic integral of the first kind. These expressions can be extended to other values of $P/\sqrt{B'}$ by standard analytic continuation. To obtain the values for the α and β periods one has to take into account the changes of definition of the cycles across the A-, B- and C-cuts.

6.2 K3 cycles and periods

As explained earlier, the $K3$ fibre (at a fixed generic value of ζ , and hence of $\sqrt{B'}$) is itself an elliptic fibration, with base parametrized by x . Accordingly, the relevant 2-cycles of the $K3$ fibre, that is, those which are in the transcendental lattice, can be constructed as circle fibrations over certain paths in the x -plane, where the circle is a 1-cycle in the torus fibre.

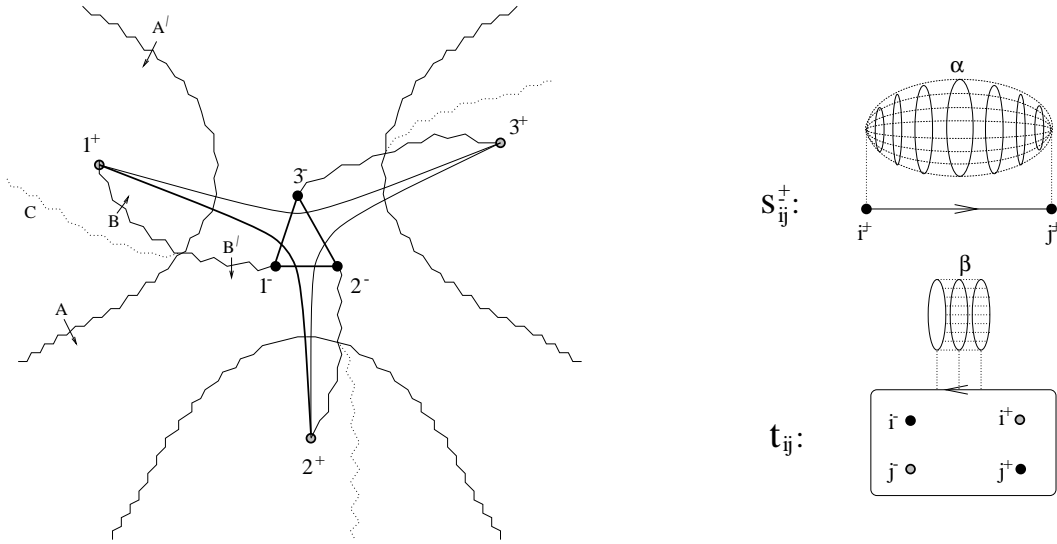


Fig5: (Elliptic) fibre singularities, cuts and cycles of the $K3$ manifold in the x -plane.

Points with degenerating elliptic fibre. The x -plane can be viewed as a 3-fold covering of the $P/\sqrt{B'}$ -plane considered in section 6.1, as ζ is fixed and P is of degree 3 in x . Therefore, in the x -plane, there are three copies of every ingredient (cuts, singularities, etc) of figure 4(b). This is shown in figure 5. In particular, the $g = 5$ Riemann surface Σ , on which α vanishes, intersects the x -plane (having a fixed value of ζ) in 6 points. As Σ splits in two branches Σ_{\pm} corresponding to the solutions of $P(x)/\sqrt{B'} = \pm 1$, we can divide those six points accordingly in two groups of three, which we label by $1^+, 2^+, 3^+$ and $1^-, 2^-, 3^-$. Choose numbering such that the B-type cuts connect i^+ with i^- (see the figure).

Cycles. The idea is to construct $K3$ 2-cycles as circle fibrations by transporting a torus 1-cycle c along a path γ in the x -plane. The path γ can either be a closed loop without monodromy for c , or an open path terminating on the points i^{\pm} , with c vanishing at both endpoints. The first possibility will produce a torus and the second a sphere.

This gives us the following 2-cycles (see figure 5):

- \mathbf{s}_{ij}^+ : $c = \alpha$ (at i^+) and γ running between i^+ and j^+ . This is a sphere.
- \mathbf{s}_{ij}^- : $c = \alpha$ (at i^-) and γ running between i^- and j^- ; again a sphere.
- \mathbf{t}_{ij} : $c = \beta$ (at i^+) and γ a closed path encircling i^+, i^-, j^+, j^- . This is a torus.

Note that it is not possible to construct a 2-cycle by taking γ to run from i^+ to j^- because such a path necessarily passes through an A-type cut: an α -cycle at one endpoint, when continued to the other endpoint, becomes $\alpha + 2\beta$ and does not vanish there.

Actually we have not yet given a precise description of the above cycles in general, only for the specific case of figure 5. To define this set in the general case, we can proceed as follows: first, we require the cycles to be compatible with the above description including

the homological relations and intersections. Any set of cycles obtained by continuation from the specific set of figure 5 will satisfy this. Because continuation is, in general, not uniquely defined (due to monodromies), there are still many possibilities, corresponding to the choice of cuts. We will not try to fix the remaining ambiguity here in general, but assume that in each case a prescription is adopted such that s_{ij}^\pm vanishes whenever i^\pm approaches j^\pm .

At the level of homology, we have the following relations:

$$\begin{aligned} t_{ij} = -t_{ji} = s_{ij}^+ - s_{ij}^- & \quad ; & \quad s_{ij}^\pm = -s_{ji}^\pm \\ s_{12}^\pm + s_{23}^\pm + s_{31}^\pm = 0 & \quad ; & \quad t_{12} + t_{23} + t_{31} = 0 . \end{aligned} \quad (6.10)$$

This implies that of the 2-cycles constructed above, only four are independent.

Intersections. Combining the intersections of the paths γ in the base (as shown in figure 5) with the known intersections of the torus 1-cycles (taking into account their transformation when passing a cut), all 2-cycle intersections can be calculated in a straightforward way:

$$\begin{aligned} s_{12}^\pm \cdot s_{12}^\pm &= -2 & s_{12}^- \cdot s_{12}^+ &= -2 & s_{12}^\pm \cdot t_{12} &= 0 \\ s_{12}^\pm \cdot s_{23}^\pm &= 1 & s_{12}^- \cdot s_{23}^+ &= 2 & s_{12}^\pm \cdot t_{23} &= 1 \\ s_{12}^- \cdot s_{31}^+ &= 0 & s_{12}^\pm \cdot t_{31} &= -1 & t_{ij} \cdot t_{kl} &= 0 \end{aligned} \quad (6.11)$$

and all cyclic permutations hereof. The first two equations can be summarized as

$$s_{ij}^\pm \cdot s_{kl}^\pm = \delta_{il} + \delta_{jk} - \delta_{ik} - \delta_{jl}. \quad (6.12)$$

Note that this is precisely (minus) the intersection of the 0-cycles $j^\pm - i^\pm$ and $l^\pm - k^\pm$. This fact will prove to be important for the reduction of the geometrical data from the Calabi–Yau to a Riemann surface in the rigid limit.

Singularities and vanishing cycles. The $K3$ degenerates when two (or more) of the points $1^\pm, 2^\pm, 3^\pm$ coincide. There are several possibilities:

- $\mathbf{B}' = \mathbf{0}$. Here $1^+ = 1^-$, $2^+ = 2^-$, $3^+ = 3^-$, and the tori t_{ij} degenerate to lines (recall that β vanishes at $B' = 0$).
- $\mathbf{B}' = (\psi_0^6 + \psi_1)^2$. Keeping in mind that we have defined $\sqrt{B'}$ to have positive real part, there are two possibilities:
 - if $\text{Re}(\psi_0^6 + \psi_1) < 0$, two of the zeros $1^+, 2^+, 3^+$ of $P = +\sqrt{B'}$ coincide, and the corresponding sphere s_{ij}^+ vanishes.
 - if $\text{Re}(\psi_0^6 + \psi_1) > 0$, two of the zeros $1^-, 2^-, 3^-$ of $P = -\sqrt{B'}$ coincide, and the corresponding sphere s_{ij}^- vanishes.

In each case, we call the vanishing sphere at this point v_a .

- $\mathbf{B}' = \psi_1^2$: Again, there are two cases: if $\text{Re}\psi_1$ is positive (negative), there is a vanishing s_{ij}^- (s_{ij}^+). Call this vanishing sphere v_b .

Define $t_a \equiv t_{ji}$ if $v_a = s_{ij}^\pm$, and similarly for t_b . The tori t_a and t_b degenerate at $B' = 0$. The set

$$c' = \begin{pmatrix} v_a \\ v_b \\ t_a \\ t_b \end{pmatrix} \quad (6.13)$$

forms a basis of the transcendental lattice, which has rank 4 here.

We have constructed different bases depending on the signs of $\text{Re}(\psi_0^6 + \psi_1)$ and $\text{Re}\psi_1$. We therefore also expect the corresponding intersection matrix to depend on these signs. To calculate this matrix when, say, $\text{Re}(\psi_0^6 + \psi_1) > 0$ and $\text{Re}\psi_1 > 0$, we consider the case where ψ_1 is very close to $\psi_1 + \psi_0^6$ (which is the case shown in figure 5). Then it is easy to see, by direct inspection of the roots of $P(x)^2 - B'$, that, choosing a suitable numbering of the roots

$$v_a = s_{12}^-; \quad v_b = s_{23}^-; \quad t_a = t_{21}; \quad t_b = t_{32}. \quad (6.14)$$

This identification, together with (6.11), provides the complete intersection matrix. An analogous procedure can be followed for the other cases.

The results are (in the basis c' (6.13)):

- If $\text{Re}\psi_1$ and $\text{Re}(\psi_1 + \psi_0^6)$ have the same sign:

$$\mathcal{I} = \begin{pmatrix} -2 & 1 & 0 & -1 \\ 1 & -2 & 1 & 0 \\ 0 & 1 & 0 & 0 \\ -1 & 0 & 0 & 0 \end{pmatrix}. \quad (6.15)$$

We recognize the $SU(3)$ Cartan matrix in the upper block and therefore call this part of moduli space the ‘ $SU(3)$ sector’. In terms of the invariants of (4.17), this sector includes the region where ν_1 is small with respect to ν_2 .

- If the real parts of $\psi_1 + \psi_0^6$ and ψ_1 have opposite sign:

$$\mathcal{I}' = \begin{pmatrix} -2 & 0 & 0 & -1 \\ 0 & -2 & 1 & 0 \\ 0 & 1 & 0 & 0 \\ -1 & 0 & 0 & 0 \end{pmatrix}. \quad (6.16)$$

Here we recognize the $SU(2) \times SU(2)$ Cartan matrix; accordingly we call this part of moduli space the ‘ $SU(2) \times SU(2)$ sector’. This sector includes the region where ν_2 is small with respect to ν_1 .

Notice that our division of the moduli space in an $SU(3)$ and an $SU(2) \times SU(2)$ sector is dependent on the sign convention for $\sqrt{B'}$ (except on the subspace $\psi_1^2 = (\psi_1 + \psi_0^6)^2$). Therefore, though the convention we have taken is quite natural, especially when we are close to a rigid limit, one can not expect the boundary between these sectors to have any

physical significance¹⁸. However, we shall see that there exists a certain region inside the $SU(3)$ sector (close to the $SU(3)$ rigid limit) where a four-dimensional low-energy observer indeed sees $SU(3)$ Yang–Mills physics (weakly) coupled to gravity, and similarly for $SU(2) \times SU(2)$. Outside these regions, four-dimensional low-energy physics might not look at all like a particular non-Abelian gauge theory.

Monodromies. We consider four monodromies:

1. The monodromy around $B' = \infty$, $M_\infty : B' \rightarrow e^{-2\pi i} B'$.
2. The monodromy around the conifold point a1 on page 23, with generator $T_a : ((\psi_0^6 + \psi_1)^2 - B') \rightarrow \exp[2\pi i]((\psi_0^6 + \psi_1)^2 - B')$.
3. The monodromy around the conifold point a2, with generator $T_b : (\psi_1^2 - B') \rightarrow \exp[2\pi i](\psi_1^2 - B')$.
4. The monodromy around the large complex structure point $B' = 0$, with generator B_0 .

The matrices realizing the monodromies depend on the choice of basis, which we have taken to depend on the sector: we will indicate the monodromy matrices corresponding to the choices in the $SU(2) \times SU(2)$ sector with a prime.

It is clear that these four monodromies are related: The exact relation depends on the choice of base point. We find

$$M_\infty^{-1} = T_b T_a B_0 , \tag{6.17}$$

which can be taken to define M_∞ in terms of the others.

The results for T_a and T_b can be computed from the Picard–Lefschetz formula (2.19): the vanishing cycles are, in both sectors, v_a and v_b , respectively. For the B_0 monodromy both t_a and t_b vanish, and the matrix is obtained by drawing some pictures. Finally the M_∞ matrix is obtained from (6.17). Working in the basis (6.13), the results are

$$\begin{aligned}
 T_a &= \begin{pmatrix} -1 & 0 & 0 & 0 \\ 1 & 1 & 0 & 0 \\ 0 & 0 & 1 & 0 \\ -1 & 0 & 0 & 1 \end{pmatrix} ; & T_b &= \begin{pmatrix} 1 & 1 & 0 & 0 \\ 0 & -1 & 0 & 0 \\ 0 & 1 & 1 & 0 \\ 0 & 0 & 0 & 1 \end{pmatrix} \\
 T'_a &= \begin{pmatrix} -1 & 0 & 0 & 0 \\ 0 & 1 & 0 & 0 \\ 0 & 0 & 1 & 0 \\ -1 & 0 & 0 & 1 \end{pmatrix} ; & T'_b &= \begin{pmatrix} 1 & 0 & 0 & 0 \\ 0 & -1 & 0 & 0 \\ 0 & 1 & 1 & 0 \\ 0 & 0 & 0 & 1 \end{pmatrix} \\
 B_0 = B'_0 &= \begin{pmatrix} 1 & 0 & -1 & 0 \\ 0 & 1 & 0 & -1 \\ 0 & 0 & 1 & 0 \\ 0 & 0 & 0 & 1 \end{pmatrix} ; & M_\infty &= \begin{pmatrix} -1 & 0 & 1 & 0 \\ 0 & -1 & 0 & 1 \\ 0 & 1 & 1 & 0 \\ -1 & -1 & 0 & 1 \end{pmatrix} . \tag{6.18}
 \end{aligned}$$

¹⁸A physically significant definition of, for example, the $SU(3)$ sector would be the region of moduli space where BPS states exist which can be identified as $SU(3)$ gauge bosons. Unfortunately, for a generic point of moduli space, the existence of these states is very difficult to check analytically, if not impossible.

The matrices T_a, T'_a, T_b and T'_b have Jordan form $\text{diag}(-1, 1, 1, 1)$, hence an expansion of the periods in a variable z around the corresponding singularity has terms of the form z^n and $z^{1/2+n}$. On the other hand, B_0 has Jordan form

$$B_{0,Jordan} = \begin{pmatrix} 1 & 1 & 0 & 0 \\ 0 & 1 & 0 & 0 \\ 0 & 0 & 1 & 1 \\ 0 & 0 & 0 & 1 \end{pmatrix}, \quad (6.19)$$

so period expansions have terms z^n and $z^n \ln z$.

The matrices T_a and T_b generate the group \mathcal{S}_3 , the Weyl group of $SU(3)$, while T'_a and T'_b generate $\mathcal{S}_2 \times \mathcal{S}_2$, the Weyl group of $SU(2) \times SU(2)$.

Periods. An integral representation for the $K3$ periods can be given by making use of the elliptic fibration structure and (6.7)-(6.9). Note, in particular, that when i^\pm and j^\pm come close to each other, we have

$$\int_{s_{i^\pm}^\pm} \Omega^{(2,0)} \approx \frac{\sqrt{6}}{2\pi i} (\pm\sqrt{B'})^{-1/2} \int_{i^\pm}^{j^\pm} dx = \frac{\sqrt{6}}{2\pi i} (\pm\sqrt{B'})^{-1/2} (x_{j^\pm} - x_{i^\pm}), \quad (6.20)$$

where the x_{i^\pm} are simply found by solving $P(x) = \pm\sqrt{B'}$.

6.3 Closed expressions

For the discussion of the main features of the rigid limit it is not really necessary to find closed expressions for the periods. But as explained in the introduction we want to also provide the explicit expressions of the basic quantities in the supergravity action for later use in explicitly constructing the expansion of that action around its rigid limit. These closed expressions can be found using first the Picard–Fuchs techniques (see appendix B for a large part based on [33]) for the periods of $K3$. These as usual do not provide an integral basis, and thus we have to find the transformation to the basis constructed above. This will be done by comparing the monodromy matrices. This will lead to a basis transformation up to an overall factor. The latter is then determined by comparing asymptotic expansions in a limit where these can be calculated easily on both sides. We will do this in a rigid limit.

The Picard–Fuchs result. The analysis of the Picard–Fuchs equations for the $K3$ -periods in appendix B.2 leads to the solution (B.23): the periods, which are functions of two variables, are linear combinations of products of two functions of one variable (each). Choosing a convenient normalization (which removes the scaling introduced in (B.21)) we write

$$\vartheta \equiv \int \Omega^{(2,0)} \equiv \begin{pmatrix} \vartheta_{12} \\ \vartheta_{21} \\ \vartheta_{11} \\ \vartheta_{22} \end{pmatrix} = \frac{\sqrt{3}}{\psi_0} \begin{pmatrix} \xi_1(r) \xi_2(s) \\ \xi_2(r) \xi_1(s) \\ \xi_1(r) \xi_1(s) \\ \xi_2(r) \xi_2(s) \end{pmatrix}, \quad (6.21)$$

where the variables r, s are given in the ‘usual gauge’ as

$$\begin{aligned} r &= \frac{1}{2} + \frac{\sqrt{(\psi_0^6 + \psi_1)^2 - B'} - \sqrt{\psi_1^2 - B'}}{2\psi_0^6} \\ s &= \frac{1}{2} + \frac{\sqrt{(\psi_0^6 + \psi_1)^2 - B'} + \sqrt{\psi_1^2 - B'}}{2\psi_0^6} . \end{aligned} \quad (6.22)$$

and the functions $\xi_{1,2}$ are given for large values of r and s in (B.27), where we choose

$$B_1 = \frac{\Gamma(\frac{2}{3})}{\Gamma^2(\frac{5}{6})} ; \quad B_2 = \frac{\Gamma(-\frac{2}{3})}{\Gamma^2(\frac{1}{6})} ; \quad B_1 B_2 = -\frac{\sqrt{3}}{4\pi} . \quad (6.23)$$

We will refer to the basis in (6.21) as our Picard–Fuchs basis.

Monodromies in the Picard–Fuchs basis. We will denote these monodromies with a superscript PF . Using (6.22) we immediately obtain for the action on the variables r and s :

$$\begin{aligned} M_\infty^{PF} &: \begin{cases} r \longrightarrow 1 - r \\ s \longrightarrow 1 - s \end{cases} \\ T_a^{PF} &: \begin{cases} r \longrightarrow 1 - s \\ s \longrightarrow 1 - r \end{cases} \\ T_b^{PF} &: \begin{cases} r \longrightarrow s \\ s \longrightarrow r \end{cases} \\ B_0^{PF} &: \begin{cases} r \longrightarrow r \\ s \longrightarrow s \end{cases} . \end{aligned} \quad (6.24)$$

To determine the action on the functions ξ_i and the periods, we have to take into account also the corresponding paths in the complex plane. For example, for B_0^{PF} , r turns around the point $r = 1$ (and s around $s = 1 + \frac{\psi_1}{\psi_0^6}$, which is however immaterial since this is not a singularity). Note that encircling the singularities for the monodromies T_a and T_b we may stay in the region where both r and s are large provided $|\psi_1| \gg |\psi_0^6|$, so that $\text{Re}\psi_1 \cdot \text{Re}(\psi_1 + \psi_0^6) > 0$. This is in the $SU(3)$ sector, which is exactly what interests us here. The expressions in (B.27) for $\xi_1(u)$ and $\xi_2(u)$ in terms of hypergeometric functions are unambiguous for $|u| > 1$ provided we specify the sixth root. We place the cut from 0 to ∞ along the negative imaginary axis, so that $u^{-1/6}$ will mean $|u|^{-1/6} \exp(-i\phi/6)$, where the phase of u is taken to obey $|\phi| < \pi$. The monodromy matrices for the T_a^{PF} and T_b^{PF} monodromies depend to a large extent on this factor. From expression (2.10.6) of [34] one finds that $\xi_1(u) = u^{-1/6} {}_2F_1(\frac{1}{6}, \frac{1}{6}, \frac{1}{3}; \frac{1}{u}) = (u-1)^{-1/6} {}_2F_1(\frac{1}{6}, \frac{1}{6}, \frac{1}{3}; \frac{1}{1-u})$. Hence, for large values of u with $\text{Im } u > 0$ we have that $\xi_1(1-u) = \exp\left(\frac{i\pi}{6}\right) \xi_1(u)$ and the opposite phase for $\text{Im } u < 0$. Similarly, $\xi_2(1-u) = \exp\left(\frac{\pm i5\pi}{6}\right) \xi_2(u)$ when $\pm \text{Im } u > 0$.

By use of (6.24) the monodromy matrices in the basis (6.21) are:

$$T_a^{PF} = \begin{pmatrix} 0 & \omega & 0 & 0 \\ \omega^2 & 0 & 0 & 0 \\ 0 & 0 & 1 & 0 \\ 0 & 0 & 0 & 1 \end{pmatrix} ; \quad T_b^{PF} = \begin{pmatrix} 0 & 1 & 0 & 0 \\ 1 & 0 & 0 & 0 \\ 0 & 0 & 1 & 0 \\ 0 & 0 & 0 & 1 \end{pmatrix} , \quad (6.25)$$

where $\omega = \exp(\pm 2\pi i/3)$ for starting with $\pm \text{Im } r > 0$ (and thus $\mp \text{Im } s > 0$). These matrices have eigenvalues $(1, 1, 1, -1)$, as we expected for A_1 monodromies.

The monodromy M_∞^{PF} is not so easily computed, but requires the continuation of the hypergeometric functions from large values of u . Indeed, when B' is large, either r is large and s is close to $\frac{1}{2}$ or vice versa. It is easier instead to obtain the matrix B_0^{PF} : the monodromy encircles the hypergeometric function singularity at $r = 1$ but leaves $\xi_i(s)$ invariant. In the rest of this paragraph we only write down the formulae for $\omega = e^{+2\pi i/3}$ in (6.25). Expanding $\xi_1(r)$ and $\xi_2(r)$ near $r = 1$ via eqs. 2.10.6 and 2.10.7 of [34]

$$\begin{aligned}\xi_1(r) &= \frac{1}{2\pi\sqrt{3}} \left[-\log(r-1)F\left(\frac{1}{6}, \frac{5}{6}, 1; 1-r\right) + \sum_{n=0}^{\infty} H_n(1-r)^n \right] \\ \xi_2(r) &= -\frac{1}{2\pi\sqrt{3}} \left[-\log(r-1)F\left(\frac{1}{6}, \frac{5}{6}, 1; 1-r\right) + \sum_{n=0}^{\infty} G_n(1-r)^n \right].\end{aligned}\quad (6.26)$$

The monodromy matrix follows from this continuation.

The combination that is regular at $r = 1$ is the sum. Using the explicit expressions for the coefficients one finds that $H_n - G_n = 2\pi\sqrt{3}\frac{(\frac{1}{6})_n(\frac{5}{6})_n}{n!^2}$, and therefore

$$\xi_1(r) + \xi_2(r) = F\left(\frac{1}{6}, \frac{5}{6}, 1; 1-r\right) \quad \text{for } r \sim 1. \quad (6.27)$$

This leads to the result

$$B_0^{PF} = \begin{pmatrix} 1 - \frac{i}{\sqrt{3}} & 0 & 0 & -\frac{i}{\sqrt{3}} \\ 0 & 1 + \frac{i}{\sqrt{3}} & \frac{i}{\sqrt{3}} & 0 \\ 0 & -\frac{i}{\sqrt{3}} & 1 - \frac{i}{\sqrt{3}} & 0 \\ \frac{i}{\sqrt{3}} & 0 & 0 & 1 + \frac{i}{\sqrt{3}} \end{pmatrix}. \quad (6.28)$$

Comparing. By comparing the monodromy matrices in the Picard–Fuchs basis, and those in (6.18) one obtains the matrix describing the basis transformation up to an overall factor. We wrote the expressions in the previous paragraph in the $SU(3)$ basis, so we have to solve $\{T_a, T_b, B_0\}S_v = S_v\{T_a^{PF}, T_b^{PF}, B_0^{PF}\}$. This leads to

$$\vartheta' = \int_{c'} \Omega^{(2,0)} = S_v \vartheta; \quad S_v = a \begin{pmatrix} -i\omega & i\omega^2 & 0 & 0 \\ -i & i & 0 & 0 \\ \frac{\omega}{\sqrt{3}} & \frac{\omega^2}{\sqrt{3}} & \frac{\omega^2}{\sqrt{3}} & \frac{\omega}{\sqrt{3}} \\ \frac{1}{\sqrt{3}} & \frac{1}{\sqrt{3}} & \frac{1}{\sqrt{3}} & \frac{1}{\sqrt{3}} \end{pmatrix}, \quad (6.29)$$

where a is a number that will be shown to be 1 by comparing the leading term in the $SU(3)$ rigid limit in section 7.3.4.

6.4 CY cycles and periods

Since the Calabi–Yau 3-fold under consideration is a $K3$ fibration, one can construct the CY 3-cycles as $K3$ cycle fibrations over paths in the base manifold (the ζ -plane). Denote

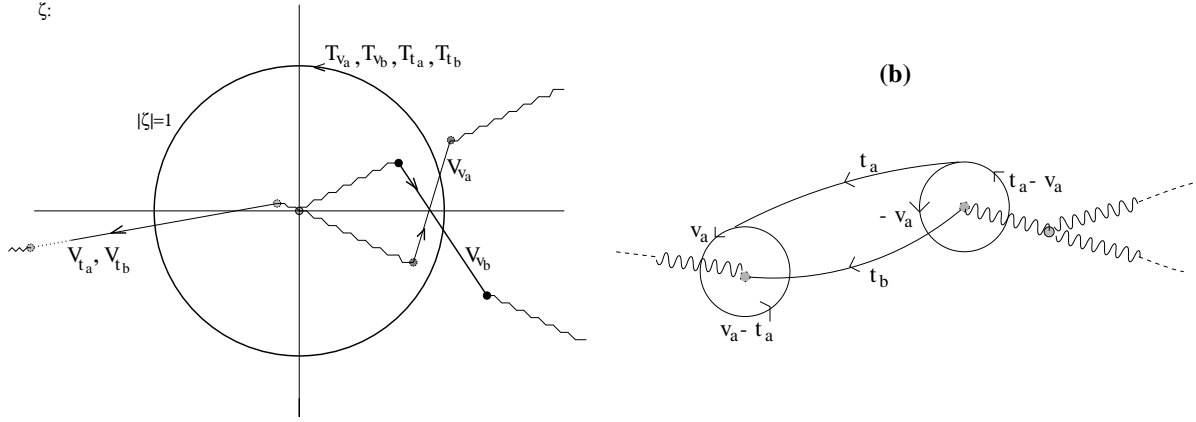


Fig. 6: (a) ($K3$) fibre singularities, cuts and cycles of the CY manifold in the ζ -plane. (b) The intersection $V_{t_a} \cdot V_{t_b}$, a detail of figure (a).

the path in the base by γ and the $K3$ cycle which is transported along γ by c ; γ can be open, with c vanishing at both endpoints, or closed, with trivial monodromy for c . The corresponding CY period is given by

$$\frac{1}{2\pi i} \int_{\gamma} \frac{d\zeta}{\zeta} \theta(\zeta), \quad (6.30)$$

where $\theta(\zeta)$ denotes the period of c in the $K3$ fibre above ζ .

A basis of 3-cycles can be constructed as follows (see fig. 6(a)):

- \mathbf{V}_{v_a} : $c = v_a$ and γ running between the two solutions of $\frac{B}{2}(\zeta + \frac{1}{\zeta}) + 1 = (\psi_0^6 + \psi_1)^2$. This is an S^3 .
- \mathbf{V}_{v_b} : $c = v_b$ and γ running between the two solutions of $\frac{B}{2}(\zeta + \frac{1}{\zeta}) + 1 = \psi_1^2$. This is also an S^3 .
- \mathbf{T}_{v_a, v_b} : $c = v_a, v_b$ and γ the unit circle. This has topology $S^1 \times S^2$.
- \mathbf{V}_{t_a, t_b} : $c = t_a, t_b$ and γ running between the two solutions of $\frac{B}{2}(\zeta + \frac{1}{\zeta}) + 1 = 0$. The topology is $S^2 \times S^1$.
- \mathbf{T}_{t_a, t_b} : $c = t_a, t_b$ and γ the unit circle. The topology is T^3 .

The intersection matrix in the basis

$$C = (V_{v_a}, V_{v_b}, V_{t_a}, V_{t_b}, T_{v_a}, T_{v_b}, T_{t_a}, T_{t_b}) \quad (6.31)$$

and in the $SU(3)$ region is

$$q = \begin{pmatrix} 0 & -1 & 0 & 0 & & \\ 1 & 0 & 0 & 0 & & \\ 0 & 0 & 0 & -2 & \mathcal{I} & \\ 0 & 0 & 2 & 0 & & \\ & & & & & \\ & & & & -\mathcal{I} & \\ & & & & & 0 \end{pmatrix}, \quad (6.32)$$

where \mathcal{I} is given in (6.15). The appearance of this matrix is clear from figure 6(a), and the T paths in ζ can be taken to be non-intersecting. The intersection $V_{t_a} \cdot V_{t_b}$ can be computed as follows. Instead of V_{t_a} , consider an 8-shaped loop in the ζ -plane around its end points, and take along the cycle $t_a - v_a$ of the fibre. After crossing the cut, this combination turns into $-v_a$, as is read off from the monodromy matrix B_0 in (6.18). The result is sketched in figure 6(b), together with V_{t_b} . Shrinking the loops around the branch points to zero one recovers V_{t_a} . The intersection with V_{t_b} can be read off from the figure before this shrinking.

7 The rigid limit

7.1 General facts and methods

The singularities of the two CY manifolds we consider, $X_8^*[1, 1, 2, 2, 2]$ and $X_{24}^*[1, 1, 2, 8, 12]$, were discussed in section 4.3, by regarding the CYs as $K3$ fibrations. The l.c.s. singularity ($B' = 0$) of the $K3$ fibre occurs, in both examples, at two points (symmetric with respect to the exchange $\zeta \rightarrow 1/\zeta$) in the base space, such that $w \equiv 1/2(\zeta + 1/\zeta) = \psi_s/B$. For the first example, these are the points e_0^\pm in figure 3; for the second one, they are the two points to the left of figure 6. In the first example, the fibre $X_4^*[1, 1, 1, 1]$ has, moreover, a conifold singularity at the points $\zeta = e_1^\pm$, see figure 3; in the second, the fibre $X_{12}^*[1, 1, 4, 6]$ of the second develops two types of conifolds at two pairs of points, appearing to the right of figure 6.

We are now interested in the neighbourhood of those CY singularities, named ‘rigid limits’ in section 4.3, that are parametrized by (4.36) and (4.41), respectively, for the two examples. In these limits, the position of the l.c.s. in the $K3$ fibre is given by

$$w \equiv \frac{1}{2} \left(\zeta + \frac{1}{\zeta} \right) = \tilde{\psi}_s = \frac{\psi_s}{2\epsilon} = -\frac{1}{2\tilde{\epsilon}}, \quad (7.1)$$

where we have introduced an expansion parameter $\tilde{\epsilon}$ invariant under (3.19) (also for the moduli we have indicated by a tilde the invariant moduli, i.e. \tilde{u})

$$\epsilon = -\psi_s \tilde{\epsilon}. \quad (7.2)$$

Thus in the rigid limit the positions of the l.c.s singularity move to $\zeta = 0$ and $\zeta = \infty$ in the base.

The position of the conifold singularities is instead independent of $\tilde{\epsilon}$:

$$\text{example 1: } w = \tilde{u} ; \quad \text{example 2: } \begin{aligned} w &= \frac{1}{2}(\tilde{u}_1 + 2\tilde{u}_0^6) + \mathcal{O}(\epsilon) , \\ w &= \frac{1}{2}\tilde{u}_1 . \end{aligned} \quad (7.3)$$

The \tilde{u} moduli will be the moduli of the rigid special geometry that emerges in the limit, that in the examples will be the one associated to the Seiberg–Witten low-energy effective action for the $SU(2)$, respectively $SU(3)$, $N = 2$, $d = 4$ SYM theory.

To deduce the behaviour of the periods in the limit $\epsilon \rightarrow 0$ one can look to the direct evaluation of the period integrals or one can analyse their monodromies under $\epsilon \rightarrow e^{2\pi i}\epsilon$. For example, suppose we have two periods v_1 and v_2 , which under $\epsilon \rightarrow e^{2i\pi}\epsilon$ transform as

$$\begin{pmatrix} v_1 \\ v_2 \end{pmatrix} \rightarrow \begin{pmatrix} e^{2i\pi q} & 0 \\ ae^{2i\pi q} & e^{2i\pi q} \end{pmatrix} \begin{pmatrix} v_1 \\ v_2 \end{pmatrix} \quad (7.4)$$

with $q > 0$. Then [35]

$$v_1(\epsilon) = \epsilon^q(a_{-n}\epsilon^{-n} + \dots + a_0 + a_1\epsilon + \dots) \quad (7.5)$$

$$v_2(\epsilon) = \frac{a}{2\pi i} \log \epsilon v_1(\epsilon) + \epsilon^q(b_{-m}\epsilon^{-m} + \dots + b_0 + b_1\epsilon + \dots) \quad (7.6)$$

where the coefficients a_i and b_i are independent of ϵ . The value of the integers n, m can usually be deduced rather easily by inspection of the behaviour of the cycles and the integrated holomorphic form. For example, when both the cycle and the holomorphic form (at a generic point of the manifold) stay bounded when $\epsilon \rightarrow 0$, the period has a finite limit [35], and therefore cannot have poles.

As we will see, such expressions for the periods contain just enough information to obtain the rigid limit of the Kähler potential. With the exact solutions we only obtain some constants, be able to compare different bases, and show the compatibility of the two methods. The extra information of the exact solutions is of course necessary to calculate gravitational corrections.

7.2 Rigid limit of the first example

7.2.1 Expansion of $K3$ periods

The CY manifold of the first example has been analysed in section 5 as a $K3$ fibration. The modulus of the $K3$ was z , see (4.32), whose expansion in the rigid limit is

$$z = -1 + 2\tilde{\epsilon}(\tilde{u} - w) + \mathcal{O}(\tilde{\epsilon}^2) . \quad (7.7)$$

The periods of the $(3, 0)$ -form $\hat{\Omega}^{(2,0)}$, (5.3), were determined as integrals over integer cycles in the form $\hat{\vartheta}_I$ (see (5.10) and (5.12) with (5.20) for their explicit values) or as $\hat{\vartheta}'_I$ after the basis transformation (5.21). For this $K3$ manifold the ϵ -monodromy thus corresponds

to the monodromy around $z = -1$, i.e. \mathcal{M}_{-1} in (5.15) or (5.22). We can diagonalize this monodromy, obtaining that the ϵ dependence of the periods is of the form

$$\begin{aligned}\hat{\vartheta}'_0 &= \eta \sqrt{2\tilde{\epsilon}(\tilde{u} - w)} + \mathcal{O}(\tilde{\epsilon}^{\frac{3}{2}}) , \\ \hat{\vartheta}'_1 &= k_1 + \ell_1 \tilde{\epsilon}(\tilde{u} - w) + \mathcal{O}(\tilde{\epsilon}^2) , \\ 2\hat{\vartheta}'_2 + \hat{\vartheta}'_0 = \vartheta_0 + \vartheta_1 &= k_2 + \ell_2 \tilde{\epsilon}(\tilde{u} - w) + \mathcal{O}(\tilde{\epsilon}^2) .\end{aligned}\tag{7.8}$$

The last two periods have a regular behaviour, i.e. starting with a constant and a $\tilde{\epsilon}$ term. In the second example the one but leading terms will be of order $\tilde{\epsilon}^{2/3}$ such that the ϵ -monodromy diagonalization will be sufficient to distinguish the constant term from the one but leading term. Here, however, we need the explicit expansions. From the explicit expressions, referred to above, we can find that

$$\begin{aligned}\hat{\vartheta}'_0 &= \eta(1+z)^{\frac{1}{2}} F\left(\frac{1}{8}, \frac{3}{8}, \frac{1}{2}; 1+z\right) F\left(\frac{7}{8}, \frac{5}{8}, \frac{3}{2}; 1+z\right) \\ \hat{\vartheta}'_1 &= k_1 \left(F^2\left(\frac{1}{8}, \frac{3}{8}, \frac{1}{2}; 1+z\right) - (1+z) F^2\left(\frac{7}{8}, \frac{5}{8}, \frac{3}{2}; 1+z\right) \right) \\ 2\hat{\vartheta}'_2 + \hat{\vartheta}'_0 &= k_2 \left(F^2\left(\frac{1}{8}, \frac{3}{8}, \frac{1}{2}; 1+z\right) + (1+z) F^2\left(\frac{7}{8}, \frac{5}{8}, \frac{3}{2}; 1+z\right) \right) ,\end{aligned}\tag{7.9}$$

and

$$\begin{aligned}\eta &= \frac{1}{\pi^2}(1+i)(1-\sqrt{2})K_1^2 = -\frac{1}{2\pi^2} \frac{\Gamma^2(\frac{1}{8})\Gamma^2(\frac{3}{8})}{\Gamma^2(\frac{1}{2})} \\ k_1 &= \frac{i\eta}{\sqrt{2}} ; \quad \ell_1 = -\frac{13}{8}k_1 ; \quad k_2 = -\frac{\eta}{2} ; \quad \ell_2 = \frac{19}{8}k_2 .\end{aligned}\tag{7.10}$$

7.2.2 Rigid limit of CY periods.

The CY periods are obtained in section 5.2 by integrating $K3$ cycles over paths indicated in figure 3. Let us first consider their ϵ -monodromy. From (7.3) and (7.1) we see that the the conifold point does not change its position under $\epsilon \rightarrow e^{2\pi i}\epsilon$, but the large complex structure point makes a complete tour. This means that for the periods \mathcal{V}_v and the three \mathcal{T}_I (integrated over the circle), we just have to consider the ϵ -monodromy of the $K3$ fibre. On the other hand, the path for \mathcal{V}_{t_a, t_b} is deformed in its beginning and end point in the ζ -plane. In this deformation, the line crosses cuts, and thus on the new path one has to consider a different cycle of the fibre. To make this concrete, let us denote the path between e_0^\pm (or between 1 and $\tilde{\psi}_s$ in w -plane) by L_0 (with $e_0^+ \sim \frac{1}{\epsilon}$ now very large in the same direction, and e_0^- very small), and the line between e_1^\pm (or between 1 and \tilde{u} in w -plane) by L_1 . So for a cycle c on the path L_0 we first have to use the ϵ -monodromy of the fibre, i.e. $\mathcal{M}_{-1}^+ c$. Following then the path starting from the point 1, it now first makes a circle in a clockwise direction for large ζ . This can be deformed to first turning around the e_1^+ point, following the outer half of the L_1 contour first with $K3$ cycle $\mathcal{M}_{-1}^+ c$, and coming back after having crossed the cuts, thus with cycle c . Then this cycle c is making its tour on the $|\zeta| = 1$ circle, before finally

being transported on the outer part of L_0 to e_0^+ . On the inner part of the contour the same deformation takes place. Adding this we obtain that the $K3$ cycle c on path L_0 , denoted as $L_0(c)$ has ϵ monodromy

$$L_0(c) \rightarrow L_1 \left(\mathcal{M}_{-1}^{+'} c \right) - L_1(c) + 2T(c) + L_0(c) . \quad (7.11)$$

The difference $\mathcal{M}_{-1}^{+'}c - L_1(c)$ is proportional to the vanishing cycle in $z = -1$, and thus that part of the CY cycle can be written in terms of V_v . The result in the basis (5.29) is

$$v \rightarrow \mathcal{M}_{CY}^\epsilon v = \begin{pmatrix} & & & & & & \\ & \mathcal{M}_{-1}^{+'} & & & & & \\ & & 0 & 0 & 0 & & \\ & & 0 & 2 & 0 & & \\ & & 0 & 0 & 2 & & \\ & 0 & & & & \mathcal{M}_{-1}^{+'} & \\ & & & & & & \end{pmatrix} v . \quad (7.12)$$

This matrix can be brought in Jordan form by defining

$$\mathcal{T}'_2 = 2\mathcal{T}_2 + \mathcal{T}_v ; \quad \mathcal{V}'_2 = 2\mathcal{V}_2 + \mathcal{V}_v - \mathcal{T}_v . \quad (7.13)$$

Indeed, reordering to the basis

$$\mathcal{C}' = \{\mathcal{V}_v, \mathcal{T}_v, \mathcal{T}_1, \mathcal{V}_1, \mathcal{T}'_2, \mathcal{V}'_2\} , \quad (7.14)$$

the ϵ -monodromy matrix is

$$\mathcal{M}_{CY,J}^\epsilon = \begin{pmatrix} -1 & 0 & 0 & 0 & 0 & 0 \\ 0 & -1 & 0 & 0 & 0 & 0 \\ 0 & 0 & 1 & 0 & 0 & 0 \\ 0 & 0 & 2 & 1 & 0 & 0 \\ 0 & 0 & 0 & 0 & 1 & 0 \\ 0 & 0 & 0 & 0 & 2 & 1 \end{pmatrix} . \quad (7.15)$$

This allows us to write the following expressions for the periods:

$$\begin{pmatrix} \mathcal{V}_v \\ \mathcal{T}_v \\ \mathcal{T}_1 \\ \mathcal{V}_1 \\ \mathcal{T}'_2 \\ \mathcal{V}'_2 \end{pmatrix} = \begin{pmatrix} \tilde{\epsilon}^{1/2} \mathcal{A}_1(\tilde{\epsilon}) \\ \tilde{\epsilon}^{1/2} \mathcal{A}_2(\tilde{\epsilon}) \\ \mathcal{A}_3(\tilde{\epsilon}) \\ \frac{\log \tilde{\epsilon}}{\pi i} \mathcal{A}_3(\tilde{\epsilon}) + \mathcal{A}_4(\tilde{\epsilon}) \\ \mathcal{A}_5(\tilde{\epsilon}) \\ \frac{\log \tilde{\epsilon}}{\pi i} \mathcal{A}_5(\tilde{\epsilon}) + \mathcal{A}_6(\tilde{\epsilon}) \end{pmatrix} = \begin{pmatrix} \tilde{\epsilon}^{1/2} (V_1 + \mathcal{O}(\tilde{\epsilon})) \\ \tilde{\epsilon}^{1/2} (V_2 + \mathcal{O}(\tilde{\epsilon})) \\ -k_1 - \tilde{\epsilon} \ell_1(\tilde{u}) + \mathcal{O}(\tilde{\epsilon}^2) \\ -\frac{1}{\pi i} \log \tilde{\epsilon} (k_1 + \tilde{\epsilon} \ell_1(\tilde{u})) + k'_1 + \tilde{\epsilon} \ell'_1(\tilde{u}) + \mathcal{O}(\tilde{\epsilon}^2) \\ -k_2 - \tilde{\epsilon} \ell_2(\tilde{u}) + \mathcal{O}(\tilde{\epsilon}^2) \\ -\frac{1}{\pi i} \log \tilde{\epsilon} (k_2 + \tilde{\epsilon} \ell_2(\tilde{u})) + k'_2 + \tilde{\epsilon} \ell'_2(\tilde{u}) + \mathcal{O}(\tilde{\epsilon}^2) \end{pmatrix} , \quad (7.16)$$

where $\mathcal{A}_\Lambda(\tilde{\epsilon})$ stand for analytic functions of $\tilde{\epsilon}$. It is not immediately clear which of the coefficients k, k', ℓ, ℓ' are functions of \tilde{u} . However, using the expressions (7.8), most integrals (5.27) and (5.26) over the base space paths are easy to perform. For example, it is trivial

to see that k_1 and k_2 in the above expressions are the constants present in (7.8), and that $\ell_{1,2}(\tilde{u}) = \tilde{u}\ell_{1,2}$. When gravity is decoupled¹⁹,

$$\text{Tr}\phi^2 \sim u = \Lambda^2 \tilde{u} , \quad (7.17)$$

where ϕ is the adjoint scalar and u the modulus of the SW theory. One immediately obtains

$$\begin{aligned} V_1 &= \eta \frac{\sqrt{2}}{\pi} \int_1^{\tilde{u}} dw \sqrt{\frac{\tilde{u}-w}{1-w^2}} = \eta \frac{\sqrt{2}}{\pi\Lambda} \int_{\Lambda^2}^u dt \sqrt{\frac{u-t}{\Lambda^4-t^2}} = \eta \frac{a_D(u; \Lambda)}{\Lambda} , \\ V_2 &= \eta \frac{\sqrt{2}}{\pi} \int_{-1}^1 dw \sqrt{\frac{\tilde{u}-w}{1-w^2}} = \eta \frac{\sqrt{2}}{\pi\Lambda} \int_{-\Lambda^2}^{\Lambda^2} dt \sqrt{\frac{u-t}{\Lambda^4-t^2}} = \eta \frac{a(u; \Lambda)}{\Lambda} , \end{aligned} \quad (7.18)$$

where $a_D(u; \Lambda)$ and $a(u; \Lambda)$ are the $SU(2)$ Seiberg–Witten periods, in the form given in the original paper [7]. One may check that in the basis (a_D, a) , the monodromy M_u around the conifold, (C.10), restricted to the periods $\mathcal{V}_v, \mathcal{T}_v$, becomes the SW monodromy around the massless monopole point $u = \Lambda^2$,

$$\begin{pmatrix} 1 & 0 \\ -2 & 1 \end{pmatrix} . \quad (7.19)$$

The only integrals which need clarification are \mathcal{V}_1 and \mathcal{V}'_2 . We have to evaluate integrals of the form

$$I = \int_{e_0^-}^{e_0^+} \frac{d\zeta}{\zeta} f(x) \quad \text{with} \quad x = 2\tilde{\epsilon}(\tilde{u} - w) . \quad (7.20)$$

The function f is regular, i.e. can be expanded as $f(x) = \sum_{n=0}^{\infty} f_n x^n$, and we get

$$\begin{aligned} I &= -2 \log \tilde{\epsilon} \left(f(0) + 2\tilde{\epsilon} f'(0) \tilde{u} + \mathcal{O}(\tilde{\epsilon}^2) \right) \\ &\quad + 2 \int_0^1 \frac{dx}{x} (f(x) - f(0)) + 2\tilde{\epsilon} \tilde{u} \int_0^1 \frac{dx}{x} (f'(x) - f'(0)) + \mathcal{O}(\tilde{\epsilon}^2) . \end{aligned} \quad (7.21)$$

This allows one to obtain the expression of \mathcal{V}_1 , and one finds that k'_1 is indeed independent of $\tilde{\epsilon}$. Finally one has²⁰

$$\mathcal{V}'_2 = \frac{1}{2\pi i} \int_{e_0^-}^{e_0^+} \frac{d\zeta}{\zeta} (2\hat{\vartheta}'_2 + \hat{\vartheta}'_0) + \frac{1}{2\pi i} \left[- \int_{e_0^-}^{e_0^+} + \int_{e_1^-}^{e_1^+} + \oint_{|\zeta|=1} \right] \frac{d\zeta}{\zeta} \hat{\vartheta}'_0 . \quad (7.22)$$

In the second term the first two integrals add up to lines between e_1^- and e_0^- and between e_0^+ and e_1^+ . Because of the symmetry $\zeta \rightarrow \zeta^{-1}$ (which changes the sign of $\zeta^{-1}d\zeta$), the integral from e_0^+ to e_1^+ is equal to the first one. Because for the function which we are considering, there is only a square root cut between e_0^- and e_1^- (and no cut to $\zeta = 0$), these first two parts add up to an integral over a cycle surrounding the point e_0^- and e_1^- . That can be deformed to the circle $|\zeta| = 1$, and thus remains in (7.22) only the integral over $(2\hat{\vartheta}'_2 + \hat{\vartheta}'_0)$, evaluated

¹⁹This scaling would also have been obtained if from the start we were to leave the ratio between b_1 and b_2 in (4.3) arbitrary, as that would lead to an arbitrary scale in the ζ -plane, which can be identified with Λ in the Seiberg–Witten curves.

²⁰Note that in this example the path of T was the unit circle in the *clockwise* direction.

in the same way as for \mathcal{V}_1 . One checks then again that the constants in (7.16) agree with their earlier definition, and that k'_2 is independent of \tilde{u} .

We thus have for \mathcal{C}' the decomposition as in (2.11) with $a = 1/2$ and

$$v_0 = \begin{pmatrix} 0 \\ 0 \\ -k_1 \\ -\frac{1}{\pi i} k_1 \log \tilde{\epsilon} + k'_1 \\ -k_2 \\ -\frac{1}{\pi i} k_2 \log \tilde{\epsilon} + k'_2 \end{pmatrix}; \quad v_1 = \begin{pmatrix} V_1 \\ V_2 \\ 0 \\ 0 \\ 0 \\ 0 \end{pmatrix}; \quad v_2 = \begin{pmatrix} \mathcal{O}(\tilde{\epsilon}^{3/2}) \\ \mathcal{O}(\tilde{\epsilon}^{3/2}) \\ -\tilde{\epsilon} \ell_1 \tilde{u} + \mathcal{O}(\tilde{\epsilon}^2) \\ -\frac{1}{\pi i} \ell_1 \tilde{u} \tilde{\epsilon} \log \tilde{\epsilon} + \tilde{\epsilon} \ell'_1 \tilde{u} + \mathcal{O}(\tilde{\epsilon}^2) \\ -\tilde{\epsilon} \ell_2 \tilde{u} + \mathcal{O}(\tilde{\epsilon}^2) \\ -\frac{1}{\pi i} \ell_2 \tilde{u} \tilde{\epsilon} \log \tilde{\epsilon} + \tilde{\epsilon} \ell'_2 \tilde{u} + \mathcal{O}(\tilde{\epsilon}^2) \end{pmatrix}. \quad (7.23)$$

The intersection matrix in the basis \mathcal{C}' is

$$q' = \begin{pmatrix} 0 & 2 & 0 & 0 & 0 & 0 \\ -2 & 0 & 0 & 0 & 0 & 0 \\ 0 & 0 & 0 & 4 & 0 & 0 \\ 0 & 0 & -4 & 0 & 0 & -4 \\ 0 & 0 & 0 & 0 & 0 & 2 \\ 0 & 0 & 0 & 4 & -2 & 0 \end{pmatrix}; \quad q'^{-1} = \frac{1}{4} \begin{pmatrix} 0 & -2 & 0 & 0 & 0 & 0 \\ 2 & 0 & 0 & 0 & 0 & 0 \\ 0 & 0 & 0 & -1 & -2 & 0 \\ 0 & 0 & 1 & 0 & 0 & 0 \\ 0 & 0 & 2 & 0 & 0 & -2 \\ 0 & 0 & 0 & 0 & 2 & 0 \end{pmatrix}. \quad (7.24)$$

Observe that this is (up to a reordering and rescaling) nearly a canonical intersection matrix (see (2.2)). To obtain the canonical form, we only have to replace \mathcal{V}_1 by $\mathcal{V}'_1 \equiv \mathcal{V}_1 + 2\mathcal{T}'_2$.

The calculation of $\langle v_0 + \tilde{\epsilon}^{1/2} v_1 + v_2, \bar{v}_0 + \tilde{\epsilon}^{1/2} \bar{v}_1 + \bar{v}_2 \rangle$ does not immediately lead to the structure of (2.12). Indeed there is an extra term due to the ℓ -terms in v_2 :

$$\begin{aligned} \langle v, \bar{v} \rangle &= iM^2(\tilde{\epsilon}) + \frac{1}{2} |\tilde{\epsilon}| \left(V_2 \bar{V}_1 - V_1 \bar{V}_2 \right) + R(\tilde{\epsilon}, \tilde{u}, \tilde{\bar{u}}) + F(\tilde{\epsilon}, \tilde{u}) - \bar{F}(\tilde{\epsilon}, \tilde{\bar{u}}) \\ M^2(\tilde{\epsilon}) &= -i v_0^T q'^{-1} \bar{v}_0 = -\frac{1}{2\pi} \left(|k_1|^2 + 2|k_2|^2 \right) \log |\tilde{\epsilon}| + \text{Im} \left(\frac{1}{2} k_1 \bar{k}'_1 + k_2 \bar{k}'_2 - k_1 \bar{k}_2 \right) \\ R(\tilde{\epsilon}, \tilde{u}, \tilde{\bar{u}}) &= \mathcal{O}(\tilde{\epsilon}^2) \\ F(\tilde{\epsilon}, \tilde{u}) &= \tilde{\epsilon} \tilde{u} (f_1 + f_2 \log \tilde{\epsilon}). \end{aligned} \quad (7.25)$$

where f_1 and f_2 are constants. If we proceed to expand the Kähler potential $\mathcal{K} = -\log(-i \langle v, \bar{v} \rangle)$ as in (2.15) we find that

$$\begin{aligned} \mathcal{K}(\tilde{\epsilon}, \tilde{u}) &= -\log M^2(\tilde{\epsilon}) + \frac{|\tilde{\epsilon}|}{M^2(\tilde{\epsilon})} K(\tilde{u}, \tilde{\bar{u}}) + \mathcal{O}(\tilde{\epsilon}^2) + \frac{i}{M^2} F(\tilde{u}) - \frac{i}{M^2} \bar{F}(\tilde{\bar{u}}) \\ K &= \frac{i|\eta|^2}{2\Lambda^2} \left(a(u, \Lambda) \bar{a}_D(\bar{u}, \Lambda) - a_D(u, \Lambda) \bar{a}(\bar{u}, \Lambda) \right). \end{aligned} \quad (7.26)$$

The terms with F and \bar{F} amount to an irrelevant Kähler transformation, and the supergravity Kähler potential reduces to the Kähler potential of the rigid $SU(2)$ theory, with a multiplicative ‘renormalization’.

7.3 The $SU(3)$ rigid limit

7.3.1 Definition

In section 6 we have considered the Calabi–Yau manifold as a torus fibration. The embedding space was parametrized by (y, ξ, ζ, x) , and for each value of (ζ, x) the equation $y(\xi)$ defines a torus. This torus degenerates on two (one complex dimensional) surfaces in the (ζ, x) -space: on Σ' the β -cycles of the torus vanish, while on Σ the α cycles vanish. The latter is a genus-5 surface defined by the equation

$$\Sigma : P^2(x) - B'(\zeta) = 0 , \quad (7.27)$$

where $B'(\zeta)$ is defined in (3.18), while $P(x)$ is given in (4.29) in the alternative gauge where ψ_4 and ψ_1 take the place of I_1 and I_2 . In in the usual gauge they are expressed in (4.20), and we thus get

$$P(x) = 2x^3 - \frac{3}{2}\psi_0^4 x - (\psi_1 - \frac{1}{2}\psi_0^6) . \quad (7.28)$$

At the A_2 point (4.40), the equation for Σ thus degenerates to

$$x^6 - \psi_1 x^3 = 0 . \quad (7.29)$$

The $SU(3)$ rigid limit is thus reached when three sheets of the Riemann surface Σ coincide, or equivalently, when the CY considered as an elliptic fibration acquires an I_3 singularity according to the Kodaira classification (i.e. a curve of A_2 singularities). However, as some periods are ill defined in this limit, we have to specify how we approach this point. This has been defined in (4.41) with $\epsilon \rightarrow 0$ while keeping \tilde{u}_1 and \tilde{u}_0 finite. In the equation for the CY (4.28) we thus have

$$\begin{aligned} P(x) &= 2x^3 - \frac{3}{2}\epsilon^{\frac{2}{3}} (\tilde{u}_0^4 + \mathcal{O}(\epsilon)) x (-\psi_s)^{-\frac{1}{3}} - \sqrt{\epsilon\tilde{u}_1 - \psi_s} - \frac{\epsilon\tilde{u}_0^6}{2\sqrt{-\psi_s}} + \mathcal{O}(\epsilon^2) \\ B'(\zeta) &= \epsilon(\zeta + \frac{1}{\zeta}) - \psi_s . \end{aligned} \quad (7.30)$$

The choice of ϵ dependence keeps the branch points in the ζ -plane with vanishing v_b or v_a at finite positions, respectively given by (7.3), while the branch points with vanishing t_a and t_b , given in (7.1) are sent to infinity. This choice gives rise to light BPS states (namely D -3-branes wrapped around the basis cycles $V_{v_a}, V_{v_b}, T_{v_a}, T_{v_b}$) which can be identified as the massive gauge bosons and dyons of the pure $N = 2$ $SU(3)$ Yang–Mills theory. Furthermore, we will show that in this limit, local special geometry indeed reduces to $SU(3)$ rigid special geometry on the rigid moduli space parametrized by \tilde{u}_1 and \tilde{u}_0 , justifying the above choice of ϵ dependence.

In the region of moduli space under consideration, the paths in the x -plane defining the $K3$ 2-cycles v_a and v_b stretch between sheets of Σ_- , the branch of the $g = 5$ Riemann surface Σ given by the equation $P(x) + \sqrt{B'(\zeta)} = 0$. Rescaling as in (7.2) and

$$x = \tilde{\epsilon}^{1/3} (-\psi_s)^{1/6} \tilde{x} , \quad (7.31)$$

and expanding the square roots in (7.30) for finite ζ :

$$\Sigma_- : \tilde{x}^3 - \frac{3}{4}\tilde{u}_0^4\tilde{x} - \frac{1}{4}(\tilde{u}_0^6 + \tilde{u}_1) + \frac{1}{4}\left(\zeta + \frac{1}{\zeta}\right) + \mathcal{O}(\tilde{\epsilon}) = 0, \quad (7.32)$$

which is the equation for the genus-2 $SU(3)$ Seiberg–Witten Riemann surface. Thus we see that in the $SU(3)$ rigid limit, a genus-2 branch of our general genus-5 Riemann surface Σ degenerates and produces the Seiberg–Witten surface, with punctures ‘at infinity’, where the rest of the genus-5 surface is attached.

7.3.2 ϵ -expansion of periods and Kähler potential

Let us calculate this ‘ ϵ -monodromy’ for the Calabi–Yau periods corresponding to the 3-cycles (6.31). First note that the equation for the Calabi–Yau (4.28) with (7.30) is transformed (to an isomorphic equation) when $\epsilon \rightarrow e^{2i\pi}\epsilon$. By the transformation (7.31) one gets rid of this complication. But we also have to perform this transformation in the (3, 0) form (6.1)

$$\Omega^{(3,0)} = \frac{\tilde{\epsilon}^{1/3}(-\psi_s)^{1/6}}{(2\pi i)^3} \frac{d\zeta}{\zeta} \wedge d\tilde{x} \wedge \frac{1}{y} \frac{d\xi}{\xi}. \quad (7.33)$$

Therefore under the ϵ -monodromy

$$\Omega^{(3,0)} \rightarrow e^{2\pi i/3} \Omega^{(3,0)}. \quad (7.34)$$

So if the basis of cycles C is transformed as $C \rightarrow MC$, the corresponding periods \mathcal{C} transform as $\mathcal{C} \rightarrow \omega MC$ where $\omega = e^{2\pi i/3}$

To calculate the action of the monodromy on the cycles, we make use of their fibred structure. In the case at hand, the $K3$ 2-cycle fibres (at fixed ζ) as well as the base paths in the ζ -plane are transformed by the monodromy. The transformation of the base paths is easily obtained by following the $K3$ degeneration points in the ζ -plane when $\epsilon \rightarrow e^{2\pi i}\epsilon$. Only the path corresponding to V_{t_a} and V_{t_b} is affected. The monodromy of our basis of $K3$ 2-cycles (at fixed ζ) can be found analogously by making use of their fibred structure. Of the four base paths in the \tilde{x} -plane, only the ones corresponding to t_a and t_b are transformed. Finally, the torus cycles α and β at $\tilde{x} = 0$ transform as follows

$$\begin{pmatrix} \alpha \\ \beta \end{pmatrix} \rightarrow \begin{pmatrix} 1 & 0 \\ 1 & 1 \end{pmatrix} \begin{pmatrix} \alpha \\ \beta \end{pmatrix}. \quad (7.35)$$

Indeed, this can be seen, because the singular points in figure 4 are from (6.2) at

$$\xi_{\pm} = -\sqrt{-\psi_s}(1 + \mathcal{O}(\tilde{\epsilon})) \pm \sqrt{\tilde{\epsilon}(2\tilde{u}_1 + \tilde{u}_0^6)}. \quad (7.36)$$

Thus the two points interchange position under the epsilon monodromy. α is therefore the vanishing cycle, to be used in the Picard–Lefschetz formula (2.19).

For the $K3$ cycles we note that in figure 5 the inner points do not move, as the equation for these is now (7.32). The outer points are determined by Σ_+ , i.e.

$$\Sigma_+ : -1 + \tilde{\epsilon} \left(\tilde{x}^3 - \frac{3}{4} \tilde{u}_0 \tilde{x} - \frac{1}{4} (\tilde{u}_0^6 + \tilde{u}_1) - \frac{1}{4} \left(\zeta + \frac{1}{\zeta} \right) \right) + \mathcal{O}(\tilde{\epsilon}^2) = 0, \quad (7.37)$$

and the solutions rotate for small ϵ under the ϵ -monodromy. Therefore the v_a and v_b paths do not change, while for t paths the rotated cycles are re-expressed as²¹

$$t_{21} \rightarrow t_{31} - s_{23}^-. \quad (7.38)$$

This equation and its cyclic permutations with (6.10) and (6.14) give

$$\begin{pmatrix} v_a \\ v_b \\ t_a \\ t_b \end{pmatrix} \rightarrow M_{K3}^\epsilon \begin{pmatrix} v_a \\ v_b \\ t_a \\ t_b \end{pmatrix} = \begin{pmatrix} 1 & 0 & 0 & 0 \\ 0 & 1 & 0 & 0 \\ 0 & -1 & -1 & -1 \\ 1 & 1 & 1 & 0 \end{pmatrix} \begin{pmatrix} v_a \\ v_b \\ t_a \\ t_b \end{pmatrix} \quad (7.39)$$

For the CY cycles, we consider figure 6. As mentioned already, only the beginning and end points of the V_{t_a} and V_{t_b} cycles are (in lowest order) ϵ dependent. They make a complete tour in this plane. Hence, for all but V_{t_a} and V_{t_b} , we just have to take the $K3$ result. The remaining two are modified by circles around the origin and infinity, and we have to consider the monodromies (6.18) of the transported $K3$ cycles when crossing cuts. This is similar to the manipulations in (7.11). This leads to

$$\begin{pmatrix} V_{v_a} \\ V_{v_b} \\ V_{t_a} \\ V_{t_b} \\ T_{v_a} \\ T_{v_b} \\ T_{t_a} \\ T_{t_b} \end{pmatrix} \rightarrow M_{CY}^\epsilon \begin{pmatrix} V_{v_a} \\ V_{v_b} \\ V_{t_a} \\ V_{t_b} \\ T_{v_a} \\ T_{v_b} \\ T_{t_a} \\ T_{t_b} \end{pmatrix} = \begin{pmatrix} & & & & 0 & 0 & 0 & 0 \\ & & & & 0 & 0 & 0 & 0 \\ & & & & 0 & 1 & 2 & 2 \\ & & & & -1 & -1 & -2 & 0 \\ & & & & & & & M_{K3}^\epsilon \\ 0 & & & & & & & \end{pmatrix} \begin{pmatrix} V_{v_a} \\ V_{v_b} \\ V_{t_a} \\ V_{t_b} \\ T_{v_a} \\ T_{v_b} \\ T_{t_a} \\ T_{t_b} \end{pmatrix}. \quad (7.40)$$

The monodromy matrix of the periods has an extra factor ω as explained above.

We can bring this monodromy matrix for the periods in Jordan form

$$\mathcal{M}_{CY,J}^\epsilon = S \omega M_{CY}^\epsilon S^{-1} = \begin{pmatrix} \omega & & & & & & & \\ & \omega & & & & & & \\ & & \omega & & & & & \\ & & & \omega & & & & \\ & & & & 1 & 0 & & \\ & & & & -2 & 1 & & \\ & & & & & & \omega^2 & 0 \\ & & & & & & -2\omega^2 & \omega^2 \end{pmatrix} \quad (7.41)$$

²¹One should see from the monodromy that the torus β cycle above t_{12} is deformed to a β cycle above t_{31} and an α cycle above s_{23}^- .

by the transformation

$$\mathcal{C}' = \begin{pmatrix} \mathcal{V}_{v_a} \\ \mathcal{V}_{v_b} \\ \mathcal{T}_{v_a} \\ \mathcal{T}_{v_b} \\ \mathcal{T}'_{11} \\ \mathcal{V}'_{11} \\ \mathcal{T}'_{22} \\ \mathcal{V}'_{22} \end{pmatrix} = S\mathcal{C} = \begin{pmatrix} 1 & 0 & 0 & 0 & 0 & 0 & 0 & 0 \\ 0 & 1 & 0 & 0 & 0 & 0 & 0 & 0 \\ 0 & 0 & 0 & 0 & 1 & 0 & 0 & 0 \\ 0 & 0 & 0 & 0 & 0 & 1 & 0 & 0 \\ 0 & 0 & 0 & 0 & -\frac{i\omega^2}{\sqrt{3}} & \frac{i}{\sqrt{3}} & -\omega^2 & 1 \\ -\frac{i\omega^2}{\sqrt{3}} & \frac{i}{\sqrt{3}} & -\omega^2 & 1 & \frac{\omega^2}{3} & -1/3 & 0 & 0 \\ 0 & 0 & 0 & 0 & \frac{i\omega}{\sqrt{3}} & -\frac{i}{\sqrt{3}} & -\omega & 1 \\ \frac{i\omega}{\sqrt{3}} & -\frac{i}{\sqrt{3}} & -\omega & 1 & \frac{\omega}{3} & -\frac{1}{3} & 0 & 0 \end{pmatrix} \begin{pmatrix} \mathcal{V}_{v_a} \\ \mathcal{V}_{v_b} \\ \mathcal{V}_{t_a} \\ \mathcal{V}_{t_b} \\ \mathcal{T}_{v_a} \\ \mathcal{T}_{v_b} \\ \mathcal{T}_{t_a} \\ \mathcal{T}_{t_b} \end{pmatrix}. \quad (7.42)$$

We will explain the choice of names for the basis vectors of \mathcal{C}' . The first four basis vectors, eigenvectors of eigenvalues ω , correspond to integrals over $\{V_{v_a}, V_{v_b}, T_{v_a}, T_{v_b}\}$, i.e. related to the v_a and v_b cycles in $K3$. The last four are simpler in terms of the $K3$ cycles in Picard–Fuchs basis. Indeed, defining the periods on the $|\zeta| = 1$ circle (see the inverse of (6.29))

$$\begin{pmatrix} \mathcal{T}_{12} \\ \mathcal{T}_{21} \\ \mathcal{T}_{11} \\ \mathcal{T}_{22} \end{pmatrix} = \int_{|\zeta|=1} \frac{1}{2\pi i} \frac{d\zeta}{\zeta} \begin{pmatrix} \vartheta_{12} \\ \vartheta_{21} \\ \vartheta_{11} \\ \vartheta_{22} \end{pmatrix}. \quad (7.43)$$

Similarly we define \mathcal{V}_{11} and \mathcal{V}_{22}

$$\begin{aligned} \mathcal{V}_{11} &= \frac{1}{\sqrt{3}} (-\mathcal{V}_{v_a} + \omega\mathcal{V}_{v_b}) + i(\mathcal{V}_{t_a} - \omega\mathcal{V}_{t_b}) \\ \mathcal{V}_{22} &= \frac{1}{\sqrt{3}} (-\mathcal{V}_{v_a} + \omega^2\mathcal{V}_{v_b}) - i(\mathcal{V}_{t_a} - \omega^2\mathcal{V}_{t_b}), \end{aligned} \quad (7.44)$$

where \mathcal{V}_I are the integrals of the $(3, 0)$ form on V_I ²². The last four elements of \mathcal{C}' are

$$\begin{pmatrix} \mathcal{T}'_{11} \\ \mathcal{V}'_{11} \\ \mathcal{T}'_{22} \\ \mathcal{V}'_{22} \end{pmatrix} = a \begin{pmatrix} i\omega^2\mathcal{T}_{11} \\ i\omega^2\mathcal{V}_{11} + \frac{\omega^2}{\sqrt{3}}\mathcal{T}_{21} \\ -i\omega\mathcal{T}_{22} \\ -i\omega\mathcal{V}_{22} + \frac{\omega}{\sqrt{3}}\mathcal{T}_{12} \end{pmatrix}. \quad (7.45)$$

The complex transformation of basis between the periods \mathcal{C} corresponding to the cycles (6.31) and those in (7.42), i.e. $\mathcal{C}' = S\mathcal{C}$, changes the inner product in (2.3). The Kähler potential on the CY complex structure moduli space is thus

$$\mathcal{K} = -\log(-i\langle \mathcal{C}, \bar{\mathcal{C}} \rangle); \quad \langle \mathcal{C}, \bar{\mathcal{C}} \rangle = \mathcal{C}^T q^{-1} \bar{\mathcal{C}} = \mathcal{C}'^T q'^{-1} \bar{\mathcal{C}}', \quad (7.46)$$

²²It may be possible to deform paths in a way similar to what we did in the first example to combine these integrals to one of ϑ_{11} and ϑ_{22} .

with q in (6.32), and the anti-Hermitian matrix q' is given by

$$q'^{-1} = S^{-1T} q^{-1} \bar{S}^{-1} = \begin{pmatrix} Q^{-1} & & & \\ & \frac{7i}{\sqrt{3}} & 1 & 0 & 0 \\ & -1 & 0 & 0 & 0 \\ & 0 & 0 & \frac{-7i}{\sqrt{3}} & 1 \\ & 0 & 0 & -1 & 0 \end{pmatrix}. \quad (7.47)$$

This anti-Hermitian matrix has a $4 + 2 + 2$ block diagonal form with as upper block

$$Q = \begin{pmatrix} 0 & -1 & -2 & 1 \\ 1 & 0 & 1 & -2 \\ 2 & -1 & 0 & 0 \\ -1 & 2 & 0 & 0 \end{pmatrix}; \quad Q^{-1} = \frac{1}{3} \begin{pmatrix} 0 & 0 & 2 & 1 \\ 0 & 0 & 1 & 2 \\ -2 & -1 & 0 & -1 \\ -1 & -2 & 1 & 0 \end{pmatrix}. \quad (7.48)$$

From the monodromy, we read off the ϵ dependence of \mathcal{C}' :

$$\begin{pmatrix} \mathcal{V}_{v_a} \\ \mathcal{V}_{v_b} \\ \mathcal{T}_{v_a} \\ \mathcal{T}_{v_b} \\ \mathcal{T}'_{11} \\ \mathcal{V}'_{11} \\ \mathcal{T}'_{22} \\ \mathcal{V}'_{22} \end{pmatrix} = \begin{pmatrix} \tilde{\epsilon}^{1/3} \mathcal{A}_1(\tilde{\epsilon}) \\ \tilde{\epsilon}^{1/3} \mathcal{A}_2(\tilde{\epsilon}) \\ \tilde{\epsilon}^{1/3} \mathcal{A}_3(\tilde{\epsilon}) \\ \tilde{\epsilon}^{1/3} \mathcal{A}_4(\tilde{\epsilon}) \\ \mathcal{A}_5(\tilde{\epsilon}) \\ \frac{-1}{\pi i} \log \tilde{\epsilon} \mathcal{A}_5 + \mathcal{A}_6(\tilde{\epsilon}) \\ \tilde{\epsilon}^{2/3} \mathcal{A}_7(\tilde{\epsilon}) \\ \frac{-1}{\pi i} \log \tilde{\epsilon} \mathcal{A}_7 + \tilde{\epsilon}^{\frac{2}{3}} \mathcal{A}_8(\tilde{\epsilon}) \end{pmatrix} = \begin{pmatrix} \tilde{\epsilon}^{1/3} (V_1 + \mathcal{O}(\tilde{\epsilon})) \\ \tilde{\epsilon}^{1/3} (V_2 + \mathcal{O}(\tilde{\epsilon})) \\ \tilde{\epsilon}^{1/3} (V_3 + \mathcal{O}(\tilde{\epsilon})) \\ \tilde{\epsilon}^{1/3} (V_4 + \mathcal{O}(\tilde{\epsilon})) \\ k + \mathcal{O}(\tilde{\epsilon}) \\ \frac{-1}{\pi i} k \log \tilde{\epsilon} + k' + \mathcal{O}(\tilde{\epsilon}, \tilde{\epsilon} \log \tilde{\epsilon}) \\ \tilde{\epsilon}^{2/3} (\ell + \mathcal{O}(\tilde{\epsilon})) \\ \tilde{\epsilon}^{\frac{2}{3}} \left(\frac{-1}{\pi i} \ell \log \tilde{\epsilon} + \ell' + \mathcal{O}(\tilde{\epsilon}, \log \tilde{\epsilon}) \right) \end{pmatrix}, \quad (7.49)$$

where $\mathcal{A}_\Lambda(\tilde{\epsilon})$ stand for analytic functions of $\tilde{\epsilon}$. The absence of poles follows from the boundedness of the $K3$ periods (for bounded B') in the limit $\tilde{\epsilon} \rightarrow 0$; therefore, \mathcal{T}'_{11} and \mathcal{T}'_{22} have a finite limit, and \mathcal{V}'_{11} and \mathcal{V}'_{22} diverge logarithmically due to the factor

$$\int_{-\tilde{\epsilon}}^{-1/(\tilde{\epsilon})} \frac{1}{2\pi i} \frac{d\zeta}{\zeta} = \frac{-1}{\pi i} \log \tilde{\epsilon}. \quad (7.50)$$

The ‘constants’ V_A^0 , k , k' , ℓ and ℓ' are independent of $\tilde{\epsilon}$, but possibly still dependent on the rigid moduli \tilde{u}_i . However, k and k' must be independent of the rigid moduli: indeed, as can be seen easily from the explicit form of $\Omega^{(3,0)}$ (and the cycles), taking derivatives of the period integrals \mathcal{T}'_{11} and \mathcal{V}'_{11} with respect to the rigid moduli gives a positive power of $\tilde{\epsilon}$ times something which is at most logarithmically divergent when $\epsilon \rightarrow 0$. Therefore²³, these

²³Actually, we have to be a bit careful here. If our cycles were such that y was bounded from below in the limit $\epsilon \rightarrow 0$, the conclusion would have been obvious. However, for the cycles under consideration, this is not the case since they contain unavoidably a piece on which y is of order $\epsilon^{1/2}$ (this is the piece close to the surface of singularities which develops when $\epsilon \rightarrow 0$). The contribution of this piece can be estimated quite easily by going to the ALE approximation, which is allowed precisely in the problematic region. Thus, for the expressions we get by taking derivatives of the periods with respect to rigid moduli, the net contribution of this piece (including the extra factor ϵ^γ produced by taking the derivative) turns out to be proportional to $\epsilon^{1/3}$. So the conclusion holds.

derivatives are zero at $\epsilon = 0$. This is only possible if both k and k' are independent of the rigid moduli. This will also be clear from the explicit expressions in section 7.3.4.

The periods of v_a and v_b for finite values of ζ thus become small in the rigid limit, and the first four CY basis cycles to give rise to the light D -brane states corresponding to gauge bosons and dyons. We have found the structure announced in section 2.3. Indeed, we have for \mathcal{C}' the decomposition as in (2.11) with $a = 1/3$ and

$$v_0 = \begin{pmatrix} 0 \\ 0 \\ 0 \\ 0 \\ k \\ \frac{-1}{\pi i} k \log \tilde{\epsilon} + k' \\ 0 \\ 0 \end{pmatrix} ; \quad v_1 = \begin{pmatrix} V_1 \\ V_2 \\ V_3 \\ V_4 \\ 0 \\ 0 \\ 0 \\ 0 \end{pmatrix} ; \quad v_2 = \begin{pmatrix} 0 \\ 0 \\ 0 \\ 0 \\ 0 \\ \tilde{\epsilon}^{2/3} \ell \\ \tilde{\epsilon}^{2/3} \left(\frac{-1}{\pi i} \ell \log \tilde{\epsilon} + \ell' \right) \end{pmatrix} + \mathcal{O}(\tilde{\epsilon}) . \quad (7.51)$$

Note that the \tilde{u} -independence of k and k' is essential to fit in this scheme. Also important is the $4 + 2 + 2$ block diagonal structure of q' in (7.47), which implies the orthogonality of v_1 , v_2 and v_3 (the latter to order $\tilde{\epsilon}$), such that (2.12) is applicable. We find

$$M^2(\tilde{\epsilon}) = -iv_0^T q'^{-1} \bar{v}_0 = |k|^2 \left(\frac{7}{\sqrt{3}} - \frac{2}{\pi} \log |\tilde{\epsilon}| \right) + 2 \operatorname{Im} (k \bar{k}') , \quad (7.52)$$

to be used in (2.15) with

$$K = iv_1^T(\tilde{u}) \begin{pmatrix} Q^{-1} & 0 \\ 0 & 0 \end{pmatrix} \bar{v}_1(\tilde{u}) . \quad (7.53)$$

From the monodromy structure of the periods V_i and the light D -brane spectrum, we can identify this as a rigid limit corresponding to a $N = 2$ $SU(3)$ pure Yang–Mills theory in four dimensions. In the next section we show how the Seiberg–Witten solution of this gauge theory is retrieved.

7.3.3 The Seiberg–Witten expression of the rigid Kähler potential

For finite ζ we obtained (6.20)

$$\int_{s_{ij}^-} \Omega^{(2,0)} = (-\psi_s)^{-1/12} \frac{\sqrt{6}}{2\pi} \tilde{\epsilon}^{1/3} (\tilde{x}_{j-} - \tilde{x}_{i-}) + \mathcal{O}(\tilde{\epsilon}^{4/3}) . \quad (7.54)$$

So for a CY cycle $\gamma \wedge s_{ij}^-$ obtained by transporting s_{ij}^- along a path γ in the ζ -plane, we find to leading order

$$\int_{\gamma \wedge s_{ij}^-} \Omega^{(3,0)} = (-\psi_s)^{-1/12} \tilde{\epsilon}^{1/3} \int_{\gamma_{j-} - \gamma_{i-}} \lambda_{SW} , \quad (7.55)$$

where

$$\lambda_{SW} = \frac{\sqrt{6}}{2\pi} \frac{1}{2\pi i} \tilde{x} \frac{d\zeta}{\zeta} , \quad (7.56)$$

and

$$\gamma_{i^-} = \gamma \text{ lifted to sheet } i \text{ of } \Sigma_- . \quad (7.57)$$

Note that $\gamma_{j^-} - \gamma_{i^-}$ is always a closed cycle on the SW Riemann surface (single loop if γ is open, double loop if closed). Thus, since λ_{SW} is also precisely the Seiberg–Witten meromorphic 1-form, we find that the leading-order part of the first four CY periods (the V_i) are nothing but the Seiberg–Witten periods²⁴.

It is interesting to retrace how the normalization of the 1-form λ_{SW} arises. In fact, at the start, the Calabi–Yau (3,0)-form can be normalized quite arbitrarily, without losing holomorphy, by multiplying it with an arbitrary holomorphic function of the moduli, in particular, the rigid moduli. The normalization we adopted arises naturally from the Griffiths representation (3.2), and after integration over 2-cycles in the $K3$ gives rise to the meromorphic form λ_{SW} , (7.55). The normalization chosen in [23] is different: $\hat{\Omega}^{(3,0)} = \psi_0 \Omega^{(3,0)}$. With this normalization, since $\psi_0 \sim \tilde{\epsilon}^{1/6} \tilde{u}_0 (-\psi_s)^{-1/12}$, it would seem to give an incorrect (\tilde{u} -dependent) normalization of λ_{SW} . However, with this normalization, the leading term of the periods v_0 ((7.51)) would not be independent of the rigid modulus \tilde{u}_0 . To recover the rigid-limit scheme of section 2.3, one could make a Kähler transformation. This effectively amounts to changing the normalization of $\Omega^{(3,0)}$ with a factor that depends on the rigid moduli²⁵.

Finally, using (6.12) and the comment below it, it is not difficult to show that the intersection matrix of the first four Calabi–Yau basis cycles is precisely equal to minus the intersection matrix of the corresponding four SW cycles, as we did in the previous sections. Thus we find

$$K(\tilde{u}, \bar{\tilde{u}}) = i \int_{\gamma_A} \lambda_{SW} (Q^{-1})^{AB} \int_{\gamma_B} \bar{\lambda}_{SW} , \quad (7.58)$$

where $(\gamma_A)_{A=1\dots 4}$ is a basis of cycles of the SW Riemann surface and Q is its intersection matrix. This completes the identification of K with the Seiberg–Witten solution for the Kähler potential of $N = 2$ $SU(3)$ Yang–Mills theory in 4 dimensions.

7.3.4 Comparison with Picard–Fuchs basis.

Consider the ϵ expansion in the Picard–Fuchs basis. Using the expansion (4.41) writing everything in terms of ψ_s , ϵ and $\tilde{u}_{1,2}$, we have that ψ_0^6 is of order ϵ (we are in the ‘ $SU(3)$ sector’), and we have as leading order

$$r, s \approx \sigma_{\mp} \tilde{\epsilon}^{-1/2} ; \quad \sigma_{\mp} = \frac{\sqrt{2\tilde{u}_0^6 + \tilde{u}_1 - (\zeta + \frac{1}{\zeta})} \mp \sqrt{\tilde{u}_1 - (\zeta + \frac{1}{\zeta})}}{2\tilde{u}_0^6} . \quad (7.59)$$

Because r and s are large, we can use (B.27). The leading order is

$$\begin{aligned} \xi_1(r), \xi_1(s) &\approx B_1 \sigma_{\mp}^{-1/6} \tilde{\epsilon}^{-1/12} \\ \xi_2(r), \xi_2(s) &\approx B_2 \sigma_{\mp}^{-5/6} \tilde{\epsilon}^{-5/12} \end{aligned} \quad (7.60)$$

²⁴Note that higher-order ϵ -corrections (gravity effects) to, for example, the SW BPS mass formula can be calculated rather easily in this set-up. There are two sources of corrections: the surface itself is corrected as well as the meromorphic 1-form.

²⁵In the first example this question did not come up because ψ_0 is independent of \tilde{u} in a first approximation.

and (using $\tilde{u}_0 = (2\sigma_-\sigma_+)^{-1/6}$)

$$\vartheta \approx -\frac{3}{4\pi}(-\psi_s)^{-1/12}2^{1/6} \begin{pmatrix} \sigma_+^{-2/3}\tilde{\epsilon}^{1/3} \\ \sigma_-^{-2/3}\tilde{\epsilon}^{1/3} \\ \frac{B_1}{B_2} \\ \frac{B_2}{B_1}(\sigma_-\sigma_+)^{-2/3}\tilde{\epsilon}^{2/3} \end{pmatrix}. \quad (7.61)$$

With (7.54) and (6.14) we can write the first two periods as

$$\begin{aligned} \int_{v_a} \Omega^{(2,0)} &= (-\psi_s)^{-1/12} \frac{\sqrt{6}}{2\pi} \tilde{\epsilon}^{1/3} (\tilde{x}_{2-} - \tilde{x}_{1-}) \\ \int_{v_b} \Omega^{(2,0)} &= (-\psi_s)^{-1/12} \frac{\sqrt{6}}{2\pi} \tilde{\epsilon}^{1/3} (\tilde{x}_{3-} - \tilde{x}_{2-}). \end{aligned} \quad (7.62)$$

On the other hand, the left-hand sides can also be written in terms of σ_{\mp} in (7.59) using (6.29) and (7.61). We thus get

$$\begin{pmatrix} \tilde{x}_{2-} - \tilde{x}_{1-} \\ \tilde{x}_{3-} - \tilde{x}_{2-} \end{pmatrix} = -2^{-4/3} \sqrt{3} a \begin{pmatrix} -i\omega & i\omega^2 \\ -i & i \end{pmatrix} \begin{pmatrix} \sigma_+^{-2/3} \\ \sigma_-^{-2/3} \end{pmatrix}. \quad (7.63)$$

On the other hand, we have for the solutions of (7.32)

$$\begin{aligned} \tilde{x}_{1-} + \tilde{x}_{2-} + \tilde{x}_{3-} &= 0 \\ \tilde{x}_{1-}\tilde{x}_{2-} + \tilde{x}_{2-}\tilde{x}_{3-} + \tilde{x}_{3-}\tilde{x}_{1-} &= -\frac{3}{4}\tilde{u}_0^4 = -2^{-8/3}3(\sigma_-\sigma_+)^{-2/3} \\ \tilde{x}_{1-}\tilde{x}_{2-}\tilde{x}_{3-} &= \frac{1}{4}\tilde{u}_0^{12}(\sigma_-^2 + \sigma_+^2) = 2^{-4}(\sigma_+^{-2} + \sigma_-^{-2}). \end{aligned} \quad (7.64)$$

Combining these equations gives $a = 1$ as announced.

These results give an independent derivation of the ϵ -monodromy results of section 7.3.2. The first two basis vectors are a recombination of v_a and v_b , see (6.29). Knowing that the paths in the $K3$ fibrations over which these cycles are integrated are independent of ϵ to first order, shows that the corresponding four CY periods behave as $\epsilon^{1/3}$. Furthermore the last two $K3$ cycles are integrated over the ϵ -independent circle $|\zeta| = 1$, which gives the behaviours of the fifth and seventh period in (7.49). There integrals over the path which for $\epsilon \rightarrow 0$ stretches to infinite length leads to extra $\log \epsilon$ -terms, see (7.50). The fact that the leading term is the constant B_1/B_2 implies indeed that k is independent of the rigid moduli \tilde{u} . In fact, this leading term comes immediately from (7.45), and we get

$$k = i\omega^2 \left(-\frac{3}{4\pi}\right) (-\psi_s)^{-1/12} 2^{1/6} \frac{B_1}{B_2}. \quad (7.65)$$

7.4 Physical interpretation of the rigid limit

Physically, taking $\tilde{\epsilon} \rightarrow 0$ means decoupling gravity. By-now-standard arguments²⁶ [16, 1, 2, 13] suggest that the running of the gauge coupling of the $N = 2$ field theory requires $-2\tilde{\epsilon} \sim (\Lambda/M)^n$ for a pure $SU(n)$ theory, where M is the scale, of the order of the Planck mass M_P , at which the bare gauge coupling is defined, and Λ is the scale at which the gauge theory becomes strongly coupled. The \tilde{u} 's are related, in the semiclassical regime of the field theory, to the masses of the W -bosons, and remain finite while gravity is decoupled.

Our analysis leads, however, to some correction to this identification. By plugging the leading terms in the $\tilde{\epsilon}$ expansion of the Kähler potential into the supergravity action, we find that the kinetic terms of matter fields get a coefficient of order $\tilde{\epsilon}^{2/n}/\log \tilde{\epsilon}$. Thus comparing the Einstein and the gauge terms in the action one obtains that $(\Lambda/M_P)^2 \sim \tilde{\epsilon}^{2/n}/\log \tilde{\epsilon}$.

8 Conclusions

Within the framework of special Kähler geometry we have discussed some aspects of the rigid limit of $N = 2$ supergravity and type IIB string theory compactified on Calabi–Yau 3-folds which admit a $K3$ fibration.

The building blocks of the corresponding supersymmetric actions are the periods of the Calabi–Yau 3-forms. We have studied in detail their structure as fibrations of $K3$ periods.

We have found it convenient to study the complex structure moduli spaces, of the CY and of its $K3$ fibre, by taking advantage of its projective structure, i.e. without making specific ‘gauge choices’. Postponing the gauge-fixing is particularly useful for the derivation of the Picard–Fuchs equations and for the discussion of the singularities. For the latter, some desingularization is automatic in the non-gauge-fixed moduli space. The Picard–Fuchs equations used to determine the $K3$ periods are differential equations for the integrals of the $(2,0)$ form over the 2-cycles. Working in the full moduli space, i.e. keeping all moduli non-gauge fixed, allows one to take derivatives with respect to these parameters and then to re-express them as derivatives with respect to the invariant variables. Borrowing ideas from toric geometry, this method avoids however the introduction of the full toric geometry machinery and leads directly to lower-order differential equations. Some aspects of the structure of the solutions are explained from group-theoretical considerations of the full moduli space of the $K3$ fibre in appendix A.

The rigid limit is a description of the behaviour of the theory in the vicinity of a singularity in the moduli space, more specifically of a point in moduli space on a conifold line at infinity, where the Calabi–Yau manifold becomes singular on the whole fibration base space \mathbb{P}^1 ; indeed the $K3$ fibre has everywhere a conifold singularity. In previous works, starting with [2], the vicinity of this point was discussed by replacing the fibre by a non-compact

²⁶Originally relying on the chain of string dualities [11] $\text{Het}(K3 \times T_2) \xrightarrow{S} \text{IIA}(X) \xrightarrow{T} \text{IIB}(X^*)$ with X and X^* $K3$ -fibrations [16, 1] that relates the IIB modulus $\tilde{\psi}_s = -1/(2\tilde{\epsilon})$ to the heterotic dilaton S , whose v.e.v. gives the bare complexified gauge coupling: $\langle S \rangle = \frac{8\pi^2}{g_0^2} + i\theta_0$, by $\tilde{\psi}_s = \exp(S/2)$. Later, for example, in [13], remaining within IIA or IIB framework, only generic requirements for the gauge theory to emerge in the rigid limit were invoked.

resolution of its singularity, an ALE space. We have considered the decoupling of gravity and the reduction of special Kähler geometry from local to rigid without going first to this ALE approximation. The general procedure by which the limit is obtained is given in section 2.3, the relevant points being the splitting of the periods according to (2.11), and the special properties of the intersection matrices. The periods are split in a leading term v_0 , a first correction vanishing at the singularity v_1 and a remainder v_2 . The term v_0 should *not* depend on the *rigid* moduli. The term v_1 contains the periods which remain in the rigid limit, and the intersection matrices which we found imply orthogonality between v_0 and v_1 . The term v_0 is generated by cycles which do not occur in the ALE manifolds. These periods contain $\log \epsilon$ terms which give in the rigid limit (infinite Planck mass) a diverging renormalization of the rigid Kähler potential. The requirement that v_0 does not depend on the rigid moduli fixes the moduli dependence of the normalization (see section 7.3.3) of the meromorphic 1-form λ whose periods specify the rigid theory.

Indeed, in the ALE approach one starts with a particular normalization of the $(3, 0)$ -form, that correctly gives in the limit the meromorphic form known on the field theory side; one may wonder what fixes the freedom of rescaling it by a holomorphic function of moduli. The above requirement on v_0 does.

Now we point out a connection with the M -theory branes. In the second example we can consider the 3-cycles as circle fibrations over certain ‘2-branes’ in the (x, ζ) -space. The circles vanish at two (one complex dimensional) surfaces in this space: Σ (α cycles vanish) and Σ' (β cycles vanish). The 2-branes can therefore either be closed with trivial monodromy for the circle fibre, or open and ending on Σ or Σ' . The topology of the 2-brane can be either a disc (gives S^3 CY 3-cycle), a cylinder ($S^1 \times S^2$ 3-cycle) or a torus (T^3 3-cycle). This is very similar to the brane picture solutions of field theories via M theory. Combining Σ with the four-dimensional spacetime M_4 , we may think of a 5-brane $M_4 \times \Sigma$ (α fibre) or $M_4 \times \Sigma'$ (β fibre) on which the 2-branes end. There are several other similarities, like the conditions for a supersymmetric state, but we will not discuss them here.

This connection with the $2/5$ brane picture generalises, at least formally, the discussion in [2] for the $\epsilon \rightarrow 0$ ALE approximation. In the full Calabi–Yau geometry at finite ϵ the surface Σ is a genus-5 Riemann surface.

Seiberg–Witten Riemann surfaces corresponding to different rigid limits emerge as degenerating branches of the genus-5 Riemann surface, defined for all values of the CY moduli. From a physical point of view we expect to approach the rigid limit when we tune the moduli in such a way that the higher-genus Riemann surface develops a branch of almost coinciding sheets. Indeed, in this case we obtain a set of small-volume 3-cycles, namely those constructed from a disc or a cylinder stretched between the sheets that approach each other. Branes wrapped around these cycles are light compared to the Planck mass and decouple from gravity. Mathematically, the required degeneration of a branch of the higher-genus surface means that the Calabi–Yau develops a complex curve of singularities.

The results of this work can be used for a full expansion of the $N = 2$ supergravity action with vector multiplets, which starts with a rigid supersymmetry action. We have developed several methods useful for such an expansion. These allow us to go beyond the usual general statements of the embedding of a Riemann surface in a Calabi–Yau manifold.

Acknowledgments.

We had stimulating discussions of various parts of the paper with Sergio Cacciatori, Ansar Fayazuddin, Albrecht Klemm, Wolfgang Lerche, Koen Vermeir and Nick Warner.

The authors acknowledge the hospitality from several institutes where they could meet and discuss. In particular, CERN, the Ecole Normale Supérieure in Paris, Nordita in Copenhagen, and the Newton Institute in Cambridge.

A Remarks on the moduli space of the $K3$ fibre

In the main text we have been concerned with the calculation of the periods $\theta_I = \int_{c_I} \Omega^{(2,0)}$ for the $K3$ fibre occurring in Calabi–Yau manifolds that are $K3$ fibrations. We have focused on two specific examples but our aim has been to illustrate the general aspects of the construction. In particular, we have stressed the implication of the fibration structure of the Calabi–Yau 3-fold for its complex structure moduli space.

In the present appendix we review some general features of $K3$ moduli spaces and give some more details on issues that were just mentioned in the main text. In particular, we give the relation between our determination of the transcendental periods and the embedding of complex structure moduli in the complete $K3$ moduli space, which is well known to be a quaternionic homogeneous space quotiented by a discrete group, see [21].

A.1 Local geometry of the complex structure moduli of $K3$

As we emphasized in the main text (see the discussion in section 3.2), differently from the case of Calabi–Yau 3-folds where the moduli space of Kähler class deformations and complex structure deformations are independent factors in the full moduli space of the Calabi–Yau 3-fold, the moduli space \mathcal{M} for string compactifications on $K3$, which includes complexified Kähler class moduli and complex structure moduli, is the quotient of a single quaternionic coset manifold with respect to a global duality group [21]:

$$\mathcal{M} = \frac{O(4, 20)}{O(4) \times O(20)} / O(4, 20; \mathbf{Z}) . \quad (\text{A.1})$$

Within \mathcal{M} , the submanifold \mathcal{M}_c of complex structure deformations also has a local coset manifold structure:

$$\mathcal{M}_c = \frac{O(3, 19)^+}{(O(2) \times O(1, 19))^+} / O(3, 19; \mathbf{Z})^+ . \quad (\text{A.2})$$

Although the total number of $(1, 1)$ -forms is always 20, in every algebraic representation Σ_{K3} of the $K3$ surface only a subset of n_{tr} of them can be traced back to a change in the coefficients of the defining polynomial. The $(1, 1)$ -forms in the Picard lattice generate deformations that induce a change of the algebraic representation of the $K3$ surface. The number n_{tr} is related

to the rank of the Picard lattice, $\rho(\Sigma_{K3})$, and to that of the transcendental one²⁷:

$$\begin{aligned} 20 = h^{(1,1)} &= \rho(\Sigma_{K3}) + n_{\text{tr}} \\ \text{rank } Pic(\Sigma_{K3}) &= \rho(\Sigma_{K3}) \\ \text{rank } \Lambda^{\text{tr}}(\Sigma_{K3}) &= n_{\text{tr}} + 2 . \end{aligned} \tag{A.3}$$

If we use²⁸ the general ideas of mirror symmetry as it is formulated, for instance, in the context of toric geometry (see e.g. [32]) to each algebraic representation Σ_{K3} we can associate a mirror one Σ_{K3}^* in which the number of algebraic and non-algebraic deformations are interchanged: $n_{\text{tr}} \leftrightarrow \rho(\Sigma_{K3})$. For instance, we can take the algebraic representation $X_4[1, 1, 1, 1]$, for which, as discussed in section 3.2, the Picard number $\rho(\Sigma_{K3}) = 1$ and $n_{\text{tr}} = 19$, and we can mod it by the action of a group $G' = \mathbb{Z}_4^2$ of identifications that acts on the homogenous coordinates as in (4.7),(4.8). The resulting manifold is the mirror algebraic representation $X_4^*[1, 1, 1, 1]$, with $\rho(\Sigma_{K3}) = 19$ and $n_{\text{tr}} = 1$. Indeed the space of parameters of the defining quartic polynomial W , invariant under G' , is one dimensional, as described in section 4.1, see (4.6). As discussed in previous sections, $X_4^*[1, 1, 1, 1]$ is the $K3$ fibre for the CY 3-fold $X_8^*[1, 1, 2, 2, 2]$ and it is the first of the two examples of algebraic representations we have studied in this paper. The second example is provided by the 2-moduli algebraic representation in (4.19). In this case the identification group that restricts the available deformations to those listed above is the \mathbb{Z}_6 group acting on the homogeneous coordinates as described in (4.11) and (4.12). Using the methods of toric geometry one can regard (4.19) as the mirror manifold of the algebraic surface $X_{12}[1, 1, 4, 6]$ with no quotienting.

As already mentioned, our main interest has been in the period vector $\vec{\theta} = (\theta_1, \dots, \theta_{n_{\text{tr}}+2})$ containing the periods of the holomorphic 2-form $\Omega^{(2,0)}$ along a basis of transcendental cycles. The period vector $\vec{\theta}$ has thus $2 + n_{\text{tr}}$ components, while it depends on n_{tr} parameters, the parameters of the defining polynomial, that we name ‘algebraic complex structure deformations’. As a consequence of (A.2) and of the constraint in (3.10), which has signature $(2, n_{\text{tr}})$, we can immediately conclude that the moduli space of algebraic complex structure deformations is given by

$$\mathcal{M}_c^{\text{alg}} = \frac{O(2, n_{\text{tr}})}{O(2) \times O(n_{\text{tr}})} / O(2, n_{\text{tr}}; \mathbb{Z}) , \tag{A.4}$$

where $O(2, n_{\text{tr}}; \mathbb{Z})$ is named the duality group. It is obtained, according to a general analysis reviewed for instance in [36] as the semidirect product of the duality group of the potential Γ_W with the monodromy group Γ_M we derive from the Picard–Fuchs equations. Following a different way of reasoning, we could have anticipated that the $n_{\text{tr}} + 2$ periods (3.9) should satisfy some constraint equation from the very fact that they depend only on n_{tr} moduli parameters. The form of this constraint equation is fixed by the *a priori* knowledge of the local geometry of the moduli space encoded in (A.4). Indeed, as noted above, (3.10) is fully equivalent to the statement that the moduli space of algebraic complex structure variations is the coset manifold (A.4).

²⁷Note, however, that none of the forms in the transcendental lattice are of purely $(1, 1)$ -type.

²⁸We skip, however, some subtle points, see [21].)

A.2 The intersection matrix of the transcendental 2-cycles and the definition of the duality group $O(2, n_{\text{tr}}, \mathbf{Z})$

If we consider a generic $K3$ manifold, the complete second homology group $H_2(K3, \mathbf{Z})$ with integer coefficients admits a basis of 22 integral cycles e_A . Their intersection matrix is

$$C_{K3}^{\text{full}} \equiv e_A \cap e_B = \begin{pmatrix} \sigma_1 & 0 & 0 & & & \\ 0 & \sigma_1 & 0 & & & \\ 0 & 0 & \sigma_1 & & & \\ & 0 & & -C(E_8) & \mathbf{0} & \\ & & & \mathbf{0} & -C(E_8) & \end{pmatrix}, \quad (\text{A.5})$$

where σ_1 denotes the standard Pauli matrix and $C(E_8)$ the Cartan matrix of the E_8 Lie algebra. The above matrix is symmetric and its signature is clearly $(3, 19)$. Canonical integral homology bases are defined up to transformations M such that

$$M \text{ is integral valued, } \quad M C_{K3} M^T = C_{K3}. \quad (\text{A.6})$$

The matrices satisfying (A.6) are the elements of the relevant $O(3, 19, \mathbf{Z})$ group.

When we introduce a specific algebraic representation Σ_{K3} the integral homology lattice contains the transcendental sublattice²⁹ $\Lambda^{\text{tr}} \subset H_2(K3, \mathbf{Z})$, and the moduli space of the algebraic deformations is the following submanifold:

$$\mathcal{M}_c^{\text{alg}} = \frac{O(2, n_{\text{tr}})}{O(2) \times O(n_{\text{tr}})} / O(2, n_{\text{tr}}, \mathbf{Z}) \subset \frac{O(3, 19)}{O(2) \times O(1, 19)} / O(3, 19, \mathbf{Z}) \quad (\text{A.7})$$

of the complex structure moduli space. The appropriate embedding (A.7) of coset manifolds is determined by the lattice embedding $\Lambda^{\text{tr}} \subset H_2(K3, \mathbf{Z})$.

Now reconsider the constraint (3.10) for the case of a generic $K3$. Allowing non-integral changes of bases \mathcal{S} , and naming $\theta'_I = \mathcal{S}_I^J \theta'_J$, it can be reduced to the form

$$0 = \theta'_I \theta'_J \eta^{IJ} \quad \text{with} \quad \theta'_I = \mathcal{S}_I^J \theta'_J \quad \text{and} \quad \eta = (\mathcal{S} \mathcal{I} \mathcal{S}^T)^{-1}, \quad (\text{A.8})$$

where \mathcal{I} is \mathcal{I}_{IJ} with $I, J = 1, \dots, 2 + n_{\text{tr}}$, and the inverse intersection matrix η^{IJ} is

$$\eta^{IJ} = \begin{pmatrix} a & 0 & \\ 0 & b & \mathbf{0} \\ \mathbf{0} & & -\mathbf{h}^{ij} \end{pmatrix}, \quad (\text{A.9})$$

$a, b > 0$ being some positive real numbers and the $n_{\text{tr}} \times n_{\text{tr}}$ matrix \mathbf{h}^{ij} being symmetric with positive-definite signature (i.e. positive eigenvalues). We recognize in (A.8) the basic constraint describing the geometry of the Kähler homogeneous manifold $\mathcal{M}_c^{\text{alg}}$ of (A.7) in

²⁹We consider here the transcendental lattice in the cycles rather than the forms, the identification between those being made by the Poincaré duality.

Calabi–Visentini coordinates [37]. The standard solution to this constraint, often considered in the literature [18, 26, 38] is given by

$$\vec{\theta} = f(\mu) \begin{pmatrix} \frac{1}{2\sqrt{a}} (1 + \vec{Y}^2) \\ \frac{i}{2\sqrt{b}} (1 - \vec{Y}^2) \\ Y_i \end{pmatrix} \quad ; \quad \begin{matrix} i = 1, \dots, n_{\text{tr}} \\ \vec{Y}^2 \equiv Y_i Y_j h^{ij} \end{matrix} . \quad (\text{A.10})$$

$f(\mu)$ is some overall holomorphic function of the n_{tr} moduli coordinates μ and henceforth, by inversion, also of the functions $Y^i(\mu)$. These latter can be utilized as a set of *special coordinates* for the moduli manifold, in place of the original ones μ . The Kähler potential of $O(2, n_{\text{tr}})/ (O(2) \times O(n_{\text{tr}}))$ is given by

$$\mathcal{K}_{\text{tr}} = \log \left[\bar{\theta}'_I \theta'_J \eta^{IJ} \right] , \quad (\text{A.11})$$

showing that the overall holomorphic factor $f(\mu)$ is immaterial for the determination of the Kähler metric since it corresponds to a Kähler transformation.

The matrix \mathcal{G} in (3.7), that relates the algebraic and transcendental cycles to the basis e_A of $H_2(K3, \mathbf{Z})$, is integral. It transforms the intersection matrix to

$$\mathcal{G} C_{K3} \mathcal{G}^T = \hat{C}_{K3} = \begin{pmatrix} \mathcal{I} & 0 \\ 0 & \star \end{pmatrix} . \quad (\text{A.12})$$

The elements $M \in O(3, 19, \mathbf{Z})$, defined by (A.6), are mapped into matrices $\hat{M} = \mathcal{G} M \mathcal{G}^{-1}$ that satisfy

$$\hat{M} \hat{C}_{K3} \hat{M}^T = \hat{C}_{K3} . \quad (\text{A.13})$$

When \mathcal{G} has determinant ± 1 all the \hat{M} matrices are integral. If $|\det \mathcal{G}| > 1$, only a subset of them is integral.

The definition of the duality group $\Gamma_D = O(2, n_{\text{tr}}, \mathbf{Z})$ which is relevant for our discussion is provided by identifying such a group with the set of *integral* $(n_{\text{tr}} + 2) \times (n_{\text{tr}} + 2)$ matrices K satisfying the equation

$$\mathcal{I} = K \mathcal{I} K^T . \quad (\text{A.14})$$

We obtain an intersection $\gamma_D \cap O(3, 19, \mathbf{Z})$ by selecting those matrices $M \in O(3, 19, \mathbf{Z})$ that, after the transformation with \mathcal{G} have the following form:

$$\hat{M} \equiv \mathcal{G} M \mathcal{G}^{-1} = \begin{pmatrix} m & \mathbf{0} \\ \mathbf{0} & \mathbf{1} \end{pmatrix} , \quad \text{with } m \text{ integral and s.t. } \mathcal{I} = m \mathcal{I} m^T . \quad (\text{A.15})$$

The monodromy matrices corresponding to the various algebraic representations of the $K3$ surface belong to such an intersection. Indeed, on one hand they must transform integral cycles into integral cycles, so that they must be in $O(3, 19, \mathbf{Z})$. On the other hand, they must transform integral transcendental cycles into integral transcendental cycles, so that they must belong to $O(2, n_{\text{tr}}, \mathbf{Z})$.

For our 2 examples, $X_4^*[1, 1, 1, 1]$ and $X_{12}^*[1, 1, 4, 6]$, the transcendental lattices are of rank 3 and 4, respectively. We can embed the transcendental lattices in the integral lattice spanned by the first four entries in (A.5). Indeed, define the matrices

$$\mathcal{G}_{(1)} = \begin{pmatrix} 1 & 0 & 0 & 0 \\ 0 & 1 & 0 & 0 \\ 1 & -2 & 2 & 1 \\ 0 & 0 & -2 & 1 \end{pmatrix}; \quad \mathcal{G}_{(2)} = \begin{pmatrix} 1 & -1 & 0 & 1 \\ 0 & 0 & 1 & -1 \\ 0 & 0 & 0 & 1 \\ 0 & -1 & 0 & 0 \end{pmatrix}. \quad (\text{A.16})$$

These transform the upper 4×4 block of the intersection matrix to

$$\mathcal{G}_{(1)} \begin{pmatrix} \sigma_1 & 0 \\ 0 & \sigma_1 \end{pmatrix} \mathcal{G}_{(1)}^T = \begin{pmatrix} \mathcal{I}_{(1)} & 0 \\ 0 & -4 \end{pmatrix}; \quad \mathcal{G}_{(2)} \begin{pmatrix} \sigma_1 & 0 \\ 0 & \sigma_1 \end{pmatrix} \mathcal{G}_{(2)}^T = \mathcal{I}_{(2)}, \quad (\text{A.17})$$

where $\mathcal{I}_{(1)}$ and $\mathcal{I}_{(2)}$ are the intersection matrices which we found in the main text for the one-modulus and two-modulus $K3$ manifolds in an integral basis, given in (5.16) and (6.15), respectively. The Picard lattice consists of the 18 basis vectors not used in this transformation, and in the first example it also has the fourth basis vector after the transformation. The transformations which we gave are not unique. For instance, we have also found another embedding of $\mathcal{I}_{(2)}$ in the full $K3$ intersection matrix, involving basis vectors corresponding to an E_8 Cartan matrix in (A.5). Note that in both cases the intersection matrix has two positive eigenvalues.

A difference between the two examples is the determinant of \mathcal{G} . For the first example the determinant is 16, while for the second one it is 1. Therefore in the second example the transcendental and algebraic lattices have as direct sum the full lattice $H^2(K3, \mathbf{Z})$, while this is not the case for the first example, where some elements of $H^2(K3, \mathbf{Z})$ can not be written as a linear combination of the basis vectors of both lattices with integer coefficients.

A.3 Embedding the monodromy group into $O(2, n_{\text{tr}}, \mathbf{z})$ and special features of the cases $n_{\text{tr}} = 1, 2$

Given an explicit algebraic representation Σ_{K3} , the Picard–Fuchs approach to be discussed in appendix B leads to a system of linear partial differential equations in n_{tr} variables that is satisfied by each component of the $2 + n_{\text{tr}}$ -dimensional period vector $\vec{\theta}$. Hence the period vector can be identified with a *basis of solutions* to this system. The analytic continuation of a particular solution around each singular point of the differential system produces the monodromy group generators. Such monodromy generators will be integer-valued pseudo-orthogonal matrices when the solution basis is brought to the integral basis where the intersection matrix is \mathcal{I} . Consequently, once a general solution of the differential system has been obtained we have to look for changes of bases that bring the monodromy matrices to be integral and such that they leave some suitable intersection matrix \mathcal{I} invariant. The form of \mathcal{I} is not determined by the Picard–Fuchs differential system so that we have to resort to different sources of information. In the main text we have obtained \mathcal{I} by a direct construction of the basis of transcendental cycles.

Summarizing our discussion, the Picard–Fuchs problem in the case of the $K3$ fibre reduces to a uniformization problem. Differently from the case of Calabi–Yau 3-folds where even the local geometry of the moduli space is not known *a priori* (apart from the fact that it is of the local special Kähler type) so that the solution of the Picard–Fuchs equations not only provides a basis of special coordinates but also determines the form of the metric, in the $K3$ case the moduli space is known *a priori*, but what we have to determine is the relation between the special coordinates Y^i (obtained by solving the algebraic constraint satisfied by the periods) and the ‘Landau–Ginzburg’ coordinates μ appearing explicitly in the potential.

For $n_{\text{tr}} \geq 3$ there is nothing more that can be stated in general. However, for $n_{\text{tr}} = 1$ and $n_{\text{tr}} = 2$ there is some more *a priori* information due to the accidental isomorphisms

$$\frac{SO(2, 1)}{SO(2)} \sim \frac{SL(2, \mathbb{R})}{SO(2)} \sim \frac{SU(1, 1)}{U(1)} \quad (\text{A.18})$$

and³⁰

$$\frac{SO(2, 2)}{SO(2) \otimes SO(2)} \sim \frac{SL(2, \mathbb{R})_1}{SO(2)} \otimes \frac{SL(2, \mathbb{R})_2}{SO(2)} \sim \frac{SU(1, 1)_1}{U(1)} \otimes \frac{SU(1, 1)_2}{U(1)}. \quad (\text{A.19})$$

In the case $n_{\text{tr}} = 1$, as in our first example of algebraic $K3$ manifold $X_4^*[1, 1, 1, 1]$, we learn from this observation that the period vector $\vec{\theta}$, which transforms as a triplet of $SO(2, 1)$ must be expressible in terms of two functions (U_1, U_2) in the doublet of $SU(1, 1)$. Of course, the triplet of $SO(2, 1)$, i.e. the $J = 1$ representation, corresponds to a symmetric product of the fundamental representation of $SU(1, 1)$, the doublet, with itself. Let us be explicit. In the case $n_{\text{tr}} = 1$, it is convenient to choose in the inverse intersection matrix η of (A.9) $a = b = 1$ and $h = 1$; the period vector is given by (A.10) with these specific choices. Explicitly if the transformation of the doublet vector is

$$\begin{pmatrix} U_1 \\ U_2 \end{pmatrix} \rightarrow \begin{pmatrix} \alpha & \beta \\ \gamma & \delta \end{pmatrix} \begin{pmatrix} U_1 \\ U_2 \end{pmatrix} \quad ; \quad \begin{pmatrix} \alpha & \beta \\ \gamma & \delta \end{pmatrix} \in SU(1, 1) \quad (\text{A.20})$$

the transformation of triplet $\vec{\theta}$ will be

$$\begin{pmatrix} \theta_1 \\ \theta_2 \\ \theta_3 \end{pmatrix} \rightarrow \begin{pmatrix} \frac{1}{2}(\alpha^2 + \beta^2 + \gamma^2 + \delta^2) & \frac{i}{2}(\alpha^2 - \beta^2 + \gamma^2 - \delta^2) & \alpha\beta + \gamma\delta \\ \frac{-i}{2}(\alpha^2 + \beta^2 - \gamma^2 - \delta^2) & \frac{1}{2}(\alpha^2 - \beta^2 - \gamma^2 + \delta^2) & -i(\alpha\beta - \gamma\delta) \\ \alpha\gamma + \beta\delta & i(\alpha\gamma - \beta\delta) & \alpha\delta + \beta\gamma \end{pmatrix} \begin{pmatrix} \theta_1 \\ \theta_2 \\ \theta_3 \end{pmatrix}. \quad (\text{A.21})$$

This amounts to expressing $\vec{\theta}$ in terms of \vec{U} as follows:

$$\vec{\theta} = f(\mu) \begin{pmatrix} \frac{1}{2}(1 + \vec{Y}^2) \\ \frac{i}{2}(1 - \vec{Y}^2) \\ Y \end{pmatrix} = \begin{pmatrix} \frac{1}{2}(U_2^2 + U_1^2) \\ \frac{i}{2}(U_2^2 - U_1^2) \\ U_1 U_2 \end{pmatrix}. \quad (\text{A.22})$$

³⁰The isomorphisms between $SL(2, \mathbb{R})$ and $SU(1, 1)$ is simply realized on doublets (P_1, P_2) of the former and (U_1, U_2) of the latter by the Cayley transformation $U_1 = P_1 + iP_2$ and $U_2 = P_1 - iP_2$.

We have seen in the main text how the above relation is retrieved while computing the periods directly. Indeed, the reader should compare the present discussion with (5.7) and (5.12). We can retrieve the same relation by solving the third order Picard–Fuchs equation. This will be done in appendix B. In that process we will also discover the meaning of the functions (U_1, U_2) . They form a basis of solutions for a second-order hypergeometric equation to which we are able to reduce the original third-order one. The monodromy of this hypergeometric equation will be generated by 2×2 matrices belonging to the $SU(1, 1)$ group. Their 3×3 image via the map (A.22) consists of integer-valued $O(2, 1)$ matrices.

Let us now turn our attention to the $n_{\text{tr}} = 2$ case, which applies to our second example, $X_{12}^*[1, 1, 4, 6]$. In this case the appropriate choices for the integers a, b and for the 2×2 matrix \mathbf{h}_{ij} are

$$2 \text{ modulus } K3 \quad : \quad a = 2, b = 6, \quad \mathbf{h}_{ij} = \begin{pmatrix} 2 & -1 \\ -1 & 2 \end{pmatrix} = A_2 \text{ Cartan matrix.} \quad (\text{A.23})$$

Indeed, consider the transcendental intersection matrix $\mathcal{I}_{(2)}$, i.e. (6.15). If we change basis with the matrix

$$\mathcal{N} = \begin{pmatrix} 1 & 1 & 1 & -1 \\ -1 & 1 & 3 & 3 \\ 1 & 0 & 0 & 0 \\ 0 & 1 & 0 & 0 \end{pmatrix}, \quad (\text{A.24})$$

the intersection form assumes the Calabi–Visentini form (A.9), with the choices (A.23):

$$\eta^{(2)} \equiv \mathcal{N} \mathcal{I} \mathcal{N}^T = \begin{pmatrix} 2 & 0 & 0 & 0 \\ 0 & 6 & 0 & 0 \\ 0 & 0 & -2 & 1 \\ 0 & 0 & 1 & -2 \end{pmatrix}. \quad (\text{A.25})$$

In this case, however, the Calabi–Visentini basis cannot be an integral basis for the transcendental lattice. Indeed, the determinant of \mathcal{N} is 6; therefore it does not transform elementary cycles to a new basis of elementary cycles. So in the basis (A.25) the monodromy generators are not necessarily integral. In fact, one can show that there does not exist an integer basis transformation matrix M with integer inverse, i.e. with $\det M = \pm 1$, which transforms the intersection matrix $\mathcal{I}_{(2)}$ in (6.15) to one of the form (A.9).

Though it is not an integral basis, the Calabi–Visentini basis defined by (A.25) is a perfectly appropriate basis to discuss the solution of Picard–Fuchs equations and their group-theoretical structure. Once that is done it suffices to change back basis with the matrix \mathcal{N} and all the considerations we are about to make are transferred to an integral basis.

This being clarified, we realize the real pseudo-orthogonal group $O(2, 2, \mathbb{R})$ as the set of real matrices M satisfying the equation:

$$M \eta^{(2)} M^T = \eta^{(2)} \quad (\text{A.26})$$

The integral subgroup $O(2, 2, \mathbb{Z}) \subset O(2, 2, \mathbb{R})$ is, however, given by those M that are integral in the integral basis in which the intersection is $\mathcal{I}_{(2)}$: that is, $\mathcal{N} M \mathcal{N}^{-1}$ must be integral.

Relying on the isomorphism (A.19) we infer from the fact that the four-dimensional fundamental representation of $O(2, 2)$ is given by the symmetric tensor product of the two fundamental representations of $SL(2, \mathbb{R})_1$ and $SL(2, \mathbb{R})_2$ that the period vector $\vec{\theta}$ should be expressible in terms of two doublets (P_1, P_2) and (Q_1, Q_2) of the two factors.

The explicit group isomorphism is expressed by mapping

$$\begin{pmatrix} a_1 & b_1 \\ c_1 & d_1 \end{pmatrix} \otimes \begin{pmatrix} 1 & 0 \\ 0 & 1 \end{pmatrix} \in SL(2, \mathbb{R})_1 \otimes SL(2, \mathbb{R})_2 \quad (\text{A.27})$$

into the $O(2, 2, \mathbb{R})$ element

$$\left(\begin{array}{cccc} \frac{a_1+d_1}{2} & \frac{\sqrt{3}(-b_1+c_1)}{2} & \frac{-a_1-\sqrt{3}b_1-\sqrt{3}c_1+d_1}{4} & \frac{a_1-d_1}{2} \\ \frac{b_1-c_1}{2\sqrt{3}} & \frac{a_1+d_1}{2} & \frac{-3a_1+\sqrt{3}b_1+\sqrt{3}c_1+3d_1}{12} & \frac{-(b_1+c_1)}{2\sqrt{3}} \\ -\frac{b_1+c_1}{\sqrt{3}} & -a_1+d_1 & \frac{3a_1-\sqrt{3}b_1+\sqrt{3}c_1+3d_1}{6} & \frac{b_1-c_1}{\sqrt{3}} \\ \frac{3a_1-\sqrt{3}b_1-\sqrt{3}c_1-3d_1}{6} & \frac{-a_1-\sqrt{3}b_1-\sqrt{3}c_1+d_1}{2} & \frac{-b_1+c_1}{\sqrt{3}} & \frac{3a_1+\sqrt{3}b_1-\sqrt{3}c_1+3d_1}{6} \end{array} \right), \quad (\text{A.28})$$

and

$$\begin{pmatrix} 1 & 0 \\ 0 & 1 \end{pmatrix} \otimes \begin{pmatrix} a_2 & b_2 \\ c_2 & d_2 \end{pmatrix} \in SL(2, \mathbb{R})_1 \otimes SL(2, \mathbb{R})_2 \quad (\text{A.29})$$

into the $O(2, 2, \mathbb{R})$ element

$$\left(\begin{array}{cccc} \frac{a_2+d_2}{2} & \frac{\sqrt{3}(-b_2+c_2)}{2} & \frac{a_2-\sqrt{3}b_2-\sqrt{3}c_2-d_2}{4} & \frac{-a_2+d_2}{2} \\ \frac{b_2-c_2}{2\sqrt{3}} & \frac{a_2+d_2}{2} & \frac{-3a_2-\sqrt{3}b_2-\sqrt{3}c_2+3d_2}{12} & \frac{b_2+c_2}{2\sqrt{3}} \\ -\frac{b_2+c_2}{\sqrt{3}} & -a_2+d_2 & \frac{3a_2+\sqrt{3}b_2-\sqrt{3}c_2+3d_2}{6} & \frac{-b_2+c_2}{\sqrt{3}} \\ \frac{-3a_2-\sqrt{3}b_2-\sqrt{3}c_2+3d_2}{6} & \frac{-a_2+\sqrt{3}b_2+\sqrt{3}c_2+d_2}{2} & \frac{b_2-c_2}{\sqrt{3}} & \frac{3a_2-\sqrt{3}b_2+\sqrt{3}c_2+3d_2}{6} \end{array} \right). \quad (\text{A.30})$$

The two matrices above commute, and their product is a generic element of $O(2, 2)$. This embedding fixes the relation between the period vector and the two doublet basis:

$$\begin{aligned} \vec{\theta} &= f(\mu) \begin{pmatrix} \frac{1}{2\sqrt{2}}(1 + 2Y_1^2 + 2Y_2^2 - 2Y_1Y_2) \\ \frac{i}{2\sqrt{6}}(1 - 2Y_1^2 - 2Y_2^2 + 2Y_1Y_2) \\ Y_1 \\ Y_2 \end{pmatrix} \\ &= \begin{pmatrix} \frac{1}{\sqrt{2}} & 0 & 0 & 0 \\ 0 & \frac{1}{\sqrt{6}} & 0 & 0 \\ 0 & 0 & \sqrt{\frac{2}{3}} & 0 \\ 0 & 0 & \frac{1}{\sqrt{6}} & \frac{1}{\sqrt{2}} \end{pmatrix} \begin{pmatrix} -\frac{1}{2}(P_1Q_2 + P_2Q_1) \\ -\frac{i}{2}(P_1Q_1 - P_2Q_2) \\ \frac{1}{2}(P_1Q_1 + P_2Q_2) \\ -\frac{1}{2}(P_1Q_2 - P_2Q_1) \end{pmatrix}. \end{aligned} \quad (\text{A.31})$$

Going to the $SU(1, 1)_1 \otimes SU(1, 1)_2$ basis of two doublets (U_1, U_2) and (V_1, V_2) , a little algebra shows that (A.31) provides the identifications

$$\begin{aligned} f &= \frac{i}{2} U_1 V_1, \\ \begin{pmatrix} Y^1 \\ Y^2 \end{pmatrix} &= \frac{1}{f(\mu)} \begin{pmatrix} \sqrt{\frac{2}{3}} & 0 \\ \frac{1}{\sqrt{6}} & \frac{1}{\sqrt{2}} \end{pmatrix} \begin{pmatrix} \frac{1}{4}(U_2 V_1 + U_1 V_2) \\ \frac{1}{4}(U_2 V_1 - U_1 V_2) \end{pmatrix} \end{aligned} \quad (\text{A.32})$$

In the next section we shall also retrieve these identifications from the solutions of the Picard–Fuchs equations obtaining the functions (U_1, U_2) , (V_1, V_2) in terms of the solutions for a pair of second-order differential equations.

B Picard–Fuchs equations

There are several ways to obtain the differential equations on the periods. One way would be to consider first the derivatives of fundamental $(2,0)$ -form $\Omega^{(2,0)}$ with respect to the moduli. This can be expressed in terms of the $(1,1)$ forms. Then the derivatives of the $(1,1)$ and $(0,2)$ forms can be expressed again in a basis of all 2-forms. These differential equations can be combined to give third-order differential equations on the fundamental $(2,0)$ form. We have followed this procedure at first, and the results are the same as the differential equations which we will present below.

We will present a simpler method, which is inspired by the one used in toric geometry [32]. We will, however, not need the full machinery of toric geometry and arrive at lower-order differential equations. A main part of the method consists in keeping all moduli non-gauge fixed. That allows one to take derivatives with respect to them which can be compared. The derivatives with respect to these parameters are then expressed as derivatives with respect to the invariant variables. To do so, we should first take a representation of the $(2,0)$ form which is gauge invariant. In the Griffiths representation of this form, W is gauge invariant, but the volume form ω is not invariant under the rescalings (it is invariant under the shifts respecting the weights). Therefore we should multiply first with a function of the moduli which compensates for the scaling weights of $x_0x_3x_4x_5$.

B.1 First example

B.1.1 The Picard–Fuchs equation

In the first example the scaling weights of the volume form can be compensated for by a factor ψ_0 . Thus we consider

$$\hat{\theta}(\mu) = \int \hat{\Omega}^{(2,0)} \propto \int \frac{\psi_0}{W^{(1)}(B', b_3, b_4, b_5)} \omega_{K3}, \quad (\text{B.1})$$

where $W^{(1)}$ is given in (4.4) and μ is the truly invariant variable

$$\mu = \frac{\psi_0}{(B'b_3b_4b_5)^{1/4}}; \quad z = -\mu^{-4}, \quad (\text{B.2})$$

for which the global identifications $\mu \sim i\mu \sim -\mu \sim -i\mu$ remain to be made. It is now straightforward to obtain *Picard–Fuchs equation* by writing

$$4^4 \frac{\partial}{\partial B'} \frac{\partial}{\partial b_3} \frac{\partial}{\partial b_4} \frac{\partial}{\partial b_5} \hat{\vartheta}(\mu) = \left(\psi_0 \frac{\partial^4}{\partial \psi_0^4} \right) \frac{1}{\psi_0} \hat{\vartheta}(\mu). \quad (\text{B.3})$$

On functions of μ we have

$$\begin{aligned} B' \frac{\partial}{\partial B'} &= b_3 \frac{\partial}{\partial b_3} = b_4 \frac{\partial}{\partial b_4} = b_5 \frac{\partial}{\partial b_5} = -\frac{\mu}{4} \frac{\partial}{\partial \mu} \\ \frac{\partial}{\partial \psi_0} &= \frac{1}{(B' b_3 b_4 b_5)^{1/4}} \frac{\partial}{\partial \mu} . \end{aligned} \tag{B.4}$$

Therefore (B.3) reduces to

$$\left(\mu \frac{\partial}{\partial \mu} \right)^4 \hat{\vartheta} = \mu \frac{\partial^4}{\partial \mu^4} \frac{1}{\mu} \hat{\vartheta} . \tag{B.5}$$

If we introduce the rescaled period $\vartheta(\mu) = \hat{\vartheta}(\mu)/\mu$, it can be immediately verified that the above (B.5) can be rewritten as the operator $\mu \frac{\partial}{\partial \mu}$ acting over the third-order equation:

$$\left(\frac{d^3}{d\mu^3} - \frac{6\mu^3}{1-\mu^4} \frac{d^2}{d\mu^2} - \frac{7\mu^2}{1-\mu^4} \frac{d}{d\mu} - \frac{\mu}{1-\mu^4} \right) \vartheta(\mu) = 0 . \tag{B.6}$$

Hence we have obtained just in one simple stroke the third-order equation that one can derive through the traditional method of considering the first-order system satisfied by the periods.

B.1.2 Solutions in terms of hypergeometric functions.

Equation (B.6) is a Fuchsian equation, with regular singular points located at infinity and in the zeros of the denominator, i.e. for $\mu^4 = 1$. It admits obviously three linearly independent solutions. The monodromy generators corresponding to non-trivial paths encircling the singular points have a matrix action on the chosen 3-vector of solutions $\vec{\vartheta}(\mu)$: $\vec{\vartheta} \rightarrow M_P \vec{\vartheta}$, where P is one of the singular points. Moreover, the $K3$ defining potential is invariant under the \mathbb{Z}_4 symmetry generated by $\mu \rightarrow i\mu$, that acts on the solution vector as a 3×3 matrix satisfying $A^4 = \mathbf{1}_{3 \times 3}$.

It was observed in [30] that the solution of (B.6) can be expressed in terms of the solution of a second-order differential equation, due to the crucial fact that the so-called W_3 -invariant of the third-order equation vanishes. It turns thus out that a generic solution of (B.6) is of the form

$$\vartheta(\mu) = \frac{1}{\sqrt{1-\mu^4}} \left(\frac{dY}{d\mu} \right)^{-1} (a + bY + cY^2) , \tag{B.7}$$

where a, b, c are constants and $Y(\mu)$ satisfies the Schwarzian equation

$$\{Y; \mu\} = \frac{\mu^2}{2} \frac{\mu^4 + 11}{(1-\mu^4)^2} . \tag{B.8}$$

This property of the PF equation is related geometrically to the fact that any basis θ_I of transcendental periods of the $K3$ (i.e. any basis of solutions to the PF equation) satisfy the quadratic constraint (3.10), where \mathcal{I}^{IJ} is the inverse intersection matrix of the transcendental cycles, with signature (2, 1). As explained in appendix A, this relation basically

tells us that the periods θ_I (over-)parametrize, in the guise of generalized Calabi–Visentini coordinates, the moduli space of the transcendental cycles that, as well known [21] has the form³¹ $\Gamma_D \backslash O(2, 1) / O(2)$. Indeed the quadratic constraint (3.10) implies that only one (and not two) of the ratios of periods are independent, in agreement with (B.7).

In the z -variable (B.2), using [34] 2.7.(11), equation (B.8) becomes

$$\{Y; z\} = \frac{1}{2} \frac{1}{z^2} + \frac{3}{8} \frac{1}{(z+1)^2} - \frac{13}{32} \frac{1}{z(z+1)} = 2I(0, \frac{1}{4}, \frac{1}{2}; -z) \quad (\text{B.9})$$

where we use the notation of [34], equation 2.7(9), and Y is a Schwarzian function $s(0, \frac{1}{4}, \frac{1}{2}; -z)$, and can therefore be expressed as $Y = \frac{y_1}{y_2}$, where $y_{1,2}(z)$ are two linear independent solutions of the Fuchsian equation

$$\frac{d^2 y}{dz^2} + I(0, \frac{1}{4}, \frac{1}{2}; -z)y = 0 . \quad (\text{B.10})$$

We also have

$$y_{1,2} = (-z)^{1/2} (1+z)^{1/4} U_{1,2}(z) , \quad (\text{B.11})$$

where $U_{1,2}$ are two linearly independent solutions of the hypergeometric equation of parameters $\{\frac{1}{8}, \frac{3}{8}, 1\}$. Recalling that the wronskian $y_1' y_2 - y_2' y_1$ is a constant since the first derivative is absent in (B.10), it follows from (B.7) and (B.11), that the rescaled period $\hat{\vartheta} = \mu \vartheta$, has the generic form

$$\hat{\vartheta}(z) = C_{\alpha\beta} U_\alpha(z) U_\beta(z) , \quad (\alpha, \beta = 1, 2) , \quad (\text{B.12})$$

As promised, by means of (B.12) we have retrieved the relation between the triplet and the doublet representation anticipated in (A.22) via group-theory arguments. Indeed the 3×3 $O(2, 1)$ -monodromy matrices of the third-order equation are nothing else but the image, in the triplet representation, of the 2×2 $SU(1, 1)$ -monodromy matrices of the associated hypergeometric equation. The construction of the third-order equation solutions as tensor products of the hypergeometric equation solutions is nothing else but a necessary consequence of this fact.

B.2 Second example

B.2.1 The Picard–Fuchs equation.

In this case as invariant (2, 0) form we take the following one (with $W^{(2)}$ as in (4.10)):

$$\hat{g}(\nu_1, \nu_2) = \int B'^{\frac{1}{12}} b_3^{\frac{1}{12}} b_4^{\frac{1}{3}} b_5^{\frac{1}{2}} \omega \frac{1}{W^{(2)}} . \quad (\text{B.13})$$

A pair of second-order differential equations satisfied by the periods can be obtained through the use of the following relations:

$$6^2 \frac{\partial}{\partial \psi_1} \frac{\partial}{\partial \psi_1} \frac{1}{W^{(2)}} = 12^2 \frac{\partial}{\partial B'} \frac{\partial}{\partial b_3} \frac{1}{W^{(2)}} \quad (\text{B.14})$$

$$4 \frac{\partial}{\partial \psi_4} \frac{\partial}{\partial \psi_4} \frac{1}{W^{(2)}} = 6 \frac{\partial}{\partial \psi_1} \frac{\partial}{\partial \psi_3} \frac{1}{W^{(2)}} . \quad (\text{B.15})$$

³¹ Γ_D is the duality group (formed by the monodromies and the symmetry of the potential). It is integer-valued in an integral basis; we give explicit matrices later.

As alternatives for the second line in (B.15) one can take various other relations but they all lead to the same final result. Applying the identities (B.15) on the invariant definition (B.13) of the period one gets the following two equations in terms of the invariants (4.17):

$$\begin{aligned} & \left(\frac{1}{2} \nu_2^{1/2} \frac{\partial}{\partial \nu_2} \nu_2^{1/2} \frac{\partial}{\partial \nu_2} \nu_1^{1/2} - \left(\nu_1 \frac{\partial}{\partial \nu_1} + \nu_2 \frac{\partial}{\partial \nu_2} \right)^2 \nu_1^{1/4} \right) \hat{g}(\nu_1, \nu_2) \\ & \left(4 \nu_1^{1/3} \frac{\partial}{\partial \nu_1} \nu_1^{2/3} \frac{\partial}{\partial \nu_1} - \nu_2^{1/2} \frac{\partial}{\partial \nu_2} \nu_2^{1/2} \frac{\partial}{\partial \nu_2} \right) \hat{g}(\nu_1, \nu_2) . \end{aligned} \quad (\text{B.16})$$

For instance, to obtain the second of the above equations from the second of the identities (B.15) it suffices to fix the gauge (4.22).

B.2.2 Lian–Yau solution.

Our goal is that of writing the general solution of such a system. This can be done by using some results already existing in the literature, in particular those obtained by Lian and Yau in [33]. They use two variables x and z , related to our ν_1 and ν_2 by

$$\nu_1^{-1} = (864x)^2 z ; \quad \nu_2 = 4\nu_1(-1 + 864x) . \quad (\text{B.17})$$

and the above equations (B.16) reduce to:

$$L_2 \hat{\vartheta} = 0 ; \quad L_1 \hat{\vartheta} = 0 , \quad (\text{B.18})$$

where

$$\begin{aligned} L_1 & \equiv x \frac{d}{dx} \left(x \frac{d}{dx} - 2z \frac{d}{dz} \right) - 12x \left(6x \frac{d}{dx} + 5 \right) \left(6x \frac{d}{dx} + 1 \right) \\ L_2 & \equiv \left(z \frac{d}{dz} \right)^2 - z \left(2z \frac{d}{dz} - x \frac{d}{dx} + 1 \right) \left(2z \frac{d}{dz} - x \frac{d}{dx} \right) . \end{aligned} \quad (\text{B.19})$$

and

$$\hat{\vartheta} = \nu_1^{1/12} \hat{g} \quad (\text{B.20})$$

which in the gauge (4.18) takes the form (using as in the first example $\hat{\Omega}^{(2,0)} = \psi_0 \Omega^{(2,0)}$)

$$\hat{\vartheta} = \int \frac{\psi_0 \omega_{K3}}{W^{(2)}} \propto \int \hat{\Omega}^{(2,0)} . \quad (\text{B.21})$$

To obtain the solutions of Lian and Yau it suffices to introduce the following differential operator:

$$L_3(u) \equiv \frac{d}{du} \left(u \frac{d}{du} \right) - \left(u \frac{d}{du} + \frac{5}{6} \right) \left(u \frac{d}{du} + \frac{1}{6} \right) = u(1-u) \frac{d^2}{du^2} + (1-2u) \frac{d}{du} - \frac{5}{36} \quad (\text{B.22})$$

and verify that a general solution to the system (B.18) of partial differential equations is of the following form

$$\hat{\vartheta}(x, z) = (a_{12}, a_{21}, a_{11}, a_{22}) \cdot \begin{pmatrix} \xi_1(r) \xi_2(s) \\ \xi_2(r) \xi_1(s) \\ \xi_1(r) \xi_1(s) \\ \xi_2(r) \xi_2(s) \end{pmatrix} \quad (\text{B.23})$$

where $(a_{12}, a_{21}, a_{11}, a_{22})$ is a set of arbitrary constants and $\xi_1(u)$ and $\xi_2(u)$ constitute a basis of solutions for the second-order equation

$$L_3(u) \xi(u) = 0 . \quad (\text{B.24})$$

The variables r and s are a pair of algebraic functions of the original variables x, z determined as **any one** of the **four** branches of the pair of algebraic equations:

$$\begin{aligned} r + s - 2rs - 432x &= 0 ; & \text{or} & & (1 - 2r)(1 - 2s) &= 2\sqrt{\frac{\nu_2}{\nu_1}} \\ rs(1 - r)(1 - s) - (432x)^2z &= 0 ; & \text{or} & & 4rs(1 - r)(1 - s) &= (4\nu_1)^{-1} . \end{aligned} \quad (\text{B.25})$$

Equation (B.24) is a hypergeometric equation of parameters $a = \frac{1}{6}$, $b = \frac{5}{6}$, $c = 1$, which admits as regular solution in the neighbourhood of $u = 0$ the hypergeometric series:

$$\xi(u) = \xi_0(u) = {}_2F_1\left(\frac{1}{6}, \frac{5}{6}, 1; u\right) . \quad (\text{B.26})$$

A complete set of linear independent solutions of the hypergeometric equation (B.24) for large values of u is given by

$$\begin{aligned} \xi_1(u) &= B_1 u^{-1/6} {}_2F_1\left(\frac{1}{6}, \frac{1}{6}, \frac{1}{3}; \frac{1}{u}\right) \\ \xi_2(u) &= B_2 u^{-5/6} {}_2F_1\left(\frac{5}{6}, \frac{5}{6}, \frac{5}{3}; \frac{1}{u}\right) , \end{aligned} \quad (\text{B.27})$$

where B_1 and B_2 are arbitrary constants.

B.2.3 Solution of the algebraic equations.

With a further change of variable:

$$r = \frac{a+1}{2} ; \quad s = \frac{b+1}{2} , \quad r = \frac{a+1}{2} ; \quad s = \frac{b+1}{2} , \quad (\text{B.28})$$

and setting

$$A \equiv \left(\sqrt{\nu_2} + \frac{1}{2}\sqrt{\nu_1}\right)^2 - 1 ; \quad B \equiv \left(\sqrt{\nu_2} - \frac{1}{2}\sqrt{\nu_1}\right)^2 - 1 . \quad (\text{B.29})$$

the system of equations (B.25) goes into the form

$$\begin{aligned} (a^2 - 1)(b^2 - 1)A &= (a + b)^2 \\ (a^2 - 1)(b^2 - 1)B &= (a - b)^2 . \end{aligned} \quad (\text{B.30})$$

Then with a few elementary manipulations one can obtain the explicit solutions of the algebraic system (B.30):

$$a = \frac{\sqrt{A} + \sqrt{B}}{\sqrt{A+1} + \sqrt{B+1}} ; \quad b = \frac{\sqrt{A} - \sqrt{B}}{\sqrt{A+1} + \sqrt{B+1}} , \quad (\text{B.31})$$

where the sign of \sqrt{A} , \sqrt{B} , $\sqrt{A+1}$ and $\sqrt{B+1}$ can be taken as arbitrary but the same in the two expressions. In other words one can take one solution, and the other possible branches of the solution can be easily obtained using the symmetries of the algebraic system:

$$r \leftrightarrow s ; \quad r \leftrightarrow (1-r) ; \quad s \leftrightarrow (1-s) . \quad (\text{B.32})$$

In the usual gauge, the invariants are given by (4.20), and

$$A = \frac{1}{B'} \left((\psi_1 + \psi_0^6)^2 - B' \right) ; \quad B = \frac{1}{B'} \left(\psi_1^2 - B' \right) , \quad (\text{B.33})$$

and one branch of the solution can be written as

$$\begin{aligned} r &= \frac{1}{2} \left(1 + \frac{\sqrt{(\psi_1 + \psi_0^6)^2 - B'} - \sqrt{\psi_1^2 - B'}}{\psi_0^6} \right) \\ s &= \frac{1}{2} \left(1 + \frac{\sqrt{(\psi_1 + \psi_0^6)^2 - B'} + \sqrt{\psi_1^2 - B'}}{\psi_0^6} \right) . \end{aligned} \quad (\text{B.34})$$

In this way we have reached an explicit solution of the Picard–Fuchs differential system. It suffices to choose the algebraic branch (B.34) and to use the basis of solutions (B.27) for the $\xi_i(r)$ and $\xi_i(s)$ functions appearing in (B.23).

The monodromy of this period vector has been obtained in the main text by considering the elliptic fibration structure or the two modulus $K3$ surface $X_6^*[1, 1, 4, 6]$ (compare with section 6). There we have related the differential equation (B.24) to the Picard–Fuchs equation of the fibre torus.

In the present appendix the derivation of the direct product structure (B.23) of the solutions was our main goal. Indeed, we wanted to verify the group-theory prediction encoded in (A.31). Once again this factorization of the solutions is a consequence of the accidental factorization of the group $SO(2, 2) \equiv SU(1, 1) \times SU(1, 1)$. The two $SU(1, 1)$ factors contain the monodromy matrices of the two hypergeometric equations in (B.24).

C The z_8 basis of integer cycles in example 1

Apart from the strategy used in the main text, there is also the possibility to construct CY cycles similar to the construction already used for the $K3$ fibre, using a fundamental cycle and its analytic continuation. This will lead us also to monodromy matrices and a formula

for the CY intersection matrix from the intersection matrix \mathcal{I} and monodromy \mathcal{M}_∞ of the $K3$ fibre. In this way we make contact with [23].

We will define a fundamental cycle C_0 (and a corresponding period $\hat{\omega}_0$) for a certain region in moduli space (ψ_0 large). This period cannot be defined globally and smoothly; as we have done before we choose cuts in the moduli space and analytically continue the period to a different region, ψ_0^4 and $\tilde{\psi}_s$ small and in the upper half-plane. Then we use the \mathbb{Z}_8 symmetry that acts on the moduli (see definitions (4.31)) as

$$(\tilde{\psi}_s, \tilde{u}) \rightarrow (e^{i\pi} \tilde{\psi}_s, e^{i\pi} \tilde{u}), \quad (\text{C.1})$$

and define a whole set of periods $\hat{\omega}_\sigma \xrightarrow{\mathbb{Z}_8} \hat{\omega}_{\sigma+1}$, $\sigma = 0, \dots, 7$. Only six of these periods are independent, since $\sum_{\sigma \text{ even}} \hat{\omega}_\sigma = \sum_{\sigma \text{ odd}} \hat{\omega}_\sigma = 0$. Finally, all the periods $\hat{\omega}_\sigma$ are analytically continued to the whole moduli space and their non-trivial monodromies around the various singularities are analysed. In the following we describe this construction in some detail.

The fundamental cycle. An integer cycle C_0 can be defined, for ψ_0 large, in complete analogy to the $K3$ fundamental cycle of (5.2):

$$C_0 = \left\{ (x_1, x_2, x_3, x_4, x_5) \mid x_5 = \text{const.}, |x_1|^2 = |x_2|^2 = |x_3| = \delta, \right. \\ \left. x_4 \text{ the solution of } W^{(1)}(x) = 0 \text{ that tends to } 0 \text{ as } \psi_0 \rightarrow \infty \right\} / (2|G|), \quad (\text{C.2})$$

where G is the discrete identification group for the CY (3.13). Here we divide by $(2|G|)$ in order to get an elementary cycle. Indeed, the subset of transformations (4.2) which leaves invariant the specified set of variables $\{x_i\}$ contains not only the group $G = \mathbb{Z}_4^3$ (i.e. arbitrary m_1, m_2 and $m_3 = m_0$ in (4.2)), but contains also the projective transformation $(x_1, x_2) \rightarrow -(x_1, x_2)$. Changing variables as in (3.16) from x_1, x_2 to ζ, x_0 , the torus $|x_1|^2 = |x_2|^2 = \delta$ covers eight times the torus $\delta|\zeta| = |x_0| = \delta$. With the notations of (5.2) and (5.4), such that $b_0 = (\gamma_0 \times \gamma_3)/|G'|$, and denoting the circle around $\zeta = 0$ as C , we have

$$C_0 = \frac{2|G|}{8|G'|} C_0 = \frac{1}{8|G'|} \gamma_1 \times \gamma_2 \times \gamma_3 = \frac{1}{|G'|} C \times \gamma_0 \times \gamma_3 = C \times b_0. \quad (\text{C.3})$$

Using (5.4) we obtain [23]

$$\hat{\omega}_0 \equiv \int_{C_0} \hat{\Omega}^{(3,0)} = \int_{C \times b_0} \hat{\Omega}^{(2,0)} \frac{d\zeta}{2\pi i \zeta} \\ = \frac{1}{2\pi i} \int_C \frac{d\zeta}{\zeta} \hat{\vartheta}_0(z(\zeta)) = \frac{1}{\pi} \int_\gamma \frac{dw \hat{\vartheta}_0(z(w))}{\sqrt{1-w^2}}. \quad (\text{C.4})$$

Note that in terms of the variable w , equation (5.25), the circle C is mapped into a contour surrounding the cut from $w = -1$ to $w = 1$ associated to the factor $1/\sqrt{1-w^2}$, i.e. twice the path γ ‘above the cut’ shown in figure 7 to describe the ‘even’ cycles.

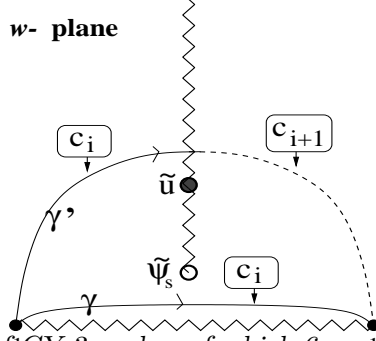


Fig. 7: A basis C_σ ($\sigma = 0, \dots, 7$) of CY 3-cycles, of which 6 are independent, is obtained by fibring (as indicated by the boxes) a basis c_i ($i = 0, \dots, 3$) of K3 2-cycles, of which 3 are independent, over the path γ (getting C_{2i}) or γ' (getting C_{2i+1}) in the base.

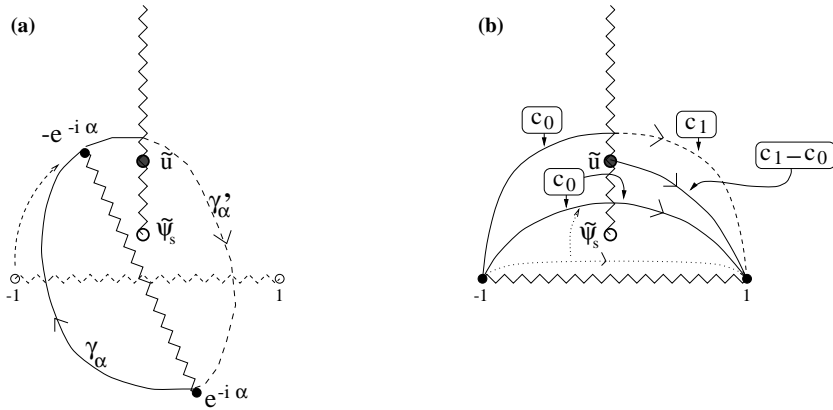


Fig. 8: (a) The rotation $(\tilde{\psi}_s, \tilde{u}) \rightarrow (e^{i\alpha}\tilde{\psi}_s, e^{i\alpha}\tilde{u})$ is discussed changing variables in the base to $w' = e^{-i\alpha}w$. The paths γ, γ' become $\gamma_\alpha, \gamma'_\alpha$; notice that with respect to figure 7 we draw γ under the square-root cut, changing its orientation. When $\alpha = \pi$, we have $\gamma_\pi = \gamma'$ and $\gamma'_\pi = \gamma$; moreover the cycles fibred over γ' have undergone a \mathbf{Z}_4 rotation. (b) The vanishing cycle V_v at the conifold: consider $C_0 \sim \gamma \times c_0$; the path γ can be lifted past the singular point $\tilde{\psi}_s$, as the K3 cycle c_0 is regular there. Then C_0 is clearly equal to $C_1 - V_v$, where V_v is the fibration of $c_1 - c_0 \equiv c'_0$, the vanishing cycle in the K3, on an open line from 1 to \tilde{u} .

Analytically continued cycles. Now consider the fundamental period for $\psi_0, \tilde{\psi}_s$ small and in the upper half-plane, i.e. the situation depicted in figure 7.

Under a rotation $(\tilde{\psi}_s, \tilde{u}) \rightarrow (e^{i\alpha}\tilde{\psi}_s, e^{i\alpha}\tilde{u})$ the modulus of the $K3$ fibre transforms, according to (4.32), as $z(w) \rightarrow z(e^{-i\alpha}w)$. Changing integration variable in (C.4), $w' = e^{-i\alpha}w$, we obtain $\hat{\omega}_0 \rightarrow \frac{1}{\pi} \int_{\gamma(\alpha)} \frac{dw'}{\sqrt{1-e^{2i\alpha}w'^2}} \hat{\vartheta}_0(z(w'))$. As explicitly shown in figure 8a, under a rotation of π , we have $\gamma \times c_0 \rightarrow \gamma' \times c_0 \rightarrow \gamma \times c_1 \rightarrow \dots$, i.e. $C_0 \rightarrow C_1 \rightarrow C_2 \rightarrow \dots$. Thus we have generated the basis of cycles C_σ described in figure 7, i.e. $C_\sigma \xrightarrow{\mathbb{Z}_8} C_{\sigma+1}$. The corresponding periods $\hat{\omega}_\sigma$ are naturally divided into ‘even’ and ‘odd’ periods

$$\begin{aligned}\hat{\omega}_{2k} &= \frac{1}{\pi} \int_{\gamma} \frac{dw}{\sqrt{1-w^2}} \hat{\vartheta}_k(z(w)) , \\ \hat{\omega}_{2k+1} &= \frac{1}{\pi} \int_{\gamma'} \frac{dw}{\sqrt{1-w^2}} \hat{\vartheta}_k(z(w)) ,\end{aligned}\tag{C.5}$$

where $\hat{\vartheta}_k, j = 0, \dots, 3$ is the \mathbb{Z}_4 -basis of $K3$ periods described previously. We will choose as a basis of independent periods $\{\hat{\omega}_\Sigma\} = (\hat{\omega}_0, \hat{\omega}_2, \hat{\omega}_4, \hat{\omega}_1, \hat{\omega}_3, \hat{\omega}_5)$.

Intersection matrix. As discussed in section 3.5, to obtain the intersection of two CY 3-cycles realized as fibrations of $K3$ 2-cycles we have to add (with the appropriate sign) the intersections of the 2-cycles in the fibre above the intersection points in the base.

Let us apply this to the basis $\{C_\Sigma\} = (C_0, C_2, C_4, C_1, C_3, C_5)$ of CY cycles (associated to the basis $\hat{\omega}$ of periods) we are considering. These cycles are described as fibrations (see figure 7 and (C.5)): $C_{2I} = \gamma \times c_I, C_{2I+1} = \gamma' \times c_I$. Using (3.22) it is immediate to see that $C_{2I} \cdot C_{2J} = C_{2I+1} \cdot C_{2J+1} = 0$, since $\gamma \cap \gamma = \gamma' \cap \gamma' = 0$. The interesting intersections are

$$C_{2I} \cdot C_{2J+1} = (+1)c_I \cdot c_J + (-1)c_J \cdot (\mathcal{M}_\infty c)_J = (\mathcal{I} - \mathcal{I}\mathcal{M}_\infty^T)_{IJ} ,\tag{C.6}$$

where $\mathcal{I}_{IJ} = c_I \cdot c_J$ is the intersection matrix (5.16) and \mathcal{M}_∞ the \mathbb{Z}_4 action (5.13) in the $K3$ fibre. Thus we obtain $C_\Lambda \cdot C_\Sigma = I_{\Lambda\Sigma}$, with

$$I = \begin{pmatrix} 0 & \mathcal{I}(\mathbf{1} - \mathcal{M}_\infty^T) \\ -(\mathbf{1} - \mathcal{M}_\infty)\mathcal{I} & 0 \end{pmatrix} ; \quad \mathcal{I}(\mathbf{1} - \mathcal{M}_\infty^T) = \begin{pmatrix} -1 & 3 & -3 \\ 1 & -1 & 3 \\ -3 & 1 & -1 \end{pmatrix} .\tag{C.7}$$

Observe that the determinant of this intersection matrix is 16^2 , while the determinant of the $K3$ intersection matrix (5.16) is -4 . We expect that fibring the $K3$ over paths in ζ with intersection matrix 1 should also lead to a construction of CY cycles, and then the determinant of the intersection matrix would be 4^2 . If this is the case, then the basis $\hat{\omega}$ of integer cycles, constructed here, is not an elementary basis. Indeed, nothing guarantees that differences between the analytic continued fundamental cycle, and the fundamental cycle itself are elementary (we just know that they are integer). In fact, below we shall construct a more elementary basis of CY cycles, removing the factor 16 in the intersection matrix.

Monodromies. First of all the monodromy around $\psi_0 = 0$ corresponds to the action of the \mathbf{Z}_8 symmetry on the ϖ basis, $\hat{\varpi} \rightarrow \mathcal{A}\hat{\varpi}$, with

$$\mathcal{A} = \begin{pmatrix} 0 & \mathbf{1} \\ \mathcal{M}_\infty & 0 \end{pmatrix}. \quad (\text{C.8})$$

Other singular points of the CY manifold are located at $\tilde{u} = \pm 1$ and $\tilde{\psi}_s = \pm 1$. Since the singularities for $+1$ are related by the \mathbf{Z}_8 symmetry to the ones for -1 , we concentrate on the $+1$ representatives. First we study the conifold singularity at $\tilde{u} = 1$.

In the main text we found at this point the ‘vanishing cycle’ V_v , equation (5.27). We now re-express it in terms of the basis C_Λ . In figure 8((b)) it is explained how the C_0 cycle is deformed to a C_1 cycle. In that procedure, it does not change by lifting it past the singularity at $w = \tilde{\psi}_s$, because the transported $K3$ cycle c_0 has no monodromy at that point, see (5.14). But lifting it through the singularity at $w = \tilde{u}$, one finds that at the right of the cut appears $\mathcal{M}_\infty c_0$, and the difference $C_1 - C_0$ is therefore a transport of

$$c_0 - \mathcal{M}_\infty c_0 = c_0 - c_1 = -c'_0 \quad (\text{C.9})$$

over the line from $w = 1$ to $w = \tilde{u}$. Thus we have $-\mathcal{V}_v = \hat{\varpi}_1 - \hat{\varpi}_0$. Knowing this expression for the singular cycle, we can obtain the monodromy around the CY conifold singularity $\tilde{u} = 1$, denoted as $M_{\tilde{u}}$, through the Picard–Lefschetz formula (2.19) with $\nu = C_1 - C_0$. Around the point $\tilde{\psi}_s = 1$ there is one more non-trivial monodromy, whose matrix action we denote by M_s . In order to compute M_s it turns out that it is easier³² to evaluate first the combined monodromy $M_{\tilde{u}}M_s$, and then obtain M_s multiplying by $M_{\tilde{u}}^{-1}$. The final result is

$$M_{\tilde{u}} = \begin{pmatrix} 2 & 0 & 0 & -1 & 0 & 0 \\ -1 & 1 & 0 & 1 & 0 & 0 \\ 3 & 0 & 1 & -3 & 0 & 0 \\ 1 & 0 & 0 & 0 & 0 & 0 \\ -3 & 0 & 0 & 3 & 1 & 0 \\ 3 & 0 & 0 & -3 & 0 & 1 \end{pmatrix}, \quad M_s = \begin{pmatrix} 1 & 0 & 0 & 0 & 0 & 0 \\ 0 & 2 & 1 & 0 & -1 & -1 \\ -3 & -4 & -2 & 3 & 4 & 3 \\ 0 & -1 & -1 & 1 & 1 & 1 \\ 3 & 4 & 3 & -3 & -3 & -3 \\ -3 & -3 & -2 & 3 & 3 & 3 \end{pmatrix}. \quad (\text{C.10})$$

All the monodromy matrices derived here agree with those given in [23].

Comparison of bases. To translate results we want to compare the basis here with that in the main text. The integrals \mathcal{T}_I in the main text over the circle correspond to the even periods $\hat{\varpi}_{2I}$, see (C.5), and the change of basis (5.21). The relation of \mathcal{V}_v to the $\hat{\varpi}$ was determined above. The same method can be used for obtaining expressions of $\mathcal{V}_{1,2}$. In fact, we can do all three at once. The three $K3$ cycles can be decomposed in one which has no monodromy at $w = \tilde{u}$, and two others which have no monodromy at $w = \tilde{\psi}_s$. Therefore in a similar way as above we can make the difference between the CY cycles C_{2I+1} and C_{2I} . The

³²The computation is simply done by manipulating the pictures of the cycles in figure 2; we first apply $M_{\tilde{u}}$ by letting \tilde{u} run around 1 in the w -plane, and then M_s by doing the same thing with $\tilde{\psi}_s$. Then by deforming the paths, we write the resulting integral in terms of our basis periods.

former consist of a transport over a γ' of a $K3$ cycle. This $K3$ cycle, say c at the left hand of the cut in figure 8**(b)**, will become $\mathcal{M}_\infty c$ at the right hand side. If we pull the path γ' through the two singular points, a cycle gets an extra part at one of the two singular points (if we write it in the basis of the cycles such that they only have monodromy in one of the points), and the difference between $C_{2I+1} - C_{2I}$ is at the end the transport over a path from $w = 1$ to either $w = \tilde{u}$ or $w = \tilde{\psi}_s$ of the cycle $(\mathbf{1} - \mathcal{M}_\infty)c_I$. We still have to express that in the c' basis, using F (5.21), and obtain

$$\hat{\omega}_{2I+1} - \hat{\omega}_{2I} = (\mathbf{1} - \mathcal{M}_\infty)F^{-1}\mathcal{V}_I. \quad (\text{C.11})$$

The full transformation matrix is then

$$\begin{pmatrix} \mathcal{V}_I \\ \mathcal{I}'_I \end{pmatrix} = \begin{pmatrix} -F(\mathbf{1} - \mathcal{M}_\infty)^{-1} & F(\mathbf{1} - \mathcal{M}_\infty)^{-1} \\ F & 0 \end{pmatrix} \begin{pmatrix} \hat{\omega}_{2I} \\ \hat{\omega}_{2I+1} \end{pmatrix}. \quad (\text{C.12})$$

Note that the matrix

$$F(\mathbf{1} - \mathcal{M}_\infty)^{-1} = \begin{pmatrix} -1 & 0 & 0 \\ \frac{3}{2} & 0 & -\frac{1}{2} \\ \frac{3}{4} & \frac{1}{2} & \frac{1}{4} \end{pmatrix} \quad (\text{C.13})$$

is non-integer. Its determinant is $-\frac{1}{4}$. As the basis $v = \{\mathcal{V}, \mathcal{I}'\}$ is build from integer cycles, this shows that the previous basis was not elementary, as we expected due to the determinant of the intersection matrix (C.7). The transformation (C.12) thus eliminates the extra factor 4^2 in the determinant of I .

One can then calculate the intersection matrix q in the basis v using (C.7), (2.17), and obtains (5.30) with a compact expression for q_{vv} :

$$q_{vv} = \mathcal{I}'(\mathbf{1} - \mathcal{M}'_\infty)^{-1T} - (\mathbf{1} - \mathcal{M}'_\infty)^{-1}\mathcal{I}'. \quad (\text{C.14})$$

References

- [1] S. Kachru, A. Klemm, W. Lerche, P. Mayr, C. Vafa, Nucl. Phys. **B459** (1996) 537; hep-th/9508155.
- [2] A. Klemm, W. Lerche, P. Mayr, C. Vafa, N. Warner, Nucl. Phys. **B477** (1996) 746; hep-th/9604034.
- [3] W. Lerche, in *Gauge Theories, Applied Supersymmetry, Quantum Gravity*, eds. B. de Wit et al., Leuven Notes in Mathematical Physics, B6, 1996, p. 53; Nucl. Phys. Proc. Suppl. 55B (1997) 83-117; Fortsch. Phys. 45 (1997); hep-th/9611190.
- [4] A. Klemm, in "1996 summer school in High Energy Physics and cosmology", Trieste 1996, World Scientific, p. 120; hep-th/9705131.

- [5] B. de Wit, P.G. Lauwers, R. Philippe, Su S.-Q. and A. Van Proeyen, Phys. Lett. **B 134** (1984) 37;
B. de Wit and A. Van Proeyen, Nucl. Phys. **B 245** (1984) 89.
- [6] G. Sierra and P.K. Townsend, in *Supersymmetry and Supergravity 1983*, ed. B. Milewski (World Scientific, Singapore, 1983), p. 396;
S. J. Gates, Nucl. Phys. **B 238** (1984) 349.
- [7] N. Seiberg and E. Witten, Nucl. Phys. **B426** (1994) 19; **B431** (1994) 484.
- [8] L. Andrianopoli, M. Bertolini, A. Ceresole, R. D’Auria, S. Ferrara, P. Frè and T. Magri, Journal of geometry and Physics **23** (1997) 111; hep-th/9605032.
- [9] N. Seiberg, Nucl. Phys. **B303** (1988) 286.
- [10] A. Klemm and S. Theisen, in *Gauge Theories, Applied Supersymmetry, Quantum Gravity*, eds. B. de Wit et al., Leuven Notes in Mathematical Physics, B6, 1996, p. 27.
- [11] S. Kachru and C. Vafa, Nucl. Phys. **B450** (1995) 69, hep-th/9505105;
S. Ferrara, J. A. Harvey, A. Strominger and C. Vafa, Phys. Lett. **B361** (1995) 59, hep-th/9505162.
- [12] J. Polchinski, Phys. Rev. Lett. 75 (1995) 4724; hep-th/9507158.
- [13] S. Katz, A. Klemm, C. Vafa, Nucl. Phys. **B497** (1997) 173; hep-th/9609239.
- [14] S. Katz, P. Mayr, C. Vafa, Adv. Theor. Math. Phys. **1** (1998) 53, hep-th/9706110.
- [15] E. Witten, Nucl. Phys. **B500** (1997) 3, hep-th/9703166.
- [16] A.Klemm, W.Lerche and P.Mayr, Phys. Lett. **B357** (1995) 313, hep-th/9506112.
- [17] P.S. Aspinwall, and J. Louis, Phys. Lett. **B369** (1996) 233, hep-th/9510234.
- [18] P. Frè, Nucl. Phys. Proc. Suppl. **45BC** (1996) 59.
- [19] B. Craps, F. Roose, W. Troost and A. Van Proeyen, Nucl. Phys. **B503** (1997) 565; hep-th/9703082.
- [20] P. Griffiths and J. Harris, *Principles of Algebraic Geometry*, Wiley-Interscience, 1978.
- [21] P. Aspinwall, *K3 surfaces and String Duality*, hep-th/9611137
- [22] S. Ferrara and J. Louis, Phys. Lett. **B 278** (1992) 240;
A. Ceresole, R. D’Auria, S. Ferrara, W. Lerche and J. Louis, Int. J. Mod. Phys.A **8** (1993) 79.
- [23] P. Candelas, X. de la Ossa, A. Font, S. Katz and D. Morrison, Nucl. Phys. **B416** (1994) 481; hep-th/9308083.

- [24] L. Castellani, R. D'Auria and S. Ferrara, Phys. Lett. **B241** (1990) 57; Class. Quantum Grav. **7** (1990) 1767,
R. D'Auria, S. Ferrara and P. Frè, Nucl. Phys. **B359** (1991) 705.
- [25] A. Strominger, Comm. Math. Phys. **133** (1990) 163.
- [26] A. Ceresole, R. D'Auria, S. Ferrara and A. Van Proeyen, Nucl. Phys. **B 444** (1995) 92, hep-th/9502072.
- [27] P. Claus, K. Van Hoof and A. Van Proeyen, in preparation.
- [28] S. Ferrara and A. Strominger, in *Strings '89*, eds. R. Arnowitt, R. Bryan, M.J. Duff, D.V. Nanopoulos and C.N. Pope (World Scientific, 1989), p. 245.
- [29] P. Griffiths, Ann. Math. **90** (1969) 460, 496.
- [30] W. Lerche, D. Smit and N. Warner, Nucl. Phys. **B372** (1992) 87.
- [31] D.R. Morrison, in *Essays on Mirror Manifolds*, ed. S.T. Yau, International Press Hong Kong, 1992.
- [32] V. Batyrev, Duke Math. Journal **69** (1993) 349; Journal Alg. Geom. **3** (1994) 493;
P.S. Aspinwall, B.R. Greene and D.R. Morrison, *The Monomial-Divisor Mirror Map*, Internat. Math. Res. Notices (1993), 319-337, alg-geom/9309007;
S. Hosono, A. Klemm, S. Theisen, S.T. Yau, Comm. Math. Phys. **167** (1995) 301;
S. Hosono, A. Klemm and S. Theisen, Commun. Math. Phys. **167** (1995) 301, hep-th/9308122; *Lectures on Mirror Symmetry*, In *Helsinki 1993, Proceedings, Integrable models and strings*, 235-280, hep-th/9403096.
- [33] B. H. Lian and S. T. Yau, *Mirror Maps, Modular Relations and Hypergeometric Series I and II*, hep-th/9507151 and hep-th/9507153.
- [34] A. Erdelyi, F. Obershettinger, W. Magnus and F.G. Tricomi, Higher Transcendental Functions, McGraw Hill, New York (1953).
- [35] V.I. Arnold: Singularity Theory, selected papers. Cambridge University Press 1981.
- [36] P. Frè and P. Soriani, *The $N = 2$ Wonderland, from Calabi-Yau manifolds to topological field-theories*, World Scientific, 1995.
- [37] E. Calabi and E. Visentini, Ann. of Math. **71** (1960) 472.
- [38] M. Billó, A. Ceresole, R. D'Auria, S. Ferrara, P. Frè, T. Regge, P. Soriani and A. Van Proeyen, Class. Quantum Grav. **13** (1996) 831; hep-th/9506075.